13. SITE 770[1]

Shipboard Scientific Party[2]

HOLE 770A

Date occupied: 21 December 1988

Date departed: 21 December 1988

Time on hole: 18 hr, 45 min

Position: 5°08.70′N, 123°40.24′E

Bottom felt (rig floor; m, drill-pipe measurement): 4518.0

Distance between rig floor and sea level (m): 11.30

Water depth (drill-pipe measurement from sea level, m): 4506.7

Total depth (rig floor; m): 4528.9

Penetration (m): 10.9

Number of cores (including cores with no recovery): 2

Total length of cored section (m): 10.9

Total core recovered (m): 1.6

Core recovery (%): 14.7

Oldest sediment cored:
Depth (mbsf): 10.9
Nature: volcanogenic silty clay
Age: Quaternary
Measured velocity (km/s): N/A

HOLE 770B

Date occupied: 21 December 1988

Date departed: 24 December 1988

Time on hole: 3 days, 30 min

Position: 5°08.69′N, 123°40.10′E

Bottom felt (rig floor; m, drill-pipe measurement): 4516.2

Distance between rig floor and sea level (m): 11.3

Water depth (drill-pipe measurement from sea level, m): 4504.9

Total depth (rig floor; m): 4990.3

Penetration (m): 474.1

Number of cores (including cores with no recovery): 21

Total length of cored section (m): 201.6

Total core recovered (m): 112.4

Core recovery (%): 55.8

Oldest sediment cored:
Depth (mbsf): 420.9
Nature: nannofossil claystone
Age: early Oligocene
Measured velocity (km/s): 1.63

Basement:
Depth (mbsf): 420.9
Nature: basalt
Measured velocity (km/s): 5.25

HOLE 770C

Date occupied: 24 December 1988

Date departed: 30 December 1988

Time on hole: 6 days, 10 hr

Position: 5°08.69′N, 123°40.11′E

Bottom felt (rig floor; m, drill-pipe measurement): 4516.2

Distance between rig floor and sea level (m): 11.3

Water depth (drill-pipe measurement from sea level, m): 4504.9

Total depth (rig floor; m): 529.5

Penetration (m): 5045.7

Number of cores (including cores with no recovery): 12

Total length of cored section (m): 115.8

Total core recovered (m): 54.8

Core recovery (%): 47.3

Oldest sediment cored:
Depth (mbsf): 423.2
Nature: nannofossil claystone
Age: early Oligocene
Measured velocity (km/s): 1.72

Basement:
Depth (mbsf): 423.2
Nature: basalt
Measured velocity (km/s): 5.57

Principal results: Three holes were drilled at Site 770 (5°08.7′N, 123°40.1′E; Table 1). Hole 770A did not properly spud in, so it was abandoned after two cores. Hole 770B was spot cored every 50 m to 340 meters below seafloor (mbsf) and then was cored continuously to 474 mbsf, including 53 m of basement. We had to abandon Hole 770B to remove 7 km of polypropylene rope that was wrapped around the drill pipe. Hole 770C was washed to basement, then cored to 529 mbsf, including 106 m of basement. We achieved excellent results in three Schlumberger logging runs and a borehole televiewer (BHTV) downhole run. The hole was reentered for an attempted packer experiment, but we could not penetrate a bridge at 56 mbsf, at which time the site was abandoned and we proceeded to Site 771 on the Cagayan Ridge.

The objectives of Site 770 were to obtain basement and logs within basement at a location close to Site 767, which had been abandoned just after hitting basement. Except for the lack of a packer run, the objectives were very well satisfied here.

Site 770 consists of two main lithologic units:

Unit I (0–296 mbsf) is middle(?) Miocene to Holocene in age, with dominant rock types composed of volcanogenic silty clay and clay with sparse thin beds of marl and volcanic ash.

Unit II (296–421 mbsf) is late middle Eocene to middle(?) Miocene in age, consisting of claystone and calcareous claystone, with sparse interbeds of silty to sandy claystone and porcellanite clay mixed sediment. The unit is divided into 3 subunits mainly on the basis of carbonate content.

Subunit IIA (296–388 mbsf) is late Oligocene to middle(?) Miocene in age. Claystone is the dominant lithology, but the subunit also contains minor interbeds of volcanogenic claystone with silt, sand, and porcellanite-mixed sediment. The claystone is grayish brown in the upper part, becoming brown to yellowish brown in the lower part.

[1] Rangin, C., Silver, E., von Breymann, M. T., et al., 1990. *Proc. ODP, Init. Repts.*, 124: College Station, TX (Ocean Drilling Program).

[2] Shipboard Scientific Party is as given in the list of participants preceding the contents.

Table 1. Coring summary, Site 770.

Core no.	Date (Dec. 1988)	Time (UTC)	Depth (mbsf)	Cored (m)	Recovered (m)	Recovery (%)
124-770A-						
1R	20	2145	0–1.4	1.4	1.43	102.0
2R	20	2240	1.4–10.9	9.5	0.15	1.6
Coring totals				10.9	1.58	14.5
124-770B-						
1R	21	0125	0–9.7	9.7	9.67	99.7
2R	21	0345	50.8–60.8	10.0	2.96	29.6
3R	21	0730	99.4–109.1	9.7	3.46	35.7
4R	21	1115	147.6–157.3	9.7	7.59	78.2
5R	21	1455	195.8–205.5	9.7	5.76	59.4
6R	21	1830	244.1–253.7	9.6	2.13	22.2
7R	21	2100	292.4–302.1	9.7	9.84	101.0
8R	22	0130	340.6–349.6	9.0	4.56	50.6
9R	22	0340	349.6–359.3	9.7	6.10	62.9
10R	22	0525	359.3–368.9	9.6	4.98	51.9
11R	22	0715	368.9–378.6	9.7	5.34	55.0
12R	22	0930	378.6–388.2	9.6	4.67	48.6
13R	22	1115	388.2–397.9	9.7	6.97	71.8
14R	22	1230	397.9–407.6	9.7	4.92	50.7
15R	22	1400	407.6–417.3	9.7	6.78	69.9
16R	22	1630	417.3–425.8	8.5	4.25	50.0
17R	22	1930	425.8–435.6	9.8	3.44	35.1
18R	22	2210	435.1–445.1	9.5	3.05	32.1
19R	23	0130	445.1–454.8	9.7	3.25	33.5
20R	23	0420	454.8–464.5	9.7	4.90	50.5
21R	23	0630	464.5–474.1	9.6	7.79	81.1
Coring totals				201.6	112.41	55.8
124-770C-						
1R	24	2030	383.8–393.3	9.5	9.33	98.2
2R	25	0130	423.2–432.9	9.7	2.42	24.9
3R	25	0515	432.9–442.6	9.7	4.40	45.3
4R	25	0800	442.6–452.2	9.6	4.09	42.6
5R	25	1035	452.2–461.9	9.7	7.83	80.7
6R	25	1230	461.9–471.5	9.6	6.75	70.3
7R	25	1555	471.5–481.1	9.6	6.49	67.6
8R	25	1815	481.1–490.8	9.7	0.90	9.3
9R	25	2030	490.8–500.5	9.7	2.10	21.6
10R	25	2300	500.5–510.2	9.7	4.20	43.3
11R	26	0125	510.2–519.9	9.7	2.40	24.7
12R	26	0420	519.9–529.5	9.6	3.90	40.6
Coring totals				115.8	54.81	47.3

Note: Depths are drill-pipe measurements corrected to sea level.

Subunit IIB (388–401 mbsf) is early to late Oligocene in age and consists of pale brown nannofossil claystone with a carbonate content up to 38%. We interpreted it as pelagic in origin.

Subunit IIC (401–421 mbsf) is late middle Eocene to early Oligocene in age. The upper part of the subunit consists of brown claystone and nannofossil claystone with a lower carbonate content than Subunit IIB (maximum of 25%). The lower part, which overlies basement, is made up of sandy clay and silty claystone.

The sedimentary section at Site 770 is about half the thickness of Site 767, yet the basal ages are identical. The difference reflects the higher elevation of Site 770, which protects the site from turbidite influence and places it just above the carbonate compensation depth (CCD) in the lowest part.

Basement was recovered from 421 to 529 mbsf. We identified nine lava units by means of their mineralogy, texture, and structure. Units 1 and 2 are pillow basalt sequences, Unit 3 is a pillow breccia, and Units 4 and 5 are brecciated, massive, amygdaloidal lavas. Unit 6 is a massive lava, which is penetrated in Hole 770C by flat-lying minor intrusions. Units 7 and 8 are dolerite sills, and Unit 9 is made up of lavas penetrated by small dikes. The boundaries, rock types, and thicknesses of these units are described below (uncertainty about exact depths is a result of core recovery of only about 50%).

Unit 1 (421–440 mbsf) is moderately plagioclase-olivine-phyric basalt. The upper part of the unit is made up mainly of small fractured and veined pillows; in the lower part of the section the pillows are larger, varying from 40 cm to 1 m in diameter.

Unit 2 (440–450 mbsf) is highly plagioclase-olivine-phyric basalt. This is a light gray, pillowed, brecciated unit.

Unit 3 (450–460 mbsf) is a moderately to highly plagioclase-olivine-phyric basalt, and pillow breccia, made up largely of angular fragments of highly porphyritic lava, 5–10 cm in diameter.

Unit 4 (460–470 mbsf) is amygdaloidal, moderately to highly plagioclase-olivine-phyric basalt, and brecciated lava, interpreted as resulting from the brecciation of an individual lava flow.

Unit 5 (470–490 mbsf) is a moderately to highly plagioclase-olivine-phyric basalt, and brecciated lava. All of the recovered section is uniform in lithology, and the unit is thought to comprise one lava flow.

Unit 6 (490–500 mbsf) is moderately to highly plagioclase-olivine-phyric basalt and lava. A number of flat intrusions with glassy chilled margins penetrate these massive lavas. It is thought to be composed of at least three separate cooling units.

Unit 7 (500–513 mbsf) is a sparsely plagioclase phyric to aphyric dolerite sill. It has a massive and uniform lithology and phaneritic texture.

Unit 8 (513–524 mbsf) is a sparsely to highly plagioclase-olivine-phyric dolerite sill. The body has a massive homogeneous lithology and a phaneritic texture.

Unit 9 (524–530 mbsf) is a moderately to highly olivine-plagioclase-phyric basalt and lavas with dikes. It is penetrated by three flay-lying minor intrusions.

Stress orientation data were obtained with the BHTV logs. Preliminary interpretation of hole ellipticity and breakout data indicate a maximum horizontal stress direction of 050°, or slightly more easterly than the results from Site 768 in the Sulu Sea.

Sites 767 and 770 documented the age, stress direction, and geologic history of the Celebes Sea, as proposed. The Celebes Sea is middle Eocene in age and was formed in a setting removed from continental or island-arc sources. During the middle Miocene, it received high amounts of continent-derived clastic debris, and in the late Miocene–Pleistocene, abundant volcanic ash. The Eocene CCD lay between Sites 767 and 770, or just below 4500 m (uncorrected for thermal subsidence).

BACKGROUND AND OBJECTIVES

The background of Site 770 is the same as that for Site 767. It is located in the Celebes Sea, 45 km from Site 767. The objectives of this site were the same as for Site 767. We returned to the Celebes Sea to complete the objectives as stated since we were not able to complete our basement objectives at Site 767 because of a hole collapse. Basement objectives for Site 770 were to measure stress in the Celebes Sea crust, to obtain sufficient basement rocks to determine their origin, and to complete the program of downhole logging.

A major objective here was to measure the direction and magnitude of the stress in the Celebes Sea. Stress orientation was made with the BHTV to measure breakouts in the borehole, and magnitude was measured with the wireline packer. We planned to determine stress directions in the Celebes Sea to test whether and to what degree collision processes are responsible for inducing long-range stress in the plate. These data could indicate whether the collision between the Sulu Ridge and Mindanao is dynamically important as well as discernible within the Celebes Sea. Alternatively, the Australia-Indonesia collision to the south could still have an influence on the stress field. The latter would be expected to produce stress vectors directed roughly north to south, whereas the former collision would be expected to orient stress northeast to southwest.

Stress magnitude is important in this kind of study to determine whether the maximum horizontal stress direction measured with the method of breakout orientations is truly the maximum principal stress. A comparison of stress magnitude with

overburden stress should solve this uncertainty. Stress directions can also be measured independently during a second BHTV run following the packer experiment by using the orientation of fractures in a hydrofrac experiment.

Our objectives in basement sampling were to date the basement rocks and to determine their petrology, chemistry, and radioisotope ratios. In this way we characterized the crust as open-ocean (MORB), back-arc basin, or thinned-arc crust. This determination is important for understanding the paleoenvironments of the basin and for better interpreting the paleoceanographic record of the cores. If successful, it can provide us with constraints for the tectonic reconstruction of the Celebes Sea region.

Site Selection

Site 770 was chosen on a raised fault block in a region where sediment thickness is about half that at Site 767. The difference in sediment thickness between the two sites was thought to reflect an absence of turbidites on the uplifted block and not a younger age of the crust. The specific site chosen had <0.5 s of sediment on the seismic line (see "Seismic Stratigraphy" section, this chapter). The thinner sediment pile was considered very important, both in terms of drilling time to basement and hole stability.

OPERATIONS

The location selected for Site 770 was about 23 nmi north-northeast of Site 767 and was located on a bathymetric rise. The target area was small, and global positioning satellite (GPS) coverage was again necessary to assure an accurate beacon emplacement. The transit was made at reduced speed to time our arrival during the GPS window, and seismic profiling began as soon as the vessel had cleared Basilan Strait.

The track took *JOIDES Resolution* southeastward to a point about 21 nmi northeast of the proposed site and intersected with the Bundesanstalt für Geowissenschaften und Rohstoffe (BGR) seismic reference Line SO49-02. The site was then approached and crossed from the northeast. The vessel continued about 6 nmi past the site, turned back to a reciprocal course and launched the positioning beacon on the second crossing at 0445 hr (UTC), 20 December 1988.

Hole 770A

Operations began slowly at Site 770, when hydraulics problems with the iron roughneck resulted in a 5¼-hr delay in the assembly of the bottom-hole assembly (BHA).

Because of the rugged bathymetry of the area, the reading from the precision depth recorder was ambiguous, with multiple side echoes. Three consecutive "water cores" were taken before sediment was recovered in the rotary core barrel (RCB) corer. After the subsequent core attempt, it was apparent that the bit was sliding down a slope and that satisfactory spud-in had not been achieved.

Hole 770B

We checked the seismic records and the precision depth recorder (PDR) and decided that the best offset was an additional 200 m south of the beacon. That offset was entered, and the bit was again lowered. This time a solid weight indication registered at about 4518 m, and the resulting core established the mud line at 4505 m below sea level (mbsl).

Drilling and coring then proceeded with a cycle of four joints drilled, a "wash barrel" recovered, and one joint cored with the barrel recovered and a new wash barrel pumped into place. Successful temperature probe measurements were taken at 61, 109, and 157 mbsf. Sediments throughout the spot-cored interval were silty clays and claystones. From 341 mbsf the sediments were cored continuously to the basement contact at about 421 mbsf with about 58% recovery.

Because of high back-pressure in the hole, a short trip was made when coring reached 379 mbsf. Basaltic basement was then cored for about 53 m at an average rate of penetration (ROP) of 5½ m/hr and a recovery rate of 44%.

We suspected that a close encounter with a floating "fish habitat" buoy the previous day had left the mooring line fouled with the drill string. Our fears were confirmed with the underwater TV camera, which revealed a heavy polypropylene rope wrapped around the drill pipe about 800 m below the rig floor. To protect the downhole science objectives, the conservative course was chosen and the bit was pulled clear of the seafloor. The rope was removed from the drill string, and the bit and bit release were inspected before the down-trip began.

The camera frame was run concurrently with the drill pipe. However, because of problems with the camera, there was little prospect of making a reentry or of detecting objects on the seafloor without a time-consuming wireline trip for repair or replacement of reentry electronics; therefore, the camera frame was recovered.

Hole 770C

Hole 770C was spudded at 1200 hr (UTC) on 24 December 1988 and was drilled without coring to 384 mbsf. At that point the center bit was recovered, a drift shot (3¼°) was taken, and a single sediment core was cut to fill a gap in the record from Hole 770B. Drilling then continued with the center bit to basement at 423 mbsf. No hole problems were encountered during drilling.

Continuous RCB cores were taken through the basaltic pillow and lava flows until the scientific drilling objectives were declared fulfilled at 529 mbsf.

Logging operations at Hole 770C began at 0435 hr (UTC) on 26 December 1988. Initial hole conditioning consisted of a wiper trip, circulation to remove 15 m of fill, a short wiper trip over the lower interval, hydraulic bit release, and pulling pipe to 433 mbsf for BHTV logging. The BHTV, with an attached L-DGO temperature tool, obtained an open-hole upcoming log for the basalts and lowermost sediments (523.5–404.8 mbsf). A short repeat section was obtained for these sediments.

The pipe was run to the bottom of the hole, the hole was filled with KCl-inhibited bentonite mud, the pipe was pulled to about 100 mbsf, and the sidewall-entry sub (SES) was rigged up. At this site the seismic stratigraphic combination consisted of long-spaced sonic, phasor resistivity, and natural gamma tools (see "Explanatory Notes" chapter, this volume). With the pipe set at 121.6 mbsf, the tool string encountered a bridge when barely into the open hole. The pipe was lowered to 433 mbsf, and a short repeat basalt log (528.4–436.1 mbsf) and a main log (527.8–0 mbsf) were obtained. The main log was obtained while pulling pipe, so that all logs except for the interval from 117.8 to 0 mbsf were open-hole logs.

The Schlumberger geochemical combination consisted of gamma spectrometry, aluminum clay, natural gamma, and general-purpose inclinometer tools (see "Explanatory Notes" chapter, this volume). With the pipe set initially at 433 mbsf, the tool string was lowered to the bottom of the hole. A through-pipe log was obtained for the interval from 449.5 to 236.5 mbsf, followed by logging while pulling pipe for the interval from 515.6 to 0 mbsf. Of the latter intervals, those from 515.6 to 125.6 mbsf were open-hole logs and from 125.6 to 0 mbsf were through-pipe logs.

Rig-up of the Schlumberger lithoporosity combination began immediately after dropping a free-fall funnel (FFF). At this site the lithoporosity combination consisted of lithodensity, neutron porosity, and natural gamma tools (see "Explanatory Notes"

chapter, this volume). With the pipe set initially at 433 mbsf, the tool string was lowered to the bottom of the hole. The open-hole interval from 513.3 to 433.0 mbsf was logged as a repeat section, followed by logging while pulling pipe for the interval from 514.6 to 102.6 mbsf. Of the latter intervals, those from 514.6 to 125.6 mbsf were open-hole logs and from 125.6 to 102.6 mbsf were through-pipe logs.

At this point a solution was found for the chronically low density log values that had been obtained, and the tool was dropped back down into the open hole for a repeat section with corrected acquisition parameters. With a fast logging speed, the interval from 232.0 to 125.6 mbsf was logged in the open hole, and the interval from 125.6 to 0 mbsf was logged through the pipe.

The reentry TV was rigged upon completion of logging and was lowered to just above the seafloor to verify that the FFF was visible and in position for reentry. Concurrently, the drill string was run back to total depth to condition the noticeably deteriorating hole for reentry with the packer.

When the special straddle-packer BHA had been made up, the drill string was run to reentry depth. The FFF was located easily, and the BHA was brought into position over the funnel for reentry.

Nearly two full stands of pipe were lowered into the hole without resistance before the reentry/clean-out bit came to a stop at 56 mbsf. The obstruction probably was a bridge or collapsed section of hole, although sidetracking in the soft sediment was not ruled out. Circulation at various rates was attempted, but no amount of circulating and "working" the pipe succeeded in advancing the bit. Rotating the pipe to "drill out" the obstruction initially was not attempted, because the packer was not designed to transmit drilling torque and because the VIT frame was still around the pipe as it was being recovered.

When the frame had been recovered, the top drive was rigged to attempt rotation as a last desperate measure to get the packer down the hole. After several minutes of working the pipe and rotating at minimum RPM and torque of under 5000 ft-lb, no progress had been made and the effort was abandoned.

The drill string was recovered, and the packer BHA was broken down. The packer had suffered no damage downhole or in passing through the FFF. Its threaded connections, as had been feared, were found to have been subjected to sufficient torque to make them difficult to break out. Both packer elements were damaged in disassembly. We found that the reentry/clean-out bit and the lowermost drill collar were plugged with sediment, confirming our suspicions that circulation had taken place through the ports in the packer body and not out the bit.

JOIDES Resolution departed Site 770 at 1000 hr (UTC), 30 December 1988.

LITHOSTRATIGRAPHY

Sedimentary Units

The holes drilled at Site 770 penetrated 420.9 m of sediments overlying the basaltic basement. Continuous coring was restricted to the interval below 340.6 mbsf. The rest of the succession was only covered by seven spot cores.

Two lithologic units were distinguished on the basis of visual descriptions and smear-slide analyses of the recovered cores (Fig. 1 and Table 2). Unit I is made up of dark greenish gray to olive gray silty clay and clay from the seafloor down to 296.05 mbsf. Unit II consists of brown claystone and light brown calcareous claystone between 296.05 and 420.9 mbsf.

Unit I

Depth: 0–296.05 mbsf
Interval: Cores 124-770A-1R through -2R and Core 124-770B-1R through Section 124-770B-7R-3

Table 2. Lithologic units for the sedimentary section, Site 770.

Unit	Subunit	Depth (mbsf)	Thickness (m)	Age
I		0–296.05	296.05	middle(?) Miocene to Holocene
II		296.05–420.90	124.85	late middle Eocene to middle(?) Miocene
	IIA	296.05–388.20	92.15	late Oligocene to middle(?) Miocene
	IIB	388.20–401.15	12.95	early to late Oligocene
	IIC	401.15–420.90	19.75	late middle Eocene to early Oligocene

Thickness: 296.05 m
Age: middle(?) Miocene to Holocene

The record of the deposits of Unit I is discontinuous as a consequence of the spot coring. The dominant rock types are volcanogenic silty clay and clay with sparse thin beds of marl and volcanic ash.

The silty clay dominates the upper five spot cores (Cores 124-770B-1R to -5R) and grades into clay in Cores 124-770B-6R and -7R. The silty clay beds are massive and dark greenish gray with gray and greenish mottling caused by bioturbation. The silt component consists mainly of volcanic ash, including glass, plagioclase, hornblende, opaques, and rock fragments. Siliceous biogenic components (sponge spicules and radiolarians) are very minor. Small amounts of calcareous grains (nannofossils) were only found at the top of the unit (Section 124-770B-1R-1).

The clay beds in the lower part of the unit are massive and moderately to heavily bioturbated. They are dark greenish gray becoming olive gray at the base. They are composed predominantly of clay minerals with minor feldspar, opaques, rock fragments, zeolites, and siliceous biogenic materials (sponge spicules and radiolarians). They grade downward into grayish brown clay beds of Unit II in Section 124-770B-7R-3.

Light greenish gray marl is present as thin, massive beds with diffuse upper and lower boundaries in Sections 124-770B-4R-3 and 124-770B-5R-4. The marl is composed predominantly of clay and micritic calcite with very minor opaques and zeolites.

Volcanic ash is present in Unit I as very thin to thin discrete layers or as burrow fills. Light greenish gray to greenish gray crystal-vitric ash beds are present in Core 124-770B-1R. They are silt- to sand-sized and are composed mainly of glass, plagioclase, and hornblende, with minor opaques and rock fragments. Interbedded within the silty clay in Cores 124-770B-4R and -5R are very thin, diffuse, grayish green to dark grayish green clay layers with silt of feldspar, glass, hornblende, and opaques. These layers are interpreted as altered fine ash.

The volcanogenic silty clay and clay in Unit I are interpreted as hemipelagic. They have a very low biogenic carbonate content, indicating deposition below the CCD. In the thin marl layers the carbonate is recrystallized, but these beds were probably deposited as turbidites. Although no structures were observed within the ash beds because of the high drilling disturbance and bioturbation, the lack of nonvolcanic materials implies air-fall deposition.

Unit II

Depth: 296.05–420.90 mbsf
Interval: Sections 124-770B-7R-3 through 124-770B-16R-3 at 60 cm
Thickness: 124.85 m
Age: late middle Eocene to middle(?) Miocene

Unit II consists of claystone and calcareous claystone, with sparse interbeds of silty to sandy claystone and porcellanite-clay mixed sediment. Unit II is divided into three subunits on the basis of the differences in carbonate content (mainly nannofossils) of the sediments.

Subunit IIA

Depth: 296.05–388.20 mbsf
Interval: Section 124-770B-7R-3 through Core 124-770B-12R
Thickness: 92.15 m
Age: late Oligocene to middle(?) Miocene

The upper part of Subunit IIA is only covered by one spot core (Core 124-770B-7R), whereas the lower part was continuously cored. Claystone is the dominant lithology and contains very minor interbeds of volcanogenic claystone with silt, silty claystone and clayey sand, and porcellanite-clay mixed sediment.

The claystone is grayish brown in the upper part, becoming brown to yellowish brown downward. It is present in massive, medium to thick beds that are slightly to moderately bioturbated. The claystone is composed mainly of clay minerals with very minor feldspar, zeolites, rock fragments, and opaque minerals. It contains variable proportions of siliceous biogenic materials (radiolarians and sponge spicules) in Cores 124-770B-10R to 124-770B-12R. The carbonate content is low (up to 6%). Dolomite (or rhodochrosite?) is present as silt-size grains in Core 124-770B-8R. Microfaults and cracks are common starting from Section 124-770B-10R-2 down to the base. The microfaults have low to steep apparent dips and have normal dip-separation. Thin laminations occur at the base of the subunit (Core 124-770-12R), and these show consistent apparent dips from 15° to 20°. The claystones are interpreted as pelagic deposits.

Very thin to thin beds of volcanogenic silty claystone, claystone with silt, and clayey sand are present in Core 124-770B-7R, Section 124-770B-9R-2, and Section 124-770B-11R-2, respectively. They are mainly composed of clay and feldspar, with minor glass, zeolites, opaques, and rock fragments. The silty claystone beds are very dark gray to greenish gray and have sharp to diffuse boundaries. They are heavily bioturbated, with numerous large round burrows. The claystone with silt is pinkish gray and is moderately to heavily bioturbated; it appears in beds with sharp bases and gradational bioturbated tops. In Section 124-770B-11R-2, thin beds of clayey sand appear as graded beds with sharp bases. They are light greenish gray to light gray in color. These beds of silty claystone, claystone with silt, and clayey sand may represent altered ashes.

Light brownish gray porcellanite-clay mixed sediment is present as very thin beds in Cores 124-770B-9R through -11R. These beds are sharp based and are commonly structureless. They consist of clay, diagenetic silica, and very minor amounts of opaques.

A medium-bedded, heavily bioturbated, yellowish brown nannofossil claystone occurs in Section 124-770B-11R-1. It has a sharp base and shows many compaction cracks. It is composed mainly of nannofossils and clay, with minor amounts of zeolites and carbonate grains.

Subunit IIB

Depth: 388.20–401.15 mbsf
Interval: Core 124-770B-13R through Section 124-770B-14R-3 at 25 cm
Thickness: 12.95 m
Age: early to late Oligocene

Subunit IIB consists of pale brown nannofossil claystone with a carbonate content of up to 38%. It is present in very thick beds that are moderately to intensely bioturbated. Clay and nannofossils (coccoliths and *Discoaster*) are the dominant components, with trace amounts of zeolites. Some black spots with high concentrations of opaque minerals (oxide or sulfide) occur in Section 124-770B-13R-4 at 22–23 and 83–84 cm. The nannofossil claystone is interpreted as pelagic in origin.

Subunit IIC

Depth: 401.15–420.90 mbsf
Interval: Sections 124-770B-14R-3 at 25 cm through 124-770B-16R-3 at 60 cm
Thickness: 19.75 m
Age: late middle Eocene to early Oligocene

The upper part of the subunit consists of brown claystone and nannofossil claystone with a lower carbonate content than Subunit IIB (a maximum of 25%). The lower part, which overlies the basement, is made up of sandy clay and silty claystone.

The claystone occurs in Core 124-770B-14R and -15R. The beds are brown, massive, and slightly bioturbated. They contain very small amounts of opaques, quartz, and feldspar. In Section 124-770B-14R-3, these are scattered because of light gray diffuse alteration patches. Manganese micronodules (< 1 mm) occur in Section 124-770B-14R-CC.

The nannofossil claystone is massive and brown with very dark gray mottling associated with bioturbation. Large, paler patches of yellowish brown color that occur throughout are diagenetic in origin. White agglutinated foraminifers are present in these patches. The principal components of the nannofossil claystone are clay minerals with varying amounts of nannofossils (coccoliths and *Discoaster*) and a minor amount of opaque minerals, which are common in darker parts of the sediment.

The nannofossil claystone and the claystone are interpreted as pelagic in origin.

Sandy clay and silty claystone occur in Sections 124-770B-16R-2 and 124-770B-16R-3. The sandy clay is medium to thick bedded with colors that vary from yellowish brown to pale yellow. It is present above the basement in Section 124-770B-16R-3, 47–54 cm (Fig. 2). In places, it is thickly laminated and shows fining-upward sequences. The sand-size fraction consists of rounded to angular, pale green aggregates of clay minerals (altered glass). The matrix is formed by clay.

The silty claystone is light brown with brown layers. The beds are bioturbated throughout and display lamination in places. Some of the burrows are infilled with coarse, altered, green glass. The silty claystone is composed of clay, feldspar, zeolite, rock fragments, and rare nannofossils.

Significant amounts of radiolarians occur at the base of the silty claystone in Section 124-770B-16R-3.

Depositional Environment and Processes

Site 770 is located on a small basement high within the Celebes Sea. Two major phases of sedimentation were recognized.

The first phase (Unit II) extended from late middle Eocene to middle(?) Miocene time. It was characterized by deposition of pelagic brown nannofossil claystone and brown hemipelagic claystone overlying basaltic basement. The base of the sedimentary succession contains hyaloclastic basement material that was eroded and redeposited. The subsequent deposition of claystone and calcareous claystone indicates that deposition took place close to the CCD. The proportion of planktonic foraminifers, calcareous benthic foraminifers, and nannofossils is variable, indicating variations in the basin of the CCD. The higher carbonate content of Subunit IIB compared with Subunit IIC indicates a deepening of the CCD from the late Eocene into the early Oligocene. Subunit IIA, which is late Oligocene to early Miocene in age, is characterized by a very low carbonate content and reflects deposition below the CCD.

The second phase (Unit I) extended from the middle(?) Miocene to the Holocene. It was characterized by deposition of greenish gray hemipelagic clay and silty clay that accumulated below the CCD. Significant amounts of carbonate only occur in

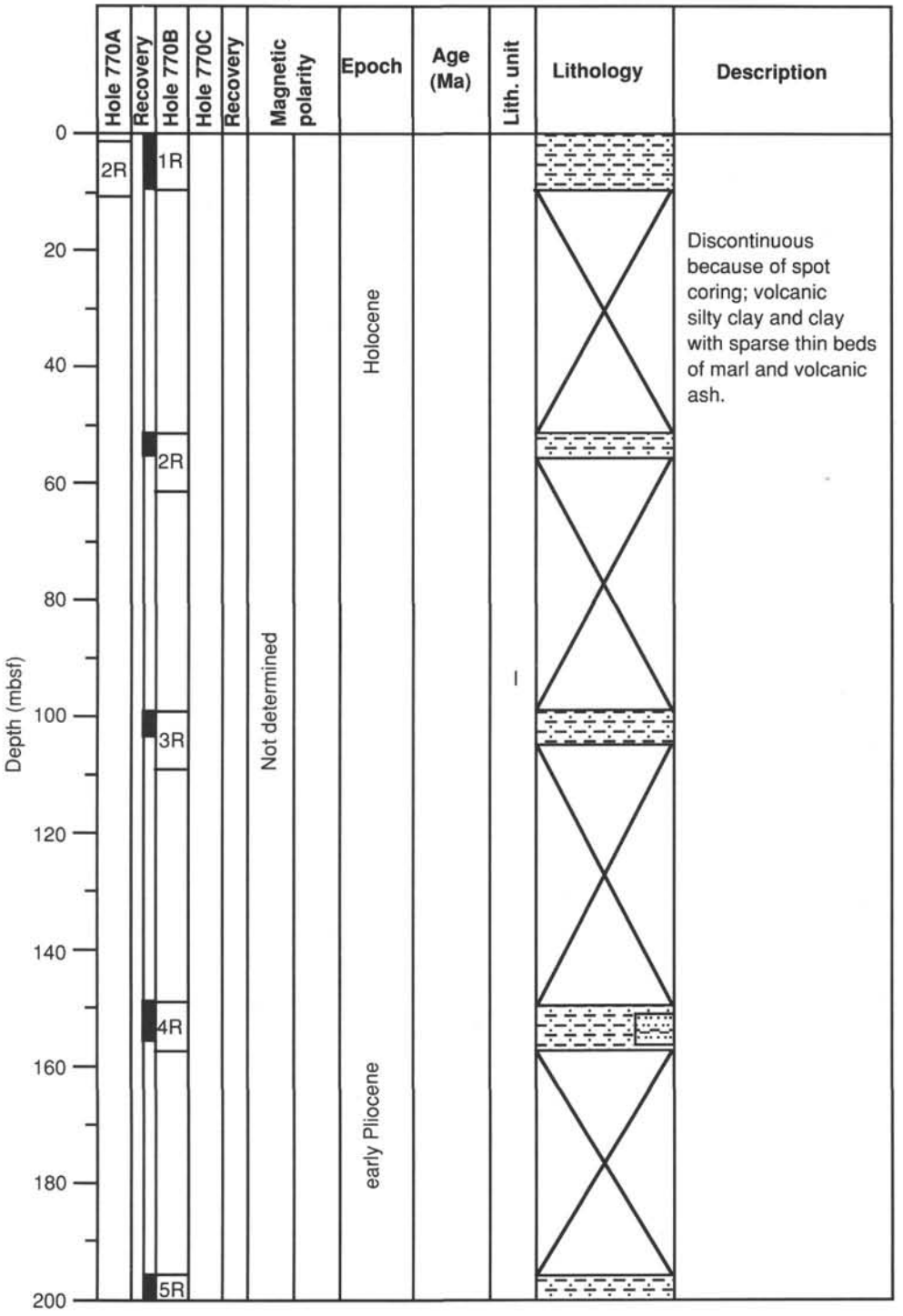

Figure 1. Graphic log of lithologic variations and units at Site 770.

sparse, thin marl layers that were probably deposited as turbidites. Volcanic activity is expressed by very thin and thin ash layers that are altered in the lower part of the unit.

Comparison of Sites 767 and 770

The lowest part of the succession at both sites consists of around 100 m of brown pelagic clay, but at Site 770 the clay contains carbonate (mainly nannofossils), indicating that this location was shallower than the CCD. In Figure 3, the paleodepths of Sites 767 and 770 have been calculated by means of the backtracking method of Sclater et al. (1985). This method assumes that basin subsidence was controlled entirely by thermal contraction similar to that of normal oceanic crust and isostatic loading by sediment. The curves were generated from the following data: the age of the sediment just above the basement, the sediment thickness, and the average sediment bulk density at both sites. The isostatic effect of the thickness of sediment has been taken into account in the position of the present depth of basement below sea level. The present-day offset from the theoretical curve of Sclater et al. (1985) for Site 767 is 637 m

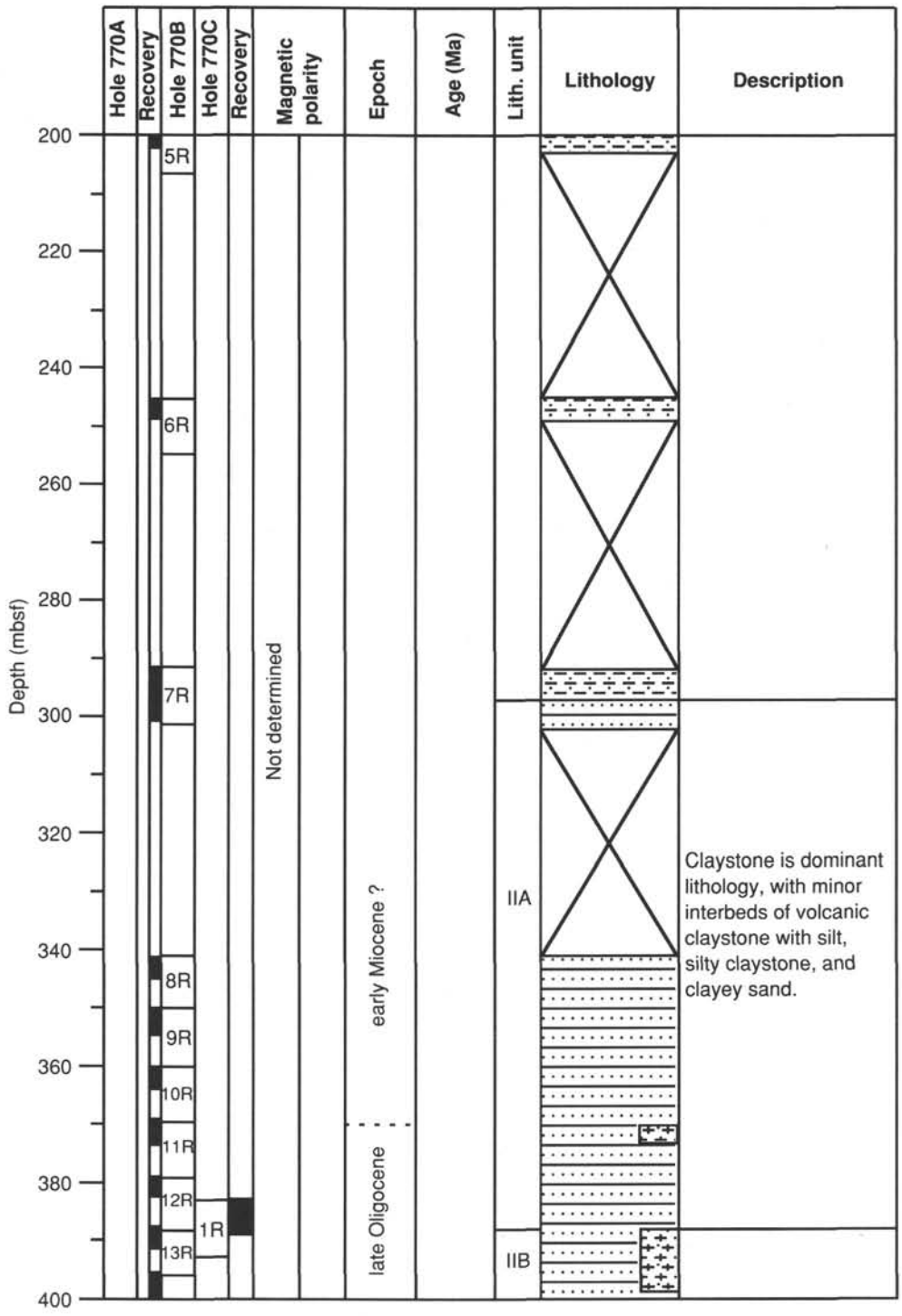

Figure 1 (continued).

and 55 m for Site 770. These curves predict that in the Eocene Site 770 was around 580 m shallower than Site 767. The sediment above the basement at Site 767 is free of carbonate, indicating sedimentation below the CCD; the lowest sediments at Site 770 contain more than 10% carbonate (mainly nannofossils), indicating sedimentation around or above the CCD. This indicates that the CCD was around 2800 mbsl in the late middle Eocene.

The middle to late Miocene interval of the sedimentary succession at Site 767 is characterized by a thick sequence of terrigenous siliciclastic turbiditic deposits. Siliciclastic turbidites were not recovered at Site 770. Similarly, calcareous turbidites are abundant in the upper Miocene to Pliocene section at Site 767, but redeposited carbonates are rare at Site 770. The overall succession at Site 770 is thinner, and it is likely that siliciclastic and carbonate turbidites were not deposited because of the elevation of the site relative to the surrounding basin. Ashes are less evident in the succession at Site 770 than at Site 767, but the greenish gray hemipelagic silty clay containing volcanic detritus is similar at the two sites.

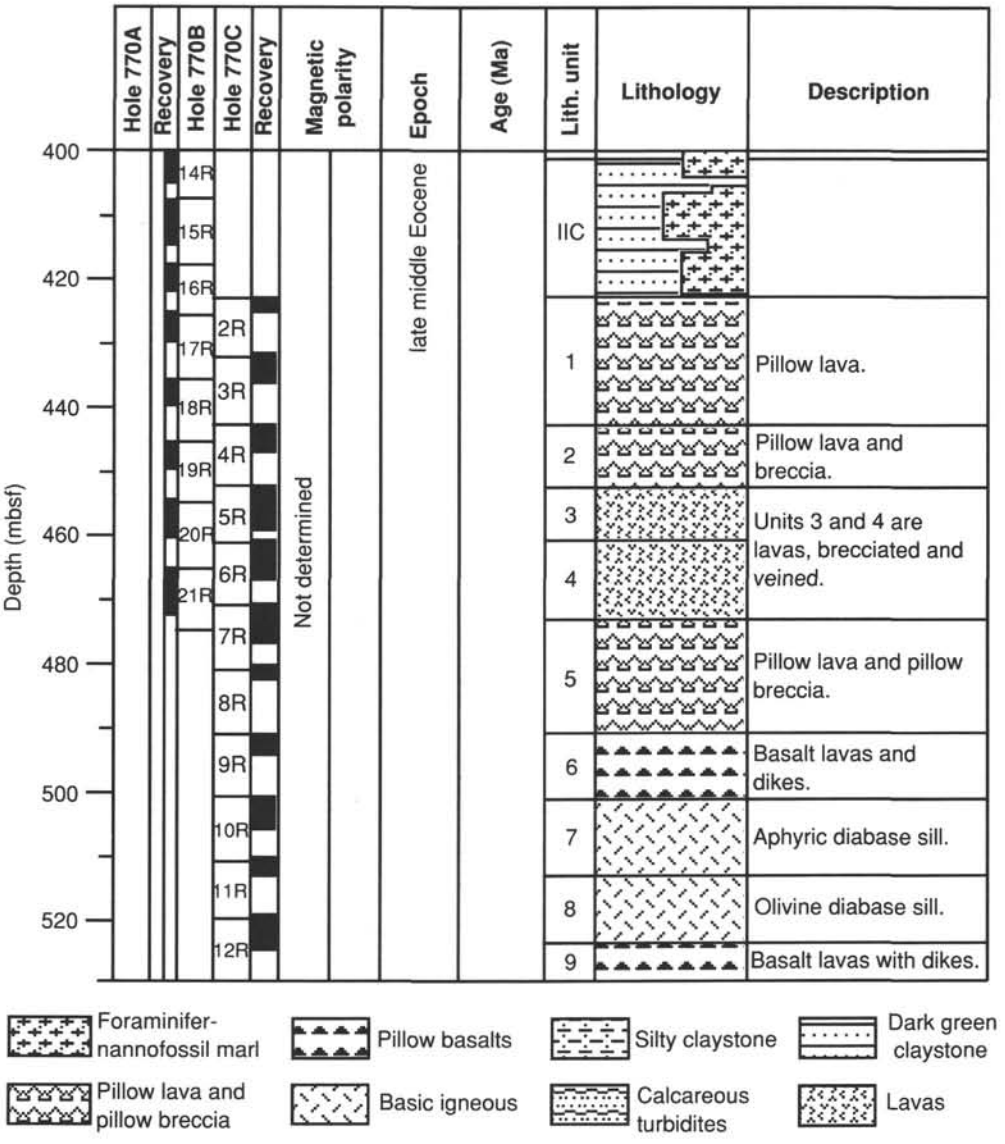

Figure 1 (continued).

BIOSTRATIGRAPHY

Summary

The sedimentary sequence of 425 m thickness overlying basalt at Site 770 ranges in age from Holocene to late middle Eocene. From Holocene to early Miocene time, the site was located below the CCD. The sediments are barren of calcareous micro- and nannofossils. Rare nannofossils and foraminifers were found in Core 124-770B-4R only, within the upper lower Pliocene.

Radiolarians and diatoms are common in the surface sediments and the Holocene, but downsection only fragments were found in the Quaternary. Rich and well-preserved radiolarian assemblages are present within Core 124-770B-6R, which also contains common volcanic ash. The radiolarians give a late Miocene age (*Didymocyrtis penultima* Zone). Radiolarians give an early Miocene age for Core 124-770B-10R. Nannofossils and radiolarians are present in Core 124-770B-11R, indicating a late Oligocene age (probably NP25).

The sediments in Cores 124-770B-13R through -16R and in Core 124-770C-1R consist of reddish nannofossil marls and clays. The calcareous fossils indicate deposition close to the CCD. Changes in preservation within these cores reflect fluctuations of the location of the CCD.

The interval represented by Zone NP23 in Hole 770B is very short (Sections 124-770B-13R-3 to 124-770B-13R-CC), which might mean that there is an unconformity coeval with the strong sea-level drop at 30 Ma (Haq et al., 1987).

The lower Oligocene (NP21 and NP22) is present in Core 124-770B-14R. A distinct lithologic change in Section 3 from marl to clay might correspond to the lowermost Oligocene. That time is characterized by an important cooling and increase in deep cold water circulation, related to the glaciation in the Southern Hemisphere.

The upper Eocene is probably present in Sections 124-770B-15R-1 to 124-770B-15R-3. However, no subdivision is possible because of the absence of zonal markers, as a result of distinct selective dissolution. In Section 124-770B-15R-2, only benthic foraminifers are present, indicating increased dissolution. This increase corresponds with the general CCD curve, which shows a rise during the middle and late Eocene. Radiolarians are very poorly preserved in Cores 124-770B-13R down to basement, but

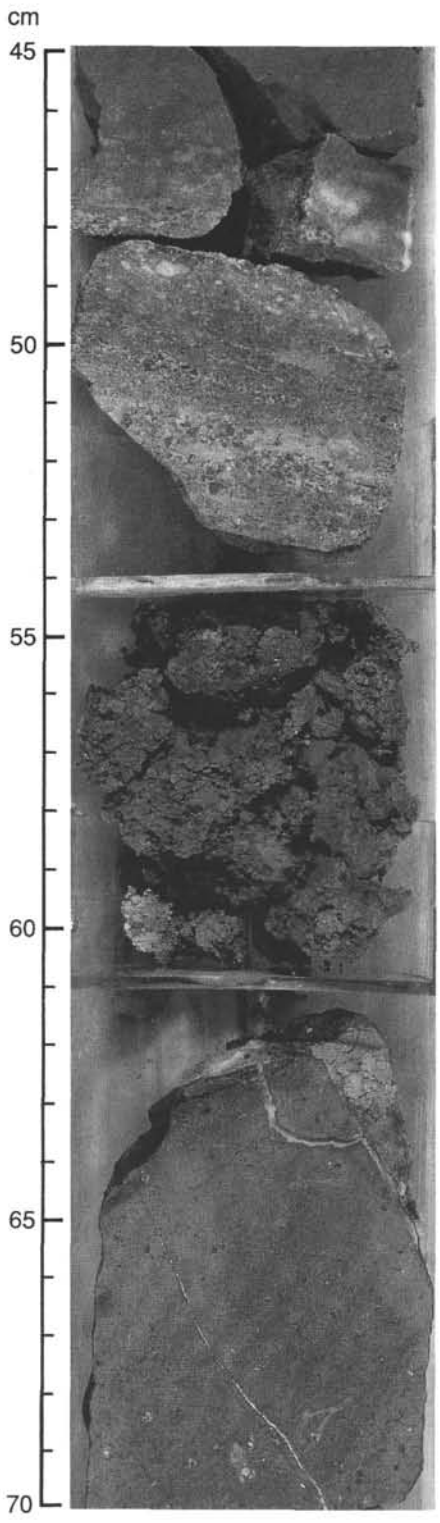

Figure 2. Contact between basaltic basement (below 61 cm) and sandy clay containing altered glass (above 54 cm) in Section 124-770B-16R-3, 45–70 cm. The interval between is filled by drilling breccia.

a diverse, moderately well-preserved assemblage of late middle Eocene age was recovered in Sample 124-770B-16R-3, 42–43 cm, immediately overlying hyaloclastite.

The sediments above the basalt are dated by nannoplankton, foraminifers, and radiolarians as upper middle Eocene (NP17, P13–P14, *P. chalara* Zone), which is in good agreement with the results obtained from radiolarians at Site 767.

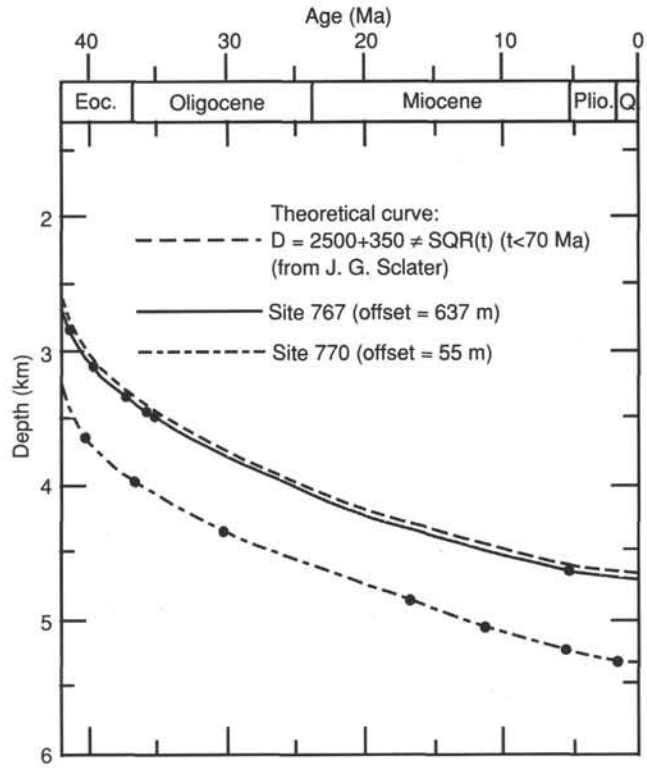

Figure 3. Backtracking curves of paleodepth at Sites 767 and 770 (see text for discussion).

Nannofossils

The age of the sedimentary sequence recovered in Hole 770B ranges from Pleistocene to late middle Eocene. The Quaternary to lower Miocene sediments were deposited below the CCD. The sediments are barren of calcareous nannoplankton. Only in Core 124-770B-4R are a few nannoplankton present, indicating a late early Pliocene age (Zone NN15) with the following species: *Discoaster asymmetricus, Discoaster brouweri, Discoaster pentaradiatus, Discoaster surculus, Sphenolithus abies, Pseudoemiliania lacunosa, Ceratolithus rugosus,* and small *Reticulofenestra pseudoumbilica.*

In Core 124-770B-6R a latest Miocene age was determined by radiolarians. This upper part of the sequence consists of gray silt and clay rich in volcanic ash. Brown clay and marls were encountered from Core 124-770B-7R downhole containing altered volcanic ash and varying amounts of carbonate. Since Oligocene time, the site has been located close to the CCD, which shows evidence of fluctuations throughout middle Eocene to Oligocene time.

In Section 124-770B-11R-1 nannofossils are common (369 mbsf). They are strongly fragmented and etched. The assemblage gives a late to late middle Oligocene age (NP25–NP24) with *Cyclicargolithus abisectus* and very rare specimens of *Sphenolithus ciperoensis* and *Sphenolithus predistentus. Dictyococcites dictyodus,* as it is known from the Philippine region and other parts of the Pacific Ocean, is absent from the upper Oligocene.

Core 124-770B-12R is barren of nannoplankton. Zone NP24–NP25 (upper to middle Oligocene) was determined down to Section 124-770B-13R-1. Rare to few specimens of *Dictyococcites dictyodus* are present. The preservation of the nannofossils is poor to moderate.

In Section 124-770B-13R-1 to the core-catcher sample, the middle Oligocene Zone NP23 was determined (389.3–398.0 mbsf). The sediments are rich in nannofossils. *Sphenolithus predistentus* together with *Sphenolithus distentus* became abundant, but *Dictyococcites dictyodus* is few to common. There are also rare reworked Eocene to lower Oligocene species.

Core 124-770B-14R belongs to the lower Oligocene (398.0–407.6 mbsf). Zone NP22 is present in Sections 124-770B-14R-1 and 124-770B-14R-2, as indicated by the presence of *Reticulofenestra umbilica*. The boundary between Zones NP22 and NP21 lies in Interval 124-770B-14R-2, 30–70 cm. The latter zone (NP21) was recovered from Samples 124-770B-14R-2, 70 cm, to 124-770B-14R-3, 16 cm. The moderately preserved nannofossils are abundant with *Helicosphaera reticulata, Ericsonia subdisticha, Cyclococcolithus formosus,* and *Reticulofenestra umbilica*. The lower part of Core 124-770B-14R is barren of nannoplankton because of its deposition below the CCD (distinct lithologic change from marl to clay). This interval might belong to the lowermost Oligocene, an interval characterized by very strong cooling and by an increase in the cold deep-water circulation related to Southern Hemisphere glaciation.

Sections 124-770B-15R-1 and 124-770B-15R-2 probably belong to the upper Eocene (NP18–NP20). No subdivision is possible because the zonal markers normally used are missing within the tropical region (Martini, 1971). The assignment of these sediments to the upper Eocene is made on the basis of the absence of *Sphenolithus obtusus* and *Chiasmolithus grandis*. According to certain authors, *Chiasmolithus grandis* has its last occurrence at the top of the middle Eocene. The last specimen of this species was observed in Sample 124-770B-15R-3, 146–147 cm. Discoasters are abundant, but very often they show dissolution of the central part, which indicates strong etching.

Sections 124-770B-15R-4 to 124-770B-16R-1 (412.0–419.0 mbsf) were assigned to Zone NP17 of the upper middle Eocene by the abundance of *Sphenolithus obtusus, Discoaster saipanensis, Discoaster barbadiensis, Reticulofenestra umbilica, Cyclococcolithus formosus,* and *Chiasmolithus grandis*. The nannofossils are common and are poorly to moderately preserved. The sediments just above the basalt at the base of Core 124-770B-16R are barren of nannoplankton.

Foraminifers

The upper part of the sedimentary sequence at Site 770 is mostly barren of calcareous foraminifers (0–389 mbsf). The sediments consist of clays that are interpreted to have been deposited below the CCD. Most washed residues contain volcanic clasts, accompanied by rare agglutinated foraminifers and fish remains. Carbonate-rich turbidites, which yielded planktonic foraminifers at nearby Site 767, are absent in Site 770 spot cores (0–340 mbsf) or are recrystallized.

Planktonic foraminifers were present in one core from the upper part of the sequence (Core 124-770B-4R) at 147.6–157.3 mbsf. The core-catcher sample contained a lower Pliocene fauna (N19/N20) that shows signs of strong carbonate dissolution. *Globorotalia tumida* is the most abundant species in this sample, accompanied by rare *Sphaeroidinella dehiscens* and *Globoquadrina altispira* and others.

Red clays and reddish marls are present from 296 to 421 mbsf (Cores 124-770B-7R through -16R) and overlay basement in Section 124-770B-16R-3. The upper part of this interval (Cores 124-770B-7R through -12R) contained red clays only, with rare agglutinated foraminifers. In the deeper cores (Core 124-770B-13R through -16R), as well as the single sediment core from Hole 770C, reddish nannofossil marls are found. These marls yield foraminiferal faunas that indicate deposition close to the CCD. All samples contain abundant calcareous benthic foraminifers and show signs of severe dissolution.

The planktonic faunas consist of dissolution-resistant forms only. The co-occurrence of *Catapsydrax dissimilis* with *Globorotalia opima nana* in Cores 124-770B-13R and -14R and in Core 124-770C-1R indicates an Oligocene or late Eocene age. Age-diagnostic forms are absent. The presence of *Globigerina senni,* accompanied by *G. opima nana* in Samples 124-770B-15R-4, 100–103 cm, and 124-770B-15R-CC give a late middle Eocene age (upper part of P14). Sample 124-770B-15R-2, 96–99 cm, contained benthic foraminifers only. Basement was encountered in Section 124-770B-16R-3. Sample 124-770B-16R-1, 127–129 cm, contained *C. dissimilis* together with *G. senni,* giving a P14 or P13 age (late middle Eocene).

Diatoms

Late Quaternary diatoms of the *Pseudoeunotia doliolus* Zone are present in Cores 124-770A-1R and 124-770B-1R. Rare diatoms were noted in >44-μm size fractions of radiolarian preparations of upper Miocene sediment in Core 124-770B-6R, but no biostratigraphically significant diatoms were found in sieved or unsieved preparations. Rare diatom fragments were encountered in radiolarian preparations from Cores 124-770B-10R and -11R, but unsieved preparations for diatom studies have not been made.

Radiolarians

Radiolarians and diatoms in Cores 124-770A-1R and 124-770B-1R display the same pattern of abundance and dissolution in upper Pleistocene–Holocene sediments as recognized at all other Leg 124 sites. Abundant, diverse, and well-preserved assemblages found at the surface abruptly degrade to fragments within the upper few meters of sediment. Spot-cored intervals from Section 124-770B-2R-CC (60.8 mbsf) through 124-770B-5R-CC (205.5 mbsf) are barren of siliceous microfossils.

Siliceous microfossils reappear in Core 124-770B-6R (244.1–253.7 mbsf). A well-preserved upper Miocene radiolarian assemblage is found throughout this core. Species present include *Didymocyrtis penultima,* a late form of *Stichocorys delmontensis* and an early form of *Stichocorys peregrina, Pterocanium charybdeum trilobum,* and *Phormostichoartus corbula.* These radiolarians indicate the *D. penultima* Zone.

The interval from Section 124-770B-7R-1 (292.4 mbsf) through 124-770B-9R-CC (359.3 mbsf) is barren of radiolarians. A well-preserved assemblage is found in Sections 124-770B-10R-1 (359.3 mbsf) through 124-770B-12R-CC (388.2 mbsf). This assemblage is very unusual. Members of the genus *Dorcadospyris* constitute up to 80% of the fauna. Samples from Cores 124-770B-10R and -11R contain *D. ateuchus* and the *simplex* form of *D. forcipata,* with rare *D. circulus* and others in the lineage. Sample 124-770B-10R-3, 125–130 cm, contains rare *Calocycletta virginis* and very rare *Stichocorys delmontensis,* indicating the *S. delmontensis* Zone of the lower Miocene. This sample also contains very abundant *Zygocircus* sp.

Specific dating of the interval down to Section 124-770B-12R-CC is difficult because of the very low diversity of the assemblage and abundance of transitional forms in the *Dorcadospyris* lineage. Detailed biometric work may be necessary to determine the *D. ateuchus–Tristylospyris triceros* transition, which defines the base of the *D. ateuchus* Zone of the upper Oligocene.

Perhaps most surprising of all is the difference between the lower Miocene through upper Oligocene radiolarian assemblage at Site 770 as compared with Site 767. Preservation is excellent in this interval at Site 770, with fine spines and other features fully represented, whereas radiolarian preservation at Site 767 is moderate to poor. Despite the poor preservation at Site 767, the assemblage is diverse. At Site 770, with good preservation, the assemblage is of very low diversity. These sites are only about 30

km from each other, with a 400-m depth difference at the present time (Site 767: 4905 mbsl; Site 770: 4505 mbsl).

The depth variance between the two sites was greater in the Paleogene, considering the thickness of Neogene turbidites at Site 767 and the thin hemipelagic Neogene sequence at Site 770. During deposition of the upper Paleogene–lower Neogene, this difference in depth may have been significant for distribution of radiolarian populations. However, such assemblage differences are not apparent elsewhere (e.g., Philippine Basin, Deep Sea Drilling Program Leg 31; Ling, 1973). It is also possible that the topographic rise led to very localized variation in circulation and upwelling, which influenced the radiolarian assemblage at Site 770.

An abrupt lithologic change occurs between the core catcher of Core 124-770B-12R and the top of Core 124-770B-13R (388.2 mbsf). The exact location and nature of the contact is unknown because of the incomplete recovery in this interval. Carbonate is present in Core 124-770B-13R to near basement in Section 124-770B-16R-3. Remains of radiolarians are present in this interval and range from rare to abundant, but preservation is generally very poor, in marked contrast to the good preservation in the overlying cores. An abundant but poorly preserved radiolarian assemblage of the *Theocyrtis tuberosa* Zone is found in Section 124-770B-13R-CC, as indicated by the presence of *T. triceros, T. tuberosa, Lithocyclia crux*(?), and *Artophormis gracilis*.

An attempt was made to recover the contact between the calcareous sediments of Core 124-770B-13R (and below) and the carbonate-free Core 124-770B-12R (and above) by spot coring that interval. Core 124-770C-1R apparently missed the contact, recovering a section roughly coeval with Core 124-770B-13R. Well-preserved radiolarians were found in one sample from this core, near the top. Sample 124-770C-1R-1, 39–41 cm, contains an assemblage consisting of abundant *T. triceros* and *D. ateuchus,* plus other species in that lineage. *Theocyrtis tuberosa* is very rare, but specimens found are highly tuberculate, as is typical of this species late in its range (Sanfilippo et al., 1985).

Also present in this core is an unidentified *Pterocanium* (*Lychnocanoma*) species (similar to an unidentified form shown in Sanfilippo et al., 1985, fig. 19-6). This assemblage is either from the upper part of the *T. tuberosa* Zone or from the lower part of the *D. ateuchus* Zone, in the mid-Oligocene, probably slightly younger than the top of Core 124-770B-13R. Several well-preserved, reworked, late Eocene radiolarians were found in this sample as well.

Radiolarians are very poorly preserved, or are absent altogether, in most of the interval from 388.2 mbsf to basement in Core 124-770B-16R-3, with one notable exception. Sediments immediately overlying hyaloclastites (Sample 124-770B-16R-3, 42 cm), 22 cm above basalt, contain an abundant and moderately preserved radiolarian assemblage. One centimeter above this level, radiolarian preservation is too poor for identification. This thin layer contains a diverse assemblage with all the forms identified as overlying basement at Site 767, but the better preservation allowed on-board identification of more than 15 taxa of the upper middle Eocene. These include common *Lithocyclia ocellus* and *Thyrsocyrtis rhizodon,* with *Sethochytris triconiscus* and its ancestor *S. babylonis, Eusyringium fistuligerum, Podocyrtis trachoides, Podocyrtis chalara, Thyrsocyrtis tricantha,* and rare *Theocotylissa ficus* and *Tristylospyris triceros*. The co-occurrence of *T. triceros, P. chalara,* and *P. trachoides* constrain the age to the lower part of the *Podocyrtis chalara* Zone, approximately 42.0–42.2 Ma (Berggren et al., 1985a, 1985b).

The lower Oligocene and upper Eocene of Site 770 contains few identifiable radiolarians. This corresponds well with a barren interval at Site 767, above and below which are found diverse upper Oligocene and upper middle Eocene assemblages, respectively. The carbonate-rich interval at Site 770 is 32 m thick, and the barren interval spanning most of the lower Oligocene to upper middle Eocene is about 20 m thick, which compares favorably with the addition of carbonate at Site 770. The occurrence of well-preserved, late Eocene radiolarians in Oligocene sediments of Site 770, but no *in-situ* late Eocene forms, implies a possible hiatus in the upper Eocene to lower Oligocene.

Ichthyoliths

At Site 770, ichthyoliths are found throughout the section, but they are always present in very low numbers and their preservation is poor. Core-catcher samples yielded only a few unbroken specimens and no age-diagnostic forms. No attempt at further analysis was made.

PALEOMAGNETICS

Following the drilling strategy of spot coring in sediment and continuous coring in basement, the purpose of paleomagnetic measurement at Site 770 was restricted to examining changes in inclination. Measurements were made primarily on discrete samples. We took 5–12 standard cube samples from each sediment core and 1 minicore sample from each basement core following Ocean Drilling Program (ODP) procedures. All the measurements were performed with a 2G-Enterprise pass-through rock magnetometer. All samples were progressively demagnetized at 2, 5, 10, 15, and 20 mT. Archive halves with continuous sections longer than 30 cm were also submitted to measurement and demagnetization.

Figure 4 shows the magnetic directions and intensities of cores from Holes 770B and 770C, with large and small dots representing discrete samples and archive halves, respectively, from sediment cores. For measurements made on archive halves of basement cores, one representative point was selected for each basalt piece and plotted similar to discrete samples. Inclinations remained low throughout most of the sedimentary column down to Core 124-770B-14R. The next two cores had scattered inclinations, and inclinations abruptly increased at the top of the basement rocks.

There are two intervals with scattered inclinations: one is in the sediment just above the basement, and the other is in the middle section of the basement. The demagnetization diagrams (Fig. 5) of the sample from the sediment interval indicate that demagnetization levels were insufficient as a result of the high coercivity. Red sediments often required thermal demagnetization treatment as well, which was the case here. In Hole 770C, the middle section of the basement included brecciated lava that caused scattered inclinations.

Excluding these scattered intervals, the mean of the absolute value of inclination and the α_{95} are 6.7° and 1.4° for sediments and 39.2° and 4.2° for basalts, respectively. These mean inclinations yield a magnetic paleolatitude difference of 18.8° or 25.6°, assuming the same or opposite signs of latitude, respectively. The duration of the gap caused by the scattered inclination at the bottom of the sediments was thoroughly determined by nannofossil biostratigraphy.

Cores 124-770B-14R (407 mbsf) and -16R (419 mbsf) were dated as NP21 and NP17, which have age assignments of 34.9–36.7 Ma and 39.8–42.3 Ma, respectively, according to Berggren et al. (1985a, 1985b). These values yield plate motions of at least 30 cm/yr. Although one cannot say that amount is completely impossible, the tilting of basement lava flows seems to explain the inclination difference better. Intensive shore-based demagnetization studies on samples from Cores 124-770B-15R and -16R will clarify this point.

Magnetic susceptibility data collected at Hole 770B are shown in Figure 6. The drilling strategy of spot coring made the

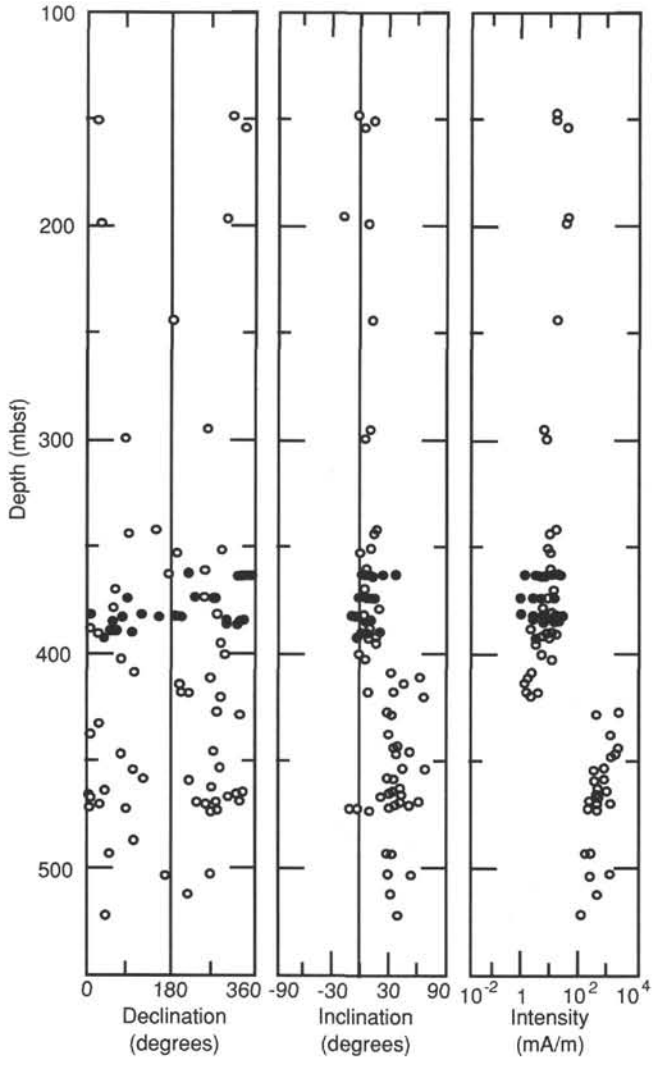

Figure 4. Magnetostratigraphic plot of declination, inclination, and intensity for Holes 770B and 770C. Solid circles are for pass-through magnetometer measurements of sediment core section. Discrete sample and archive half-piece measurements in basalts are represented by open circles.

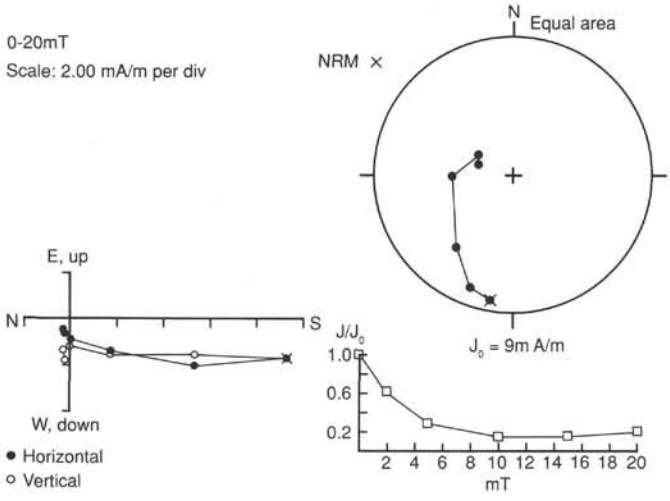

Figure 5. Zijderveld vector diagram for Sample 124-770B-16R-3, 8-10 cm.

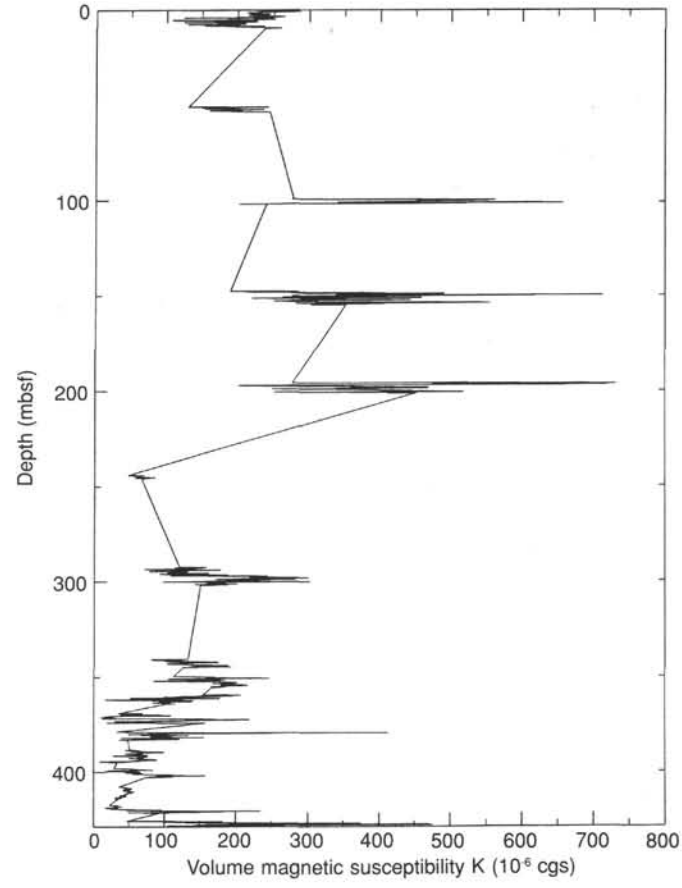

Figure 6. Magnetic susceptibility data, Hole 770B.

unit classification difficult at this site. However, we can generally see that magnetic susceptibility starts with values around 200 × 10^{-6} cgs, increases at about 100 mbsf to 300–700 × 10^{-6}, and begins to decrease from about 200 mbsf at the bottom of the sedimentary column to about 20 × 10^{-6} cgs.

SEDIMENT ACCUMULATION RATES

Sediment accumulation rates were determined at Site 770 by means of biostratigraphic data. The upper seven cores at this site were spot cores taken approximately every 50 m, and all cores were rotary drilled. Magnetostratigraphic studies were not undertaken at this site because of the discontinuous coring operation and the disturbed nature of the cores.

The time scale of Berggren et al. (1985a, 1985b) was used for the assignment of ages to biostratigraphic zones. Calcareous nannoplankton zones are described in Martini (1971), and radiolarian zones are defined by Riedel and Sanfilippo (1978). Sedimentation rates calculated from biostratigraphic markers are shown in Figure 7. Ages and intervals in which respective biozones are identified are found in Table 3.

Few confident biozones and no zonal boundaries were identified in the top 350 m at Site 770 because of the poor preservation of fossil assemblages and the discontinuous nature of drilling. The poor preservation of calcareous fossils indicates that this site has been below the CCD since the lower Miocene. Nannofossil Zone NN15 and foraminifer Zone N19 were located in Core 124-770B-4R. Radiolarian Zone *Didymocyrtis penultima* was observed in Core 124-770B-6R (244.1–253.7 mbsf). A very poorly constrained sedimentation rate of 36 m/m.y. is indicated for the upper 254 m of Site 770.

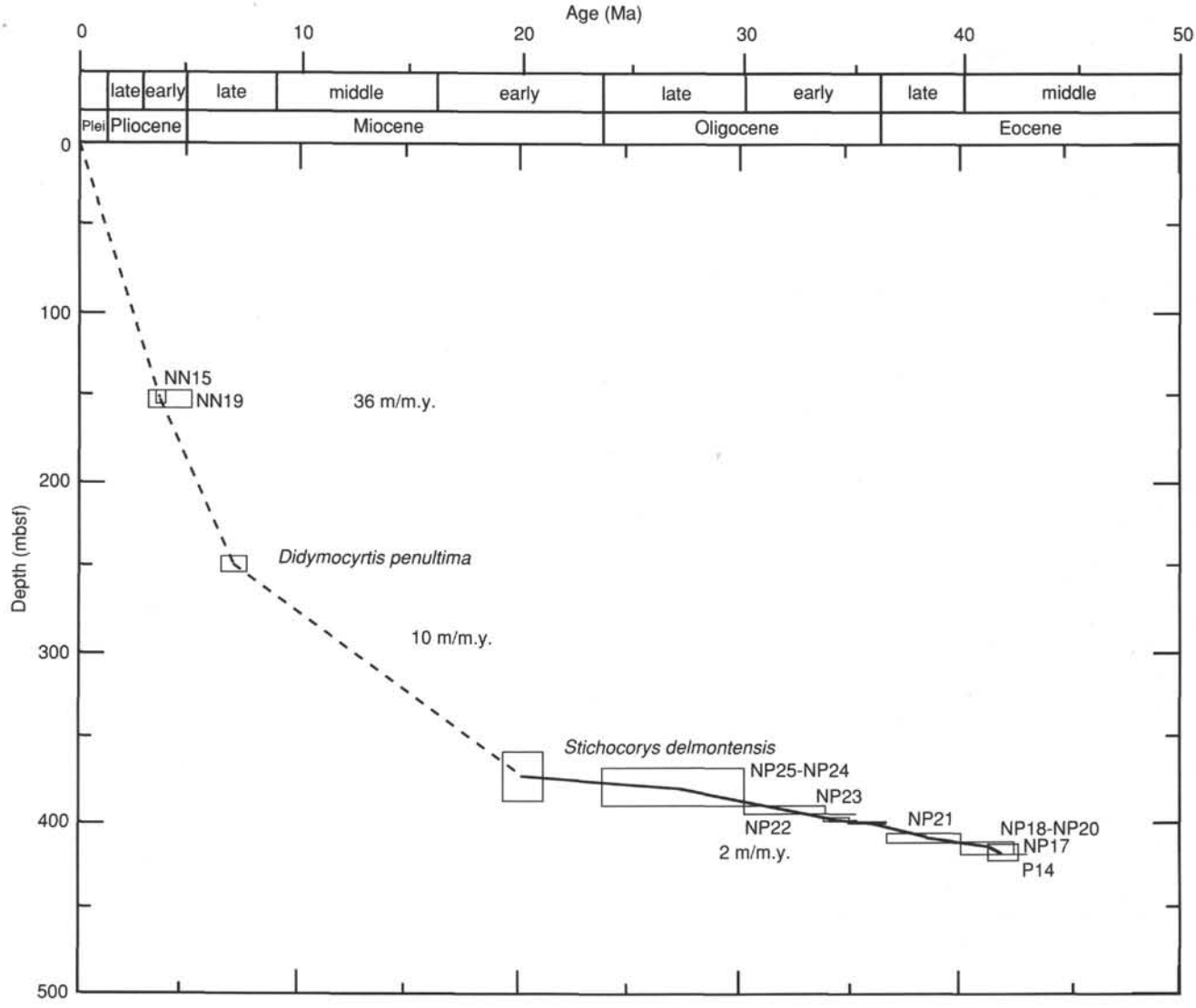

Figure 7. Sedimentation rates calculated from biostratigraphic data, Site 770.

Table 3. Ages and depths for individual biozones identified at Site 770.

Biozone	Age (Ma)	Depth (mbsf)
NP25–NP24	23.7–30.2	369–388
NP23	30.2–33.8	388–398
NP22	33.8–34.9	398–400
NP21	34.9–36.7	400–408
NP18–NP20	36.7–39.8	408–411
NP17	39.8–42.3	411–419
D. penultima	6.4–7.5	244.1–253.7
S. delmontensis	19.2–21.0	359.3–388.2
T. tuberosa	31.2–35.2	395.2
P. chalara	41.8–42.3	420.2
N19	3.0–5.0	147.6–157.3
P14	41.3–42.6	413.1–423.3
P14–P13	41.3–43.0	418.6

From the *D. penultima* (Core 124-770B-6R, 244.1–253.7 mbsf) to the *Stichocorys delmontensis* (Core 124-770B-10R, 359.3–368.9 mbsf) zones, there are no identifiable biozones. Connecting these two widely spaced zones results in an unreliable sedimentation rate of 10 m/m.y.

Continuous coring commenced with Core 124-770B-8R (340.6 mbsf). The preservation of calcareous micro- and nannofossils varied below this depth in response to the shifting CCD (see "Lithostratigraphy" section, this chapter). Biostratigraphic zones confine the sedimentation rates well from 360 mbsf to the bottom of the hole. Sedimentation rates remain consistently low throughout the interval with an average of 2 m/m.y. and with fluctuations around this average of no more than 2 m/m.y.

Biostratigraphic constraints are poor at Site 770 from the present to the early Miocene, but sedimentation rates at this site can generally be compared with sedimentation rates at Site 767. Site 767 received approximately 700 m of sediment since the early Miocene (22 m.y.), for an average sedimentation rate of 32 m/m.y. Over the same interval, Site 770 received approximately 380 m of sediment, for a calculated sedimentation rate of approximately 17 m/m.y., indicating that Site 770 was more isolated from sedimentary input even though the two sites are fairly close to each other.

Sedimentation rates at Sites 767 and 770 are very similar prior to the early Miocene with sedimentation rates of approximately 2–3 m/m.y.

SEDIMENT INORGANIC GEOCHEMISTRY

Carbonate analyses were performed routinely on all the cores, and the distribution of carbonate is indicative of sedimentation below the CCD except in the lower section of the hole. The dissolved constituents analyzed in the interstitial water of the sediments at Site 770 include pH, alkalinity, magnesium, calcium, sulfate, and silica. The distribution of dissolved sulfate reflects decomposition of organic matter by sulfate reduction. The Ca^{2+} and Mg^{2+} profiles indicate the alteration of volcanic material and the formation of smectite.

Calcium Carbonate

We analyzed a total of 47 sediment samples for their inorganic carbon content at Site 770, by means of the ODP standard shipboard method (see the "Explanatory Notes" section, this volume). The results are given in Table 4, and the depth distribution is shown in Figure 8. Samples from Unit I (0–296 mbsf) have very low carbonate levels, which correspond to the hemipelagic clays deposited below the CCD (see "Lithostratigraphy" section, this chapter). Below 382 mbsf, $CaCO_3$ levels increase to maximum values of 39%. This increase is evident in the sediments because of the presence of foraminifers and nannoplankton fossils. The higher carbonate content of this unit (Subunit IIB) can be used to determine paleodepth variations of the CCD for this basin (see "Lithostratigraphy" section, this chapter).

Interstitial Water Chemistry

A total of seven interstitial water (IW) samples were collected for analyses at Site 770. We took 5–10-cm, whole-round samples from selected cores, and the IW was obtained by means of the standard ODP squeezing technique (see "Explanatory Notes" chapter, this volume). The results are summarized in Table 5, and the depth distributions are shown in Figure 9.

pH

The downcore pH distribution (Fig. 9) shows similar features to those observed at previous sites. Compared with bottom-water values of around 7.6, the value of 8.3 at 153 mbsf represents a maximum, corresponding to similar features at the other sites in the Celebes and Sulu seas. The high pH values are probably the result of the alteration of volcanic material. Below 153 mbsf, pH decreases with depth, indicating a release of hydrogen ions by alteration reactions in the basement.

Sulfate and Alkalinity

The sulfate distribution observed (Fig. 9) is the result of the decomposition of organic matter by sulfate reduction. Compared with Site 767 (also in the Celebes Sea), Site 770 shows a slower sulfate usage rate. This difference is probably a result of the lower sediment accumulation rates at Site 770 relative to Site 767 (See "Sediment Accumulation Rates" section, this chapter).

Results from the alkalinity analysis are not conclusive because of the lack of data in the uppermost sections of the core.

Calcium and Magnesium

Dissolved calcium and magnesium distributions at Site 770 are shown in Figure 9. The increase observed in Ca^{2+} concurrent with the decrease observed in Mg^{2+} are characteristic of the alteration of volcanic material. This observation is consistent with the pH distribution, as well as with observations made at Sites 767, 768, and 769.

Table 4. Results of calcium carbonate analysis, Site 770.

Core, section, interval (cm)	Depth (mbsf)	$CaCO_3$ (%)
124-770A-		
1R-1, 20–22	0.20	0.1
124-770B-		
1R-1, 64–66	0.64	0.2
1R-1, 108–110	1.08	0.2
1R-2, 89–91	2.39	0.2
1R-3, 30–32	3.30	0.2
1R-7, 18–20	9.18	0.2
2R-1, 50–52	51.30	0.2
2R-1, 100–102	51.80	0.2
2R-2, 50–52	52.80	0.2
2R-2, 100–102	53.30	0.2
3R-1, 56–58	99.96	0.2
3R-2, 56–58	101.46	0.8
4R-1, 60–62	148.20	0.6
4R-2, 60–62	149.70	0.3
4R-3, 60–62	151.20	0.5
4R-4, 60–62	152.70	0.3
4R-5, 60–62	154.20	0.2
5R-1, 75–77	196.55	0.2
5R-2, 74–76	198.04	0.2
5R-4, 88–90	201.18	0.3
6R-1, 8–10	244.18	0.2
6R-2, 35–36	245.95	0.2
7R-1, 33–35	292.73	0.2
7R-3, 42–44	295.82	0.2
7R-4, 68–70	297.58	0.2
7R-6, 106–108	300.96	0.2
8R-1, 29–31	340.89	0.4
8R-2, 29–31	342.39	0.2
8R-3, 101–103	344.61	0.2
9R-1, 146–148	351.06	0.2
9R-2, 61–63	351.71	0.4
9R-4, 42–44	354.52	0.2
10R-1, 111–113	360.41	0.1
10R-2, 26–28	361.06	0.2
10R-3, 51–53	362.81	0.1
11R-1, 80–82	369.70	5.4
11R-2, 53–55	370.93	0.3
11R-3, 89–91	372.79	0.2
12R-1, 52–54	379.12	0.7
12R-2, 103–105	381.13	0.3
12R-3, 103–105	382.63	35.7
13R-1, 63–65	388.83	25.7
13R-2, 138–140	391.08	38.3
13R-3, 88–90	392.08	20.0
13R-4, 88–90	393.58	38.6
13R-5, 69–71	394.89	0.3
14R-1, 124–126	399.14	33.2
14R-2, 122–124	400.62	31.8
14R-3, 141–143	402.31	0.3
15R-1, 39–41	407.99	18.2
15R-2, 121–123	410.31	21.3
15R-4, 111–113	413.21	25.3
16R-1, 26–28	417.56	14.4

ORGANIC GEOCHEMISTRY

The scientific purposes of Leg 124 shipboard organic geochemistry studies were previously outlined in Site 767 (see "Organic Geochemistry" section, "Site 767" chapter, this volume). The following summarizes the preliminary shipboard results of Site 770 (Celebes Sea).

Samples

We collected 19 sediment samples from Site 770: 1 sample from Hole 770A and 18 from Hole 770B. We then analyzed 15 of these sediments for the composition of light hydrocarbons by means of headspace gas analyses. The total organic carbon

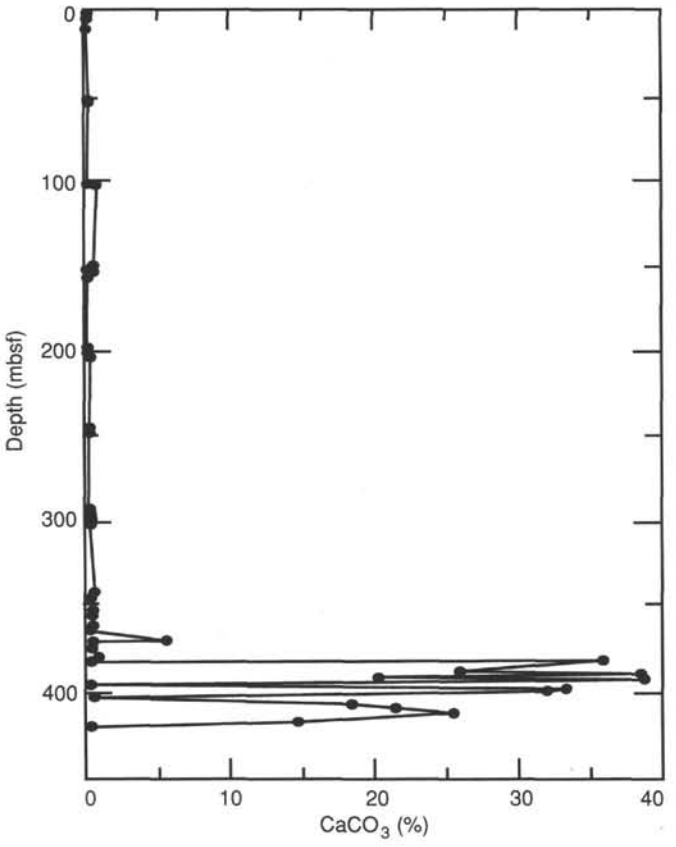

Figure 8. Downcore distribution of calcium carbonate, Site 770.

(TOC) content was determined by Rock-Eval pyrolysis on all samples. The details of the analytical methods used are given in the "Explanatory Notes" chapter (this volume).

Results and Discussion

Amount, Type, and Maturity of Organic Matter

The TOC values are below 0.5% and generally decrease downward (Table 6 and Fig. 10). From 0 to 300 mbsf (Cores 124-770B-1R to -7R), values range from 0.06% to 0.45%. This interval consists of green clayey sediments that correspond to the upper part of Site 767, where similar TOC values were observed. Below 300 mbsf, TOC values range from 0% to 0.25%. A decrease in TOC is observed with increasing depth. This interval corresponds to brown clayey sediments (Cores 124-770B-8R to -16R), which possibly correspond to the lower part of Site 767 (from Core 124-767B-62X to basement).

Because of the low concentrations of organic matter, no reliable maturity data (T_{max}) or information on the type of organic matter were obtained from the Rock-Eval analyses. Answers concerning these open questions will be provided by further shore-based investigations (vitrinite reflectance or liptinite fluorescence analyses). However, the low gas concentrations (see below) indicate a low thermogenic maturity of the organic matter.

Hydrocarbon Gases

Background concentrations of methane were observed in all headspace gas samples (Table 6), indicating that no biogenic or thermogenic gas production occurs in the sediments of Site 770.

Conclusions

The sediments contained only low amounts of organic matter, and a decrease in TOC was observed with increasing depth. No gas generation was observed in the sediments at Site 770.

PHYSICAL PROPERTIES

Introduction

The physical properties determined from the materials recovered at Site 770 include index properties (i.e., bulk density, grain density, porosity, water content, and void ratio), as determined from measurements by pycnometer and balance; compressional wave velocity measured on discrete samples with the Hamilton Frame apparatus; and thermal conductivity. The testing procedures are described in the "Explanatory Notes" chapter (this volume).

The lithologic units used in this section are those described in the "Lithostratigraphy" section (this chapter). Only spot coring was performed in the sediment column of Site 770. Because of the limited amount of data, interpretations of physical property variations and depths of property boundaries are only approximate. Velocities and index properties were measured on all of the cores taken at Site 770. Thermal conductivity measurements were made on a representative number of sediment and rock samples. The values of the various physical properties measured are listed in Tables 7–9, and the variations of these properties with depth are illustrated in Figures 11–13.

Results

Index Properties

Bulk density, grain (or matrix) density, porosity, water content (dry basis), and void ratio of the samples from Site 770 are listed in Table 7 and plotted vs. depth in Figure 11.

Figure 11 shows a pattern of smoothly increasing density with depth through Units I and II (0–421 mbsf). The bulk density in Unit I ranges from 1.4 to 1.6 g/cm^3 at the seafloor and increases to 1.8 g/cm^3 at the base of the unit (296 mbsf). The bulk density in Unit II shows more variability with depth and

Table 5. Interstitial water analyses, Site 770.

Core, section, interval (cm)	Depth (mbsf)	Vol. (cm^3)	pH	Alk. (mM)	Sal. (g/kg)	Mg^{2+} (mM)	Ca^{2+} (mM)	SO_4^{2-} (mM)	SiO^2 (μM)	Mg^{2+}/Ca^{2+}
124-770B-										
3R-2, 145–150	102.35	5			35.3	42.22	17.45	25.09	673	2.42
4R-4, 140–150	153.50	35	8.30	1.867	35.0	28.54	27.21	22.26	174	1.05
6R-1, 140–150	245.50	37	7.52	1.684	34.9	17.68	36.89	19.48	858	0.48
7R-5, 140–150	299.80	7			33.3	21.08	37.79	18.09	199	0.56
8R-2, 140–150	343.50	9			33.8	20.28	41.27	19.82	326	0.49
11R-1, 140–150	370.30	20	7.27	3.359	34.0	18.75	42.57	17.74	864	0.44
14R-2, 140–150	400.80	20	7.25	1.435	33.8	18.37	43.03	19.25	539	0.43

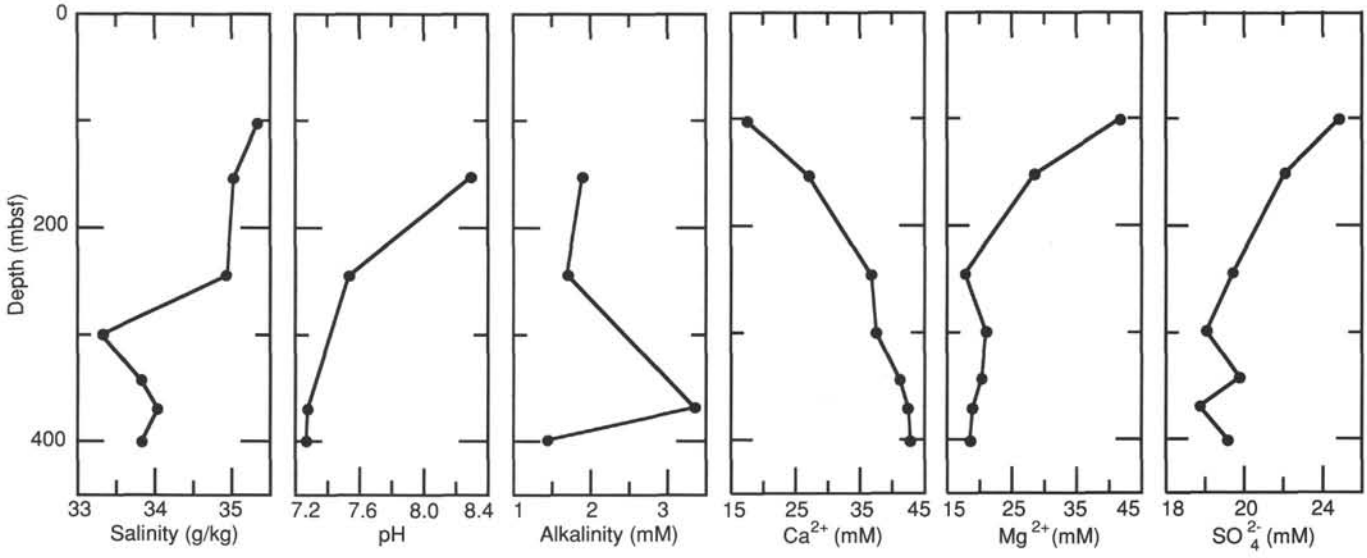

Figure 9. Summary of interstitial water analyses, Site 770, as a function of depth.

Table 6. Total organic carbon content and methane concentration of headspace gases (Carle GC) from sediments of Site 770.

Core, section, interval (cm)	Depth (mbsf)	TOC (%)	Methane (ppm)
124-770A-			
1R-1, 0–3	0	0.24	
124-770B-			
1R-5, 0–3	6.00	0.35	
2R-1, 76–79	51.56	0.34	
2R-2, 0–3	52.30	0.45	2.40
3R-1, 67–70	100.07	0.14	
3R-2, 0–3	100.90	0.08	2.20
4R-5, 0–3	153.60	0.15	2.30
5R-4, 0–3	200.30	0.06	2.30
6R-2, 0–3	245.60	0.25	2.40
7R-6, 0–3	299.90	0.20	2.50
8R-2, 0–3	342.10	0.09	2.40
9R-4, 0–3	354.10	0.08	3.05
10R-3, 0–3	362.30	0.07	3.23
11R-3, 0–3	371.90	0.13	3.14
12R-3, 0–3	381.60	0.24	3.28
13R-3, 0–3	391.20	0	2.50
14R-3, 0–3	400.90	0.01	2.28
15R-3, 0–3	410.60	0	2.17
16R-3, 0–3	420.30	0.18	2.17

increases to about 1.95 g/cm^3 at the base of the unit. The abrupt increase in bulk density below 421 mbsf coincides with the basement basalt. The bulk density of the basalt is consistently 2.70–2.90 g/cm^3. Some intervals, however, have bulk densities as low as 2.20 g/cm^3.

The grain density at Site 770 shows a slight increase with depth, but the scatter of the profile is large (Fig. 11). The grain density of the surface sediment ranges from 2.5 to 2.6 g/cm^3, and increases to nearly 2.75 g/cm^3 at the base of the sediment section. The pillow basalt and dolerite sills of the oceanic basement at Site 770 have grain densities similar to those of the overlying sediment, with most values falling between 2.65 and 2.85 g/cm^3.

The material drilled at Site 770 shows a pattern of smoothly decreasing porosity with depth in the sediment section, implying compaction caused by gravitational loading through continued deposition (Fig. 11). The porosity of the surface sediment is 70%–80% at the seafloor and decreases to approximately 50% at the base of the sediment section at 421 mbsf. The porosity of the basaltic basement is consistently $<10\%$, with the exception of two measurements of 15%–20% porosity.

The plot of water content vs. depth (Fig. 11) shows a decrease downward in the sediment column, with seafloor values of 85%–135%. Water content decreases to levels of 30%–40% at the base of the sediment section, with values of 1%–9% in the igneous oceanic crustal rocks at the base of the hole.

Figure 11 shows that the void ratio (the ratio of voids to solids) follows a nearly coincident pattern as the water content. This is as expected for sediment that is completely saturated with fluid.

Velocity

The compressional wave velocities of discrete samples from Holes 770B and 770C are presented in Table 8 and plotted in Figure 12. This figure shows no increase in velocity with depth in the sediments. The velocities fall within a narrow range near 1.55 km/s, with no apparent increase in velocity downsection until the basement interface is reached. The contact between the sediment and the basalt is reflected in an abrupt increase in velocity from 1.55 km/s in the sediments to more than 5.0 km/s in the basalt.

Thermal Conductivity

The thermal conductivities of cores from Holes 770B and 770C are given in Table 9 and are graphically presented in Figure 13. All values in the sediments were obtained with needle probes inserted through core liners into full core sections. An attempt was made to insert the probes at locations along each core section that were the least disturbed. However, an annulus of disturbed sediment and drill fluid was often present along the inside of the liner that prevented visual identification of the more intact segments in the core.

The thermal conductivity of the basaltic basement was determined by means of the half-space technique with polished 8–15-cm segments of the split core.

Thermal conductivity at Site 770 ranges from 0.8 to 1.0 W/m · K at the seafloor and increases to an average of about 1.2 W/m · K at the base of the sediments. The thermal conductiv-

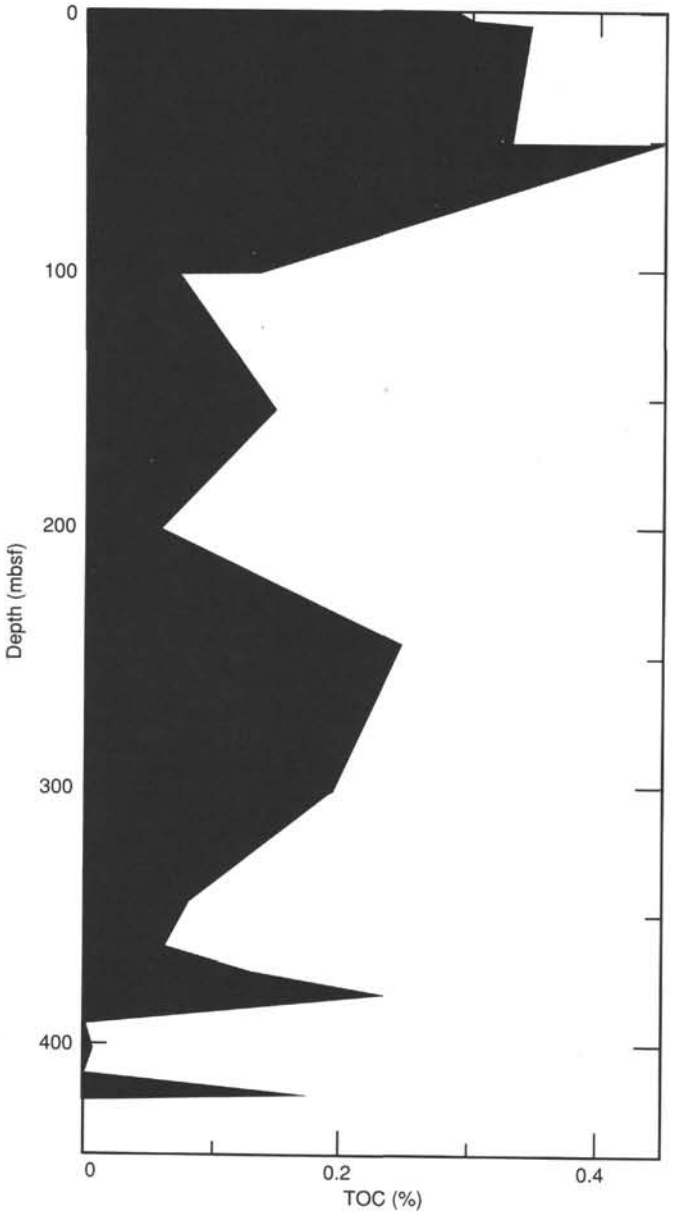

Figure 10. Total organic carbon content of sediment samples, Site 770.

ity of the basement is highly variable, with an average value of about 1.4 W/m · K.

Conclusions

In general, all of the physical properties measured at Site 770 displayed the expected depth-dependent variations. Bulk density increases with depth, almost certainly a result of compaction caused by gravitational loading. This observation is corroborated by the values obtained for porosity, water content, and void ratios, which all decrease with depth. Grain densities show a broad range of values, but they display little increase with depth.

Compressional wave velocity provides the most obvious indicator of the contacts between the sediment and basalt. The basalt has a much higher velocity than the sediments, and the interface between the two is extremely sharp. Thermal conductivity values are variable but show an increase with depth near the seafloor.

BASEMENT LITHOLOGY

Basaltic rocks were recovered at about 420 mbsf (Cores 124-770B-16R and 124-770C-2R). These mafic rocks underlie red pelagic clays that contain green hyaloclastite fragments immediately above the volcanic rocks and are of late middle Miocene age (see "Biostratigraphy" section, this chapter). The depth at which the igneous rocks are present corresponds closely to that of the acoustic basement estimated on the basis of seismic velocity values, and there were no sedimentary intercalations within the sequence. It is regarded as the basement of the Celebes Sea.

A total of nine separate units can be recognized in the igneous sequence recovered at Site 770 by means of their mineralogy, texture, and structure. Only six of these units are present in Hole 770B. Units 1 and 2 are pillow basalt sequences. Unit 3 is a pillow breccia, and Units 4 and 5 are brecciated amygdaloidal lavas. Unit 6 is composed of massive lava or lavas, which are penetrated in Hole 770C by a number of flat-lying minor intrusions. Units 7 and 8 are identified as sills, and Unit 9 is made up of thin lavas penetrated by small dikes. The boundaries, rock types, and thicknesses of these units are described below for each hole.

Hole 770B

Basaltic rocks were first recovered at 420.92 mbsf (Core 124-770B-16R), and a total of 53.18 m of igneous rocks were penetrated. The lithology, depth, and recovery data for the igneous rocks at Hole 770B are summarized in Figure 14A. Igneous rocks comprise 20% of the core recovered from Core 124-770B-16R and 100% of the rock recovered from Cores 124-770B-17R through -21R. Total recovery of igneous rock averaged 47.0% and ranged in individual cores from a low of 32.1% in Core 124-770B-18R to a high of 81.1% in Core 124-770B-21R.

We examined 16 thin sections of the igneous rocks recovered from Hole 770B under the microscope: four from Unit 1, three from Unit 2, two from Unit 3, one from Unit 4, four from Unit 5, and two from Unit 6. The lithologic units are named according to their dominant rock types. Olivine and plagioclase phenocrysts are present in all of these units as single crystals and glomeroporphyritic aggregates. The results are summarized in Table 10; more complete details can be obtained from the visual core descriptions and the thin section descriptions at the back of the book.

Unit 1

Moderately plagioclase-olivine-phyric basalt and pillow lava

Unit 1 occurs between 420.92 and 439.34 mbsf or between Sections 124-770B-16R-3 at 62 cm and 124-770B-18R-3 at 76 cm. It has a thickness of 18.42 m, of which approximately 7.0 m was recovered. There are 5 cm of laminated brown clay containing hyaloclastic fragments immediately above the basalts in Core 124-770B-16R. No individual cooling units were defined in this unit. The upper part of the unit is composed mainly of small fractured and veined pillows; in the lower part of the section, the pillows are larger, varying from 40 cm to 1 m in diameter. Remnants of thin (< 5 mm) glassy and variolitic pillow margins, some containing skeletal quenched olivine crystals, are present throughout the sequence. Interpillow material, comprising green glass fragments and lithic fragments suspended in a green clay matrix, is scarce. Vesicles are unevenly distributed, average about 1%–2% by volume, range from 0.5 to 2.00 mm, and are filled with layers of green clay, limonite, and calcite. Sparse irregular fractures ranging from 0.5 to 1.0 cm wide are filled with mixtures of green and brown clays containing glass shards, calcite, and limonite.

The rocks of Unit 1 are generally moderately plagioclase-olivine-phyric basalts, and parts of the unit are highly phyric and have more than 10% phenocrysts. The basalts contain 2%–10%

Table 7. Index property data, Site 770.

Core, section, interval (cm)	Depth (mbsf)	Wet-bulk density (%)	Grain density (%)	Porosity (%)	Water content (%)	Void ratio
124-770A-						
1R-1, 20–22	0.20	1.55	2.54	69.3	84.9	2.26
1R-1, 64–66	0.64	1.47	2.52	76.3	113.5	3.23
1R-1, 108–110	1.08	1.42	2.54	78.1	129.5	3.57
124-770B-						
1R-1, 64–66	0.64	1.48	2.58	77.1	113.6	3.36
1R-2, 89–91	2.39	1.48	2.55	77.1	114.7	3.37
1R-3, 30–32	3.30	1.46	2.56	78.6	123.6	3.68
1R-7, 18–20	9.18	1.43	2.68	79.5	133.0	3.89
2R-1, 50–52	51.30	1.34	2.67	85.5	190.4	5.88
2R-1, 100–102	51.80	1.35	2.63	84.0	176.6	5.24
2R-2, 50–52	52.80	1.36	2.67	83.6	169.7	5.11
2R-2, 100–102	53.30	1.40	2.51	80.2	141.8	4.05
3R-1, 56–58	99.96	1.45	2.73	78.5	123.8	3.65
3R-2, 56–58	101.46	1.41	2.57	79.1	135.0	3.79
4R-1, 60–62	148.20	1.54	2.54	70.5	88.3	2.39
4R-2, 60–62	149.70	1.47	2.58	75.9	112.1	3.15
4R-3, 60–62	151.20	1.49	2.61	74.9	105.8	2.99
4R-4, 60–62	152.70	1.52	2.75	76.4	105.6	3.23
4R-5, 60–62	154.20	1.55	2.69	75.0	98.7	3.00
5R-1, 75–77	196.55	1.74	2.57	84.8	100.2	5.58
5R-2, 74–76	198.04	1.56	2.83	54.2	55.2	1.18
5R-3, 76–78	199.56	1.68	2.57	87.3	114.5	6.85
5R-4, 88–90	201.18	1.57	2.54	70.4	84.6	2.38
6R-1, 8–10	244.18	1.42	2.64	80.9	140.8	4.23
6R-2, 35–36	245.95	1.46	2.76	84.2	144.6	5.33
7R-1, 33–35	292.73	1.68	2.69	66.0	67.0	1.94
7R-3, 42–44	295.82	1.83	2.78	61.0	51.6	1.56
7R-4, 68–70	297.58	1.75	2.74	63.1	58.5	1.71
7R-6, 106–108	300.96	1.95	2.77	82.7	77.1	4.79
8R-1, 29–31	340.89	1.96	2.81	62.1	47.9	1.64
8R-2, 29–31	342.39	1.95	2.78	57.8	43.8	1.37
8R-3, 101–103	344.61	1.89	2.68	59.7	47.9	1.48
9R-1, 146–148	351.06	1.85	2.81	63.6	54.4	1.75
9R-2, 61–63	351.71	1.75	2.74	65.4	61.9	1.89
9R-4, 42–44	354.52	1.69	2.42	76.7	86.8	3.29
10R-1, 111–113	360.41	1.80	2.51	57.2	48.3	1.33
10R-2, 26–28	361.06	1.73	2.70	64.6	62.2	1.83
10R-3, 51–51	362.81	1.71	2.54	63.2	60.7	1.72
11R-1, 80–82	369.70	1.80	2.76	64.0	57.2	1.78
11R-2, 53–55	370.93	1.75	2.76	65.4	61.8	1.89
11R-3, 89–91	372.79	1.77	2.73	65.2	60.8	1.87
12R-1, 52–54	379.12	1.54	2.58	73.7	95.7	2.80
12R-2, 103–105	381.13	1.50	2.41	73.1	100.0	2.71
12R-3, 103–105	382.63	1.56	2.62	72.6	91.6	2.65
13R-1, 63–65	388.83	1.85	2.72	58.2	47.5	1.39
13R-2, 138–140	391.08	1.92	2.65	51.8	38.2	1.07
13R-3, 88–90	392.08	1.87	2.67	54.1	42.3	1.18
13R-4, 17–19	392.87	1.90	2.63	52.0	39.0	1.08
13R-5, 69–71	394.89	1.92	2.71	51.6	38.0	1.07
14R-1, 124–126	399.14	1.89	2.68	52.5	39.6	1.10
14R-2, 122–124	400.62	1.95	2.72	50.3	35.8	1.01
14R-3, 141–143	402.31	1.91	2.72	53.5	40.2	1.15
15R-1, 39–41	407.99	1.98	2.71	47.5	32.5	0.90
15R-2, 121–123	410.31	1.98	2.73	48.8	33.7	0.95
15R-4, 111–113	413.21	2.02	2.65	48.6	32.7	0.95
16R-1, 26–28	417.56	1.93	2.77	53.1	39.3	1.13
16R-3, 32–34	420.02	1.69	2.76	67.2	68.5	2.05
16R-3, 73–75	420.43	2.80	2.82	5.8	2.2	0.06
16R-4, 26–28	421.41	2.86	2.85	1.7	0.6	0.02
17R-1, 22–24	426.02	2.80	2.80	4.2	1.6	0.04
17R-3, 21–23	428.94	2.76	2.80	6.1	2.3	0.07
18R-1, 57–59	436.17	2.83	2.83	3.1	1.2	0.03
18R-2, 108–110	438.12	2.81	2.84	6.0	2.2	0.06
19R-1, 96–98	446.06	2.22	2.74	3.3	1.5	0.03
19R-2, 31–33	446.91	2.67	2.65	6.7	2.7	0.07
20R-1, 27–29	455.07	2.45	2.65	18.1	8.2	0.22
20R-2, 94–96	457.10	2.75	2.74	4.6	1.8	0.05
20R-3, 12–14	457.62	2.81	2.79	3.4	1.3	0.04
20R-4, 77–79	459.63	2.69	2.73	7.4	2.9	0.08
21R-2, 91–93	466.84	2.76	2.78	4.8	1.8	0.05
21R-4, 101–103	469.42	2.78	2.78	3.2	1.2	0.03
21R-6, 93–95	472.08	2.78	2.79	3.8	1.4	0.04

Table 7 (continued).

Core, section, interval (cm)	Depth (mbsf)	Wet-bulk density (%)	Grain density (%)	Porosity (%)	Water content (%)	Void ratio
124-770C-						
1R-2, 24–26	385.54	1.83	2.69	57.7	47.9	1.36
1R-4, 48–50	388.71	1.90	2.77	56.2	43.5	1.28
1R-6, 19–21	391.42	2.02	2.71	48.4	32.6	0.94
2R-2, 80–82	425.47	2.84	2.85	4.0	1.5	0.04
3R-2, 72–74	435.12	2.78	2.79	4.0	1.5	0.04
3R-3, 23–25	436.13	2.70	2.78	7.4	2.9	0.08
3R-4, 102–104	438.42	2.80	2.81	4.9	1.8	0.05
4R-1, 29–31	442.89	2.82	2.80	1.8	0.7	0.02
4R-3, 38–40	445.98	2.59	2.72	13.6	5.7	0.16
5R-1, 67–69	452.87	2.84	2.84	1.9	0.7	0.02
5R-3, 40–42	454.96	2.82	2.81	2.6	0.9	0.03
5R-4, 37–39	456.19	2.84	2.83	3.0	1.1	0.03
5R-7, 27–29	460.21	2.82	2.83	2.6	1.0	0.03
6R-1, 82–84	462.72	2.69	2.72	4.9	1.9	0.05
6R-3, 116–118	465.90	2.78	2.80	3.6	1.3	0.04
6R-5, 107–109	468.81	2.81	2.81	3.8	1.4	0.04
7R-1, 27–29	471.77	2.64	2.67	6.0	2.4	0.06
7R-3, 84–86	475.17	2.76	2.76	4.2	1.6	0.04
7R-5, 107–109	478.21	2.86	2.84	1.8	0.7	0.02
9R-2, 29–31	492.59	2.79	2.84	4.4	1.7	0.05
9R-2, 120–122	493.50	2.81	2.81	3.0	1.1	0.03
10R-1, 140–142	501.90	2.85	2.85	2.4	0.9	0.02
10R-2, 9–11	502.09	2.88	2.87	2.6	0.9	0.03
10R-3, 8–10	503.47	2.90	2.89	3.2	1.2	0.03
11R-1, 91–93	511.11	2.79	2.80	3.9	1.5	0.04
11R-2, 99–101	512.52	2.86	2.85	3.3	1.2	0.03
12R-1, 8–10	519.98	2.89	2.87	2.0	0.7	0.02

euhedral to subhedral olivine phenocrysts (0.2–1.0 mm) and 2%–10% plagioclase phenocrysts (0.3–4.0 mm). The olivine phenocrysts are totally altered to a mixture of clay and calcite, and the plagioclase phenocrysts (An_{50-70}), which show normal compositional zoning, contain patches and zones of devitrified glass. The groundmass varies from cryptocrystalline to fine grained and is medium grained in the larger pillows. The rocks are generally hypocrystalline, with hyalopilitic to intersertal textures.

The groundmass of the less well-crystallized samples comprises from 15% to 60% plagioclase (An_{50-70}) in the form of thin skeletal and hollow laths, generally 0.15–1.0 mm long, set in a cryptocrystalline matrix of turbid, devitrified glass full of tiny grains of iron oxide in which the individual minerals cannot be recognized. In the better crystallized samples, the groundmass is made up of 30% plagioclase laths up to 2 mm, with 25% anhedral grains and skeletal prisms of clinopyroxene. The rocks contain unevenly distributed (maximum 2%) spherical, lobate, and irregular vesicles up to 2.0 mm, filled with calcite and clay. Many of the rocks are nonvesicular. Alteration is generally slight, consisting of the replacement of olivine by clays and calcite as well as the devitrification of the glassy groundmass.

Unit 2

Highly plagioclase-olivine-phyric basalt, pillow lava, and pillow breccia

Unit 2 is a light gray pillowed unit that is present between 439.34 and 454.8 mbsf, or between Section 124-770B-18R-3 at 76 cm and the top of Section 124-770B-20R-1. The total thickness drilled in this unit is 15.46 m, and approximately 5 m was recovered. The upper contact with Unit 1 is missing; it occurs in Section 124-770B-18R-3 at 76 cm between Pieces 9 and 10, where an unnumbered rock piece is found. The common presence of curved, glassy, and variolitic chilled margins and patches

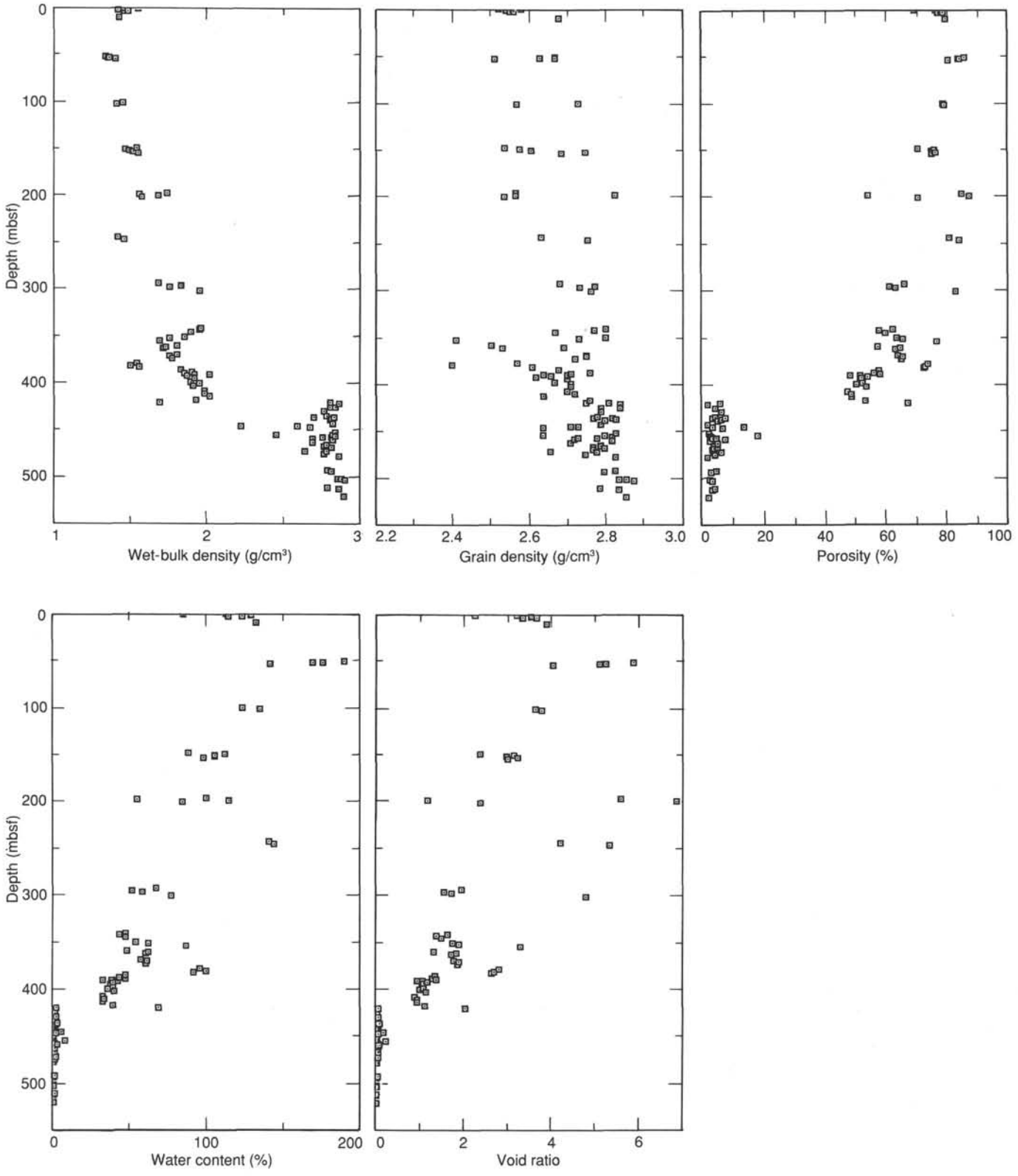

Figure 11. Downhole changes in index properties (wet-bulk density, grain density, porosity, water content, and void ratios), Site 770.

Table 8. Compressional wave velocity data, Site 770.

Core, section, interval (cm)	Depth (mbsf)	Velocity (km/s)
124-770B-		
5R-3, 76–78	199.56	1.63
5R-4, 88–90	201.18	1.65
6R-1, 8–10	244.18	1.57
7R-7, 25–27	301.65	1.61
8R-3, 101–103	344.61	1.65
9R-1, 134–136	350.94	1.64
10R-1, 148–150	360.78	1.62
10R-3, 51–53	362.81	1.63
11R-1, 80–82	369.70	1.62
12R-1, 52–54	379.12	1.61
12R-2, 103–105	381.13	1.61
12R-3, 103–105	382.63	1.64
13R-1, 63–65	388.83	1.69
13R-2, 138–140	391.08	1.70
13R-3, 88–90	392.08	1.67
13R-4, 17–19	392.87	1.66
13R-5, 69–71	394.89	1.68
14R-1, 124–126	399.14	1.68
14R-2, 122–124	400.62	1.69
14R-3, 141–143	402.31	1.68
15R-1, 39–41	407.99	1.69
15R-2, 121–123	410.31	1.67
15R-4, 111–113	413.21	1.72
16R-1, 26–28	417.56	1.67
16R-2, 32–34	419.12	1.63
16R-3, 73–75	420.43	5.26
16R-4, 26–28	421.41	5.72
17R-1, 22–24	426.02	5.50
17R-3, 21–23	428.94	5.04
18R-1, 57–59	436.17	5.23
18R-2, 108–110	438.12	5.24
19R-1, 96–98	446.06	4.70
19R-2, 31–34	446.91	4.90
20R-1, 27–29	455.07	4.02
20R-2, 94–96	457.10	4.70
20R-3, 12–14	457.62	5.60
20R-4, 77–79	459.63	5.25
21R-2, 91–93	466.84	5.14
21R-4, 101–103	469.42	5.30
21R-6, 93–95	472.08	5.25
124-770C-		
1R-2, 24–26	385.54	1.67
1R-4, 48–50	388.71	1.69
1R-6, 19–21	391.42	1.72
2R-2, 80–82	425.47	5.17
3R-2, 72–74	435.12	5.12
3R-3, 23–25	436.13	4.69
3R-4, 102–104	438.42	5.05
4R-1, 29–31	442.89	5.42
4R-3, 38–40	445.98	4.96
5R-1, 67–69	452.87	5.58
5R-3, 40–42	454.96	5.39
5R-4, 37–39	456.19	5.66
5R-7, 27–29	460.21	5.42
6R-1, 82–84	462.72	4.98
6R-3, 116–118	465.90	5.42
6R-5, 107–109	468.81	5.27
7R-1, 27–29	471.77	5.01
7R-3, 84–86	475.17	4.99
7R-5, 107–109	478.21	5.76
9R-2, 29–31	492.59	5.06
9R-2, 120–122	493.50	5.21
10R-1, 140–142	501.90	5.39
10R-2, 9–11	502.09	5.37
10R-3, 8–10	503.47	5.55
11R-1, 91–93	511.11	5.08
11R-2, 99–101	512.52	5.30
12R-1, 8–10	519.98	5.46
12R-2, 66–68	521.89	5.57

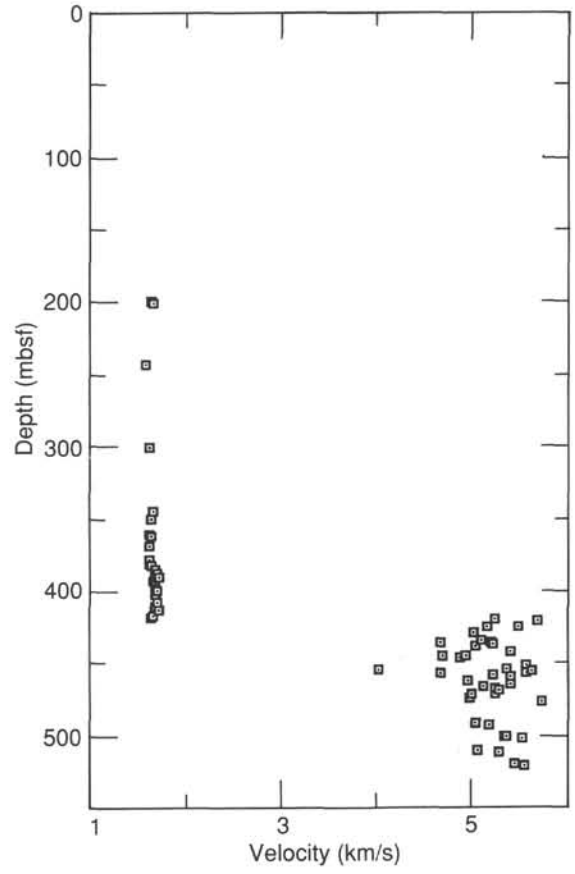

Figure 12. Hamilton Frame compressional wave velocity vs. depth, Site 770.

of hyaloclastic breccia indicates that the unit is made up of pillows 10–20 cm in diameter. No individual cooling units were recognized.

Vesicles are small (<1.0 mm) and scarce in this sequence, ranging from 0% to 2%, and are filled or lined with green clay. In the upper part of the unit, the fractures and veins are few and irregular. They do not exceed 5 mm in width and are filled with limonite, carbonate, and green clay. Near the base of the section the fractures are more common and larger, up to 1 cm wide, and are filled with green clay that contains glassy fragments, as well as limonite and carbonate.

The rocks of Unit 2 are highly plagioclase-olivine-phyric basalts, containing 5%–10% euhedral to subhedral olivine phenocrysts (0.3–3.0 mm) and 5%–15% euhedral to subhedral plagioclase phenocrysts (0.3–5.0 mm). The olivine phenocrysts are totally altered to brown clay, and the plagioclase phenocrysts (An_{70}), which show some normal compositional zoning, contain angular patches and zones of devitrified glass. The groundmass varies from cryptocrystalline to fine grained. The rocks are generally hypocrystalline, with hyalopilitic to intersertal textures.

The groundmass comprises from 10% to 25% of very thin, hollow and skeletal plagioclase laths and microliths, generally 0.1–1.0 mm long, set in a cryptocrystalline matrix (48%–66%) of turbid, iron-stained devitrified glass full of tiny grains and plates of iron oxide, in which the individual minerals cannot be recognized. A maximum of 2% of poorly developed skeletal prisms of clinopyroxene are present in the groundmass. The rocks contain unevenly distributed (maximum 2%) spherical vesicles up to 1.0 mm, filled with brown clays. Many of the rocks are nonvesicular. Alteration is generally slight and consists

Table 9. Thermal conductivity data, Site 770.

Core, section, interval (cm)	Depth (mbsf)	Thermal conductivity (W/m · K)
124-770B-		
1R-1, 75–76	0.75	0.93
1R-3, 75–76	3.75	0.87
1R-5, 75–76	6.75	0.91
1R-7, 35–36	9.35	0.93
2R-1, 75–76	51.55	0.83
2R-2, 75–76	53.05	0.80
3R-1, 75–76	100.15	0.90
3R-2, 75–76	101.65	0.85
4R-2, 75–76	149.85	0.97
4R-3, 65–66	151.25	0.95
4R-4, 75–76	152.85	0.97
4R-5, 75–76	154.35	1.01
5R-1, 50–51	196.30	0.86
5R-2, 70–71	198.00	0.98
5R-3, 80–81	199.60	0.92
5R-4, 87–88	201.17	0.99
6R-1, 11–12	244.21	0.79
6R-1, 66–67	244.76	0.77
7R-1, 80–81	293.20	1.17
7R-3, 80–81	296.20	1.20
7R-4, 80–81	297.70	1.17
7R-6, 80–81	300.70	1.13
8R-1, 88–89	341.48	1.26
8R-2, 102–103	343.12	1.40
8R-2, 50–51	342.60	1.32
8R-3, 97–98	344.57	1.23
9R-1, 75–76	350.35	1.37
9R-2, 75–76	351.85	1.38
9R-3, 75–76	353.35	1.34
9R-4, 75–76	354.85	1.25
10R-1, 75–76	360.05	1.25
10R-2, 75–76	361.55	1.04
10R-3, 80–81	363.10	0.85
10R-4, 22–23	364.02	0.91
11R-1, 75–76	369.65	1.15
11R-2, 75–76	371.15	1.07
11R-3, 75–76	372.65	1.14
11R-4, 40–41	373.80	1.11
12R-1, 75–76	379.35	1.08
12R-2, 75–76	380.85	0.99
12R-3, 75–76	382.35	0.97
14R-1, 74–75	398.64	1.33
14R-2, 90–91	400.30	1.41
14R-3, 48–49	401.38	1.26
14R-4, 16–17	402.56	1.29
15R-1, 45–46	408.05	1.37
15R-2, 64–65	409.74	1.40
15R-4, 75–76	412.85	1.46
15R-5, 24–25	413.84	1.39
16R-1, 30–31	417.60	1.28
16R-1, 65–66	417.95	1.13
16R-2, 40–41	419.20	1.22
16R-3, 23–24	419.93	1.00
17R-2, 24–25	427.47	1.44
19R-2, 35–36	446.95	0.97
21R-4, 92–93	469.33	1.70
124-770C-		
1R-1, 72–73	384.52	1.39
1R-3, 71–72	387.44	1.22
1R-4, 45–46	388.68	1.17
1R-6, 89–90	392.12	1.46
3R-3, 45–46	436.35	1.49
5R-6, 55–56	459.01	1.67
7R-1, 42–43	471.92	1.73
9R-2, 20–21	492.50	1.50
11R-2, 132–133	512.85	1.71

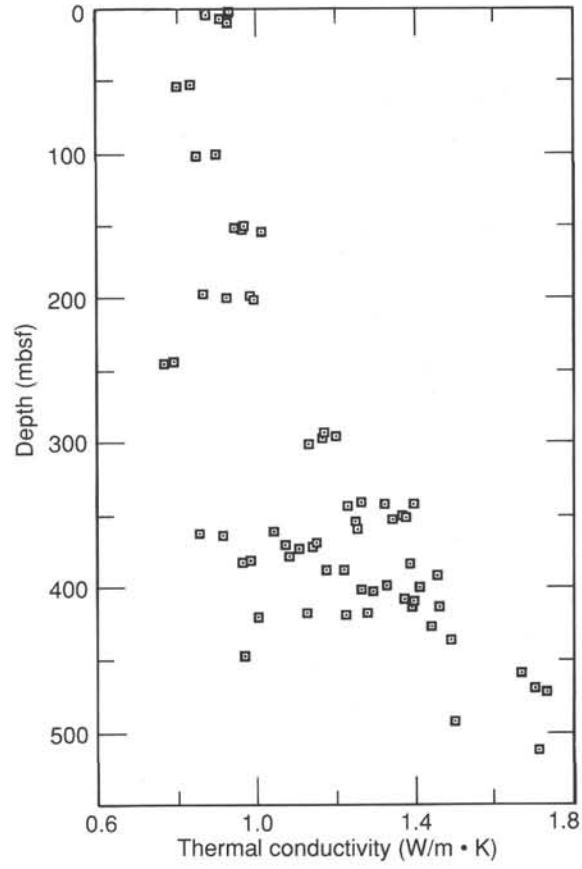

Figure 13. Thermal conductivity vs. depth, Site 770.

of the replacement of olivine by clays and the devitrification of the glassy groundmass.

Unit 3

Moderately to highly plagioclase-olivine-phyric basalt and pillow breccia

Unit 3 occurs between 454.8 and 458.6 mbsf, or between the top of Section 124-770B-20R-1 and Section 124-770B-20R-3 at 80 cm. The total thickness of the unit penetrated by drilling is 3.8 m, and approximately 2.5 m was recovered. There is a gap of more than 10.0 m in the core above the top of this unit, and the nature of the contact with Unit 2 is unknown. The unit is essentially a volcanic breccia made up largely of angular fragments of highly porphyritic lava, 5–10 cm in diameter (Pieces 5a and 7c in Section 124-770B-20R-1 have chilled margins).

The larger clasts are surrounded by a finer-grained matrix 1–10 mm in diameter, suspended in a green clay matrix. The small fragments show all of the features associated with chilled pillow margins, including banded and fragmental glass, variolitic and cryptocrystalline material, and quenched olivine crystals. A few green clay veins, <5 mm wide and containing glassy fragments, penetrate the breccia.

The rocks of Unit 3 are pillow brecciated and comprise highly plagioclase-olivine-phyric basalts. They contain 5%–10% euhedral to subhedral olivine phenocrysts (0.2–2.0 mm) and 5%–20% euhedral to subhedral plagioclase phenocrysts (1.0–5.0 mm). The olivine phenocrysts are totally altered to brown clay, and the plagioclase phenocrysts (An_{50-70}) show some normal compositional zoning and contain angular patches and zones of devitrified glass.

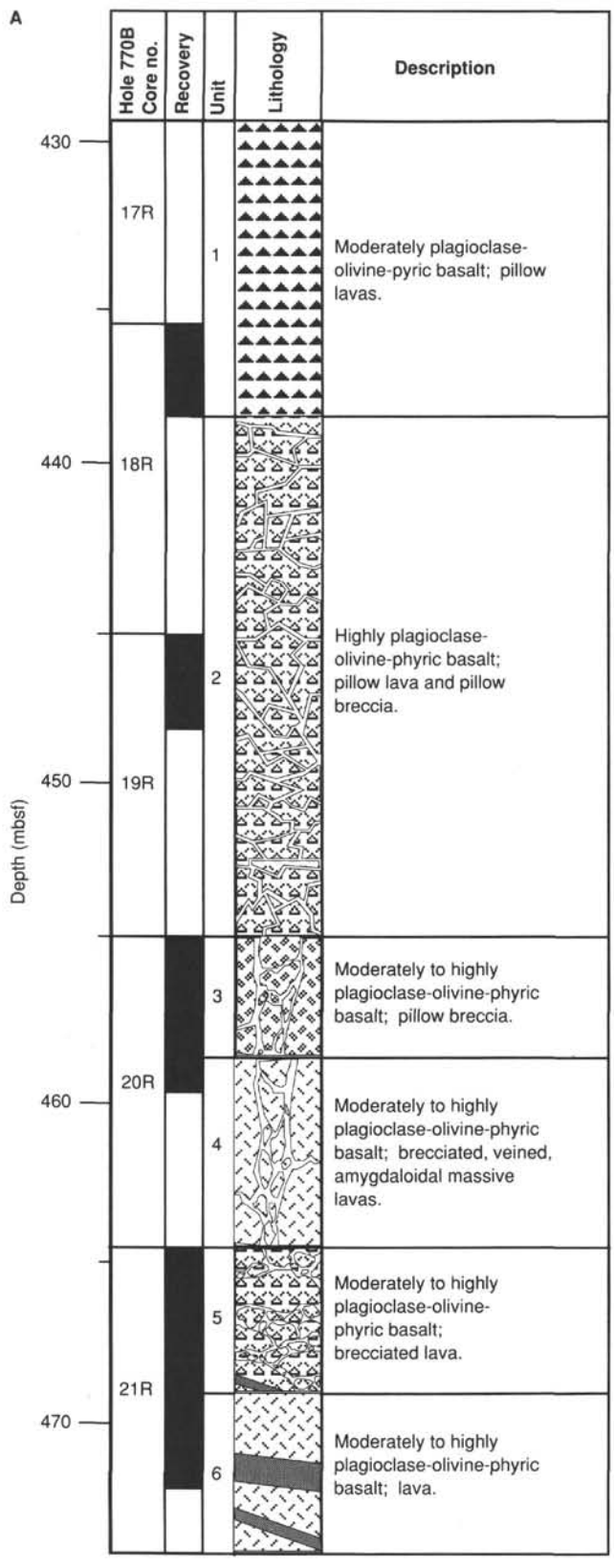

Figure 14. Lithology and recovery of basement rocks, Holes 770B (A) and 770C (B).

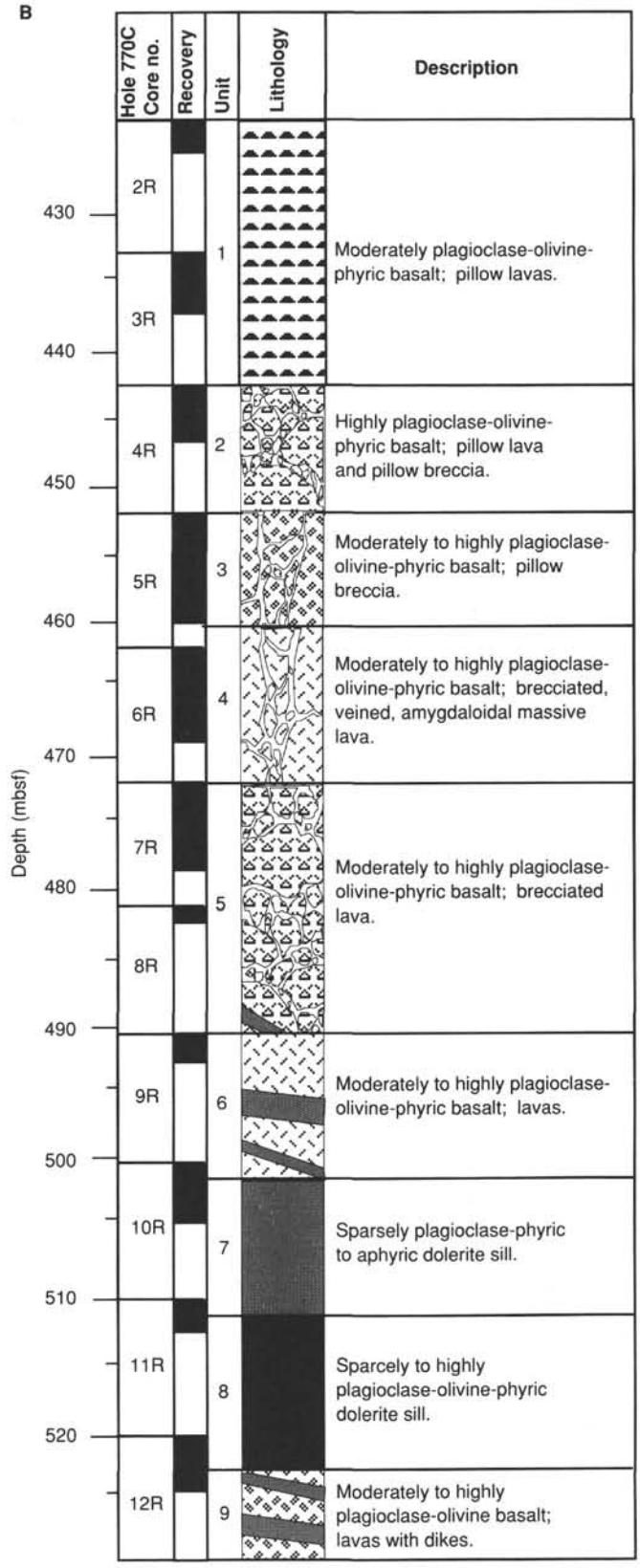

Figure 14 (continued).

Table 10. Petrographic data on basement rocks, Hole 770B.

Core, section, interval (cm)	Phenocryst		Groundmass					Secondary minerals[a]
	Ol	Pl	Pl	Cpx	Mes	Acc	Ves	
Unit 1 (moderately plagioclase-olivine-phyric basalt pillows):								
16R-3, 64–65	2	3	30	—	63	—	2	12
16R-4, 95–96	3	3	15	—	79	—	—	1
17R-3, 134–137	2	3	60	—	34	—	1	33
18R-2, 90–93	2	2	30	25	41	—	—	2
Unit 2 (highly plagioclase-olivine-phyric basalt pillows):								
18R-3, 144–145	10	15	15	2	58	—	—	12
19R-1, 98–99	6	20	25	—	48	—	1	7
19R-2, 42–45	4	20	10	—	64	—	2	6
Unit 3 (highly plagioclase-olivine-phyric brecciated basalt pillows):								
20R-2, 101–102	10	20	32	30	5	—	2	17
20R-3, 12–14	5	10	39	30	12	1	3	—
Unit 4 (moderately to highly plagioclase-olivine-phyric amygdaloidal basalt):								
20R-4, 135–140	10	5	51	13	5	—	15	30
Unit 5 (moderately to highly plagioclase-olivine-phyric basalt):								
21R-1, 99–100	5	3	37	34	5	1	15	25
21R-1, 123–126	8	1	45	25	10	1	10	28
21R-3, 34–35	5	10	38	37	—	—	5	10
21R-4, 34–35	10	6	35	28	5	1	15	30
Unit 6 (moderately to highly plagioclase-olivine-phyric basalt):								
21R-4, 77–78	5	5	39	27	20	1	3	25
21R-6, 19–20	5	15	24	34	—	2	15	25

Note: Ol = olivine, Pl = plagioclase, Cpx = clinopyroxene, Mes = mesostasis, Acc = accessory minerals, and Ves = vesicles.
[a] Secondary minerals include vesicle filling.

The groundmass varies from fine to medium grained, is generally hypocrystalline, with intersertal, intergranular, and subophitic textures. It comprises 30%–40% of broad, euhedral to subhedral plagioclase laths, generally 0.25–1.0 mm long, and up to 30% clinopyroxene prisms and grains that are intergrown with the plagioclase or are present among the plagioclase laths. About 1% skeletal, dendritic, and platy ilmenite (<0.2 mm) is also present. There is 5%–15% devitrified glass in angular patches set between the plagioclase laths. The rocks contain unevenly distributed (maximum 3%) 1.0–4.0-mm spherical vesicles filled with clay and calcite. Alteration is generally slight and consists of the replacement of olivine by brown clays and the replacement of the intersertal glass by a mixture of clay and calcite.

Unit 4

Moderately to highly plagioclase-olivine-phyric basalt and brecciated, veined lava

Unit 4 is a massive gray to brownish gray unit that occurs between 458.6 and 464.5 mbsf, or between Section 124-770B-20R-3 at 80 cm and the top of Section 124-770B-21R-1. The thickness of the unit as defined by coring is 5.9 m, and <1.5 m were recovered. The rock is made up of angular fragments 1 mm to 8 cm in diameter, of lithologically uniform amygdaloidal highly porphyritic basalt, cemented together by a mixture of silica, carbonate, and clay that forms a vein network unevenly distributed throughout the unit. The structure of the unit is interpreted as resulting from the brecciation of an individual lava flow of amygdaloidal, highly plagioclase-olivine-phyric basalt. The amygdules (0.5–9.0 mm) are irregularly distributed and make up 5%–20% of the rock. The dominant filling is calcite with subordinate green clay.

The rocks of Unit 4 comprise highly brecciated and veined, highly plagioclase-olivine-phyric basalt. They contain about 10% euhedral to subhedral olivine phenocrysts (0.5–1.0 mm) and approximately 5% euhedral to subhedral plagioclase phenocrysts (1.0–5.0 mm). The olivine phenocrysts are totally altered to brown clay and calcite, and the plagioclase phenocrysts show some normal compositional zoning. They also contain angular patches and zones of devitrified glass.

The groundmass varies from fine to medium grained, is generally hypocrystalline, and has intersertal, intergranular, and subophitic textures. The groundmass comprises about 50% euhedral to subhedral plagioclase laths (approximately An_{50}), generally 1.0–2.0 mm long, and approximately 15% clinopyroxene prisms and grains that are intergrown with the plagioclase or are present among the plagioclase laths. About 1% large, skeletal plates of ilmenite (<1.0 mm) also occur. There is 5% devitrified glass in angular patches set between the plagioclase laths.

The rocks are extremely vesicular and contain up to 20% unevenly distributed spherical and lobate vesicles 0.3–3.0 mm, and rarely 9.0 mm, filled with clay and calcite. Alteration is generally slight and consists of the replacement of olivine by brown clays and calcite and the replacement of intersertal glass by a mixture of sericite and calcite.

Unit 5

Moderately to highly plagioclase-olivine-phyric basalt and brecciated lava

Unit 5 is a massive dark gray to brownish gray unit that occurs between 464.5 and 469.0 mbsf, or between the top of Section 124-770B-21R-1 and the top of Section 124-770B-21R-4. It is 4.5 m thick, according to the drilling logs, and approximately 2 m was recovered. There is a gap of about 10 cm in the core recovered between the bottom of Unit 4 and the top of Unit 5, and the nature of the contact between them cannot be seen.

All of the recovered section is uniform in lithology, and the unit is thought to comprise one lava flow. It comprises finely to coarsely brecciated angular to subrounded fragments of amygdaloidal basalt in a matrix of fine glass clasts cemented by a network of veins that contain a mixture of silica, clay, and carbonate. The subrounded fragments are vesicular in the center and fine grained at the margin, which indicates that they may be the result of autobrecciation of a lava flow. The amygdules make up about 10%–20% of the rock and are spherical, ovoid, and lobate in form. They range in size from 1 to 5 mm.

The rocks of Unit 5 comprise highly brecciated and veined (moderately for the most part, but also highly in part) plagioclase-olivine-phyric basalt. They contain 5%–10% euhedral to subhedral olivine phenocrysts (0.4–1.5 mm) and 1%–10% euhedral to subhedral plagioclase phenocrysts (1.0–5.0 mm; approximately An_{65}). The olivine phenocrysts are totally altered to brown clay, and the plagioclase phenocrysts show some normal compositional zoning and contain angular patches and zones of devitrified glass.

The groundmass varies from fine to medium grained, is generally hypocrystalline, and has intersertal, intergranular, and intrafasciculate textures. The groundmass comprises 35%–50% euhedral to subhedral plagioclase laths (approximately An_{65}), generally 1.0–2.0 mm long, and approximately 25%–40% clinopyroxene prisms and grains that are intergrown in radial and parallel aggregates with the plagioclase or are present among the plagioclase laths. About 1% large skeletal plates and grains of ilmenite (0.1–0.5 mm) are also present.

Some samples contain 5%–10% angular, intersertal areas of glass that are altered to clay. The rocks are extremely vesicular and contain 5%–20% uniformly to unevenly distributed, spherical, lobate, and irregular vesicles 0.5–5.0 mm, with clay rims

and cores that are filled with mixtures of clay and calcite. Alteration is generally moderate and consists of the replacement of olivine by brown clays and calcite and the replacement of interstitial glass by clay.

Unit 6

Moderately to highly plagioclase-olivine-phyric basalt and lava

Unit 6 is a massive brownish gray unit that occurs between 469.0 mbsf and the bottom of the hole at 474.10 mbsf, or between the top of Section 124-770B-21R-4 and the bottom of Section 124-770B-21R. It is 5.1 m thick, according to the drilling records, and <2.5 m was recovered. At least 40 cm of core is missing above the top of this unit, and the nature of the contact with Unit 5 was not seen. The bottom of the hole lies within the unit, and thus its base was not seen.

The rock is coarsely brecciated, with clasts ranging in size from 1 to 35 cm. They are angular, subrounded, and lobate with vesicles in the core and fine-grained margins. The fragments are cemented together by a network of veins that are filled with a mixture of clay, carbonate, and silica. The rocks contain 5%–15% spherical, ovoid, and irregular vesicles filled with clay and calcite.

The rocks of Unit 6 comprise highly brecciated and veined, moderately to highly plagioclase-olivine-phyric basalt. They contain from about 5% euhedral to subhedral olivine phenocrysts (0–1.0 mm) and 5%–15% euhedral to subhedral plagioclase phenocrysts (1.0–3.0 mm; approximately An_{55}). The olivine phenocrysts are totally altered to brown clay, and the plagioclase phenocrysts show some normal compositional zoning and contain angular patches and zones of devitrified glass.

The groundmass is fine grained and is generally hypocrystalline, with intersertal, intergranular, and intrafasciculate textures. It comprises 25%–40% euhedral to subhedral plagioclase laths (approximately An_{50-60}), generally 0.1–1.0 mm long, and approximately 25%–30% clinopyroxene prisms and grains that are intergrown in radial and parallel aggregates with the plagioclase or are present between the plagioclase laths. About 1% large skeletal plates and euhedral grains of ilmenite (0.1–0.5 mm) are also present.

From 5% to 20% angular, intersertal areas of glass altered to clay are present. The rocks are extremely vesicular and contain 3%–15% uniformly to unevenly distributed spherical, ovoid, and irregular vesicles 1.0–4.0 mm, with clay rims and cores filled with mixtures of clay and calcite. Alteration is slight to moderate and consists of the replacement of olivine by brown clays and the replacement of interstitial glass to clay.

Hole 770C

Basaltic rocks were first recovered from Hole 770C at 423.2 mbsf (Core 124-770C-2R), and a total of 106.3 m of igneous rocks was penetrated. The bottom of the hole is at 529.5 mbsf and lies within a sequence of brecciated basalt lavas penetrated by small dikes.

The lithology, depth, and recovery data for the igneous rocks at Site 770C are summarized in Figure 14B. The average recovery of the igneous rocks in Cores 124-770C-2R to -12R was 42.8% and ranged from a high of 80.7% in Core 124-770C-5R to a low of 9.3% in Core 124-770C-8R. Nine separate units were recognized in the sequence by means of the differences in structure, lithology, mineralogy, and texture.

We examined 11 thin sections of igneous rocks from Hole 770C under the microscope: two from Unit 1, one from Unit 2, one from Unit 3, one from Unit 4, two from Unit 5, two from Unit 7, one from Unit 8, and one from Unit 9. No thin sections of rocks from Unit 6 were examined. The units are named according to their dominant rock types. Plagioclase and olivine phenocrysts occur in all of the lithologic units as single crystals and as glomerophyric aggregates. The results are summarized in Table 11; more complete details can be obtained from the visual core descriptions and the thin section descriptions at the back of the book.

Unit 1

Moderately plagioclase-olivine-phyric basalt and pillow lava

Unit 1 is a gray to brownish gray unit that occurs between 423.2 and 442.7 mbsf, or between the top of Section 124-770C-2R and Section 124-770C-4R-1 at 10 cm. It has a thickness of 19.5 m, of which approximately 6.0 m was recovered. A piece of red mud is present in the core immediately above but not in contact with the basalts. This suggests that they are directly overlain by sediments similar to those that are present in Hole 770B. No individual cooling units were defined in this unit.

In the first two sections of Core 124-770C-2R, the material recovered was very fragmental; however, in Section 124-770C-2R-3 and in Sections 124-770C-3R-1 to 124-770C-3R-4, the pieces are larger, and many have preserved the curved black glass and variolitic margins of pillow lavas, in which the pillows generally seem to be up to 30 cm in diameter. Small amounts of hyaloclastic interpillow breccia are also preserved in the lower sections of the core.

Spherical vesicles are scattered in occurrence and never exceed 2% by volume. They generally range from 0.5 to 1.00 mm, with a few up to 2.00 mm, and are filled or partly filled with layers of green clay, calcite, and silica. Sparse irregular fractures ranging from 0.5 cm to 1.0 cm wide are present in Sections 124-770C-3R-1 to 124-770C-3R-4 and are filled with mixtures of

Table 11. Petrographic data on basement rocks, Hole 770C.

Core, section, interval (cm)	Phenocryst		Groundmass						Secondary minerals[a]
	Ol	Pl	Ol	Pl	Cpx	Mes	Acc	Ves	
Unit 1 (moderately plagioclase-olivine-phyric basalt pillows):									
2R-3, 61–62	1	2	—	25	5	42	—	—	41
3R-3, 128–129	2	2	—	33	56	5	—	—	5
Unit 2 (highly plagioclase-olivine-phyric basalt pillows):									
4R-1, 26–27	3	15	—	10	—	70	2	—	3
Unit 3 (moderately to highly plagioclase-olivine-phyric brecciated basalt pillows):									
5R-7, 70–71	3	2	—	44	33	15	1	2	5
Unit 4 (moderately plagioclase-olivine-phyric basalt):									
6R-3, 44–45	1	4	—	50	34	2	—	8	9
Unit 5 (moderately to highly plagioclase-olivine-phyric basalt):									
7R-5, 3–6	4	15	—	5	—	74	1	1	5
7R-6, 43–44	3	8	—	10		75	1	3	6
Unit 6 (moderately plagioclase-olivine-phyric basalt):									
Not represented									
Unit 7 (sparsely plagioclase-phyric to aphyric dolerite sill):									
10R-2, 42–43	—	1	4	31	42	20	2	—	24
10R-1, 96–98	—	3	—	38	38	20	1	—	21
Unit 8 (sparsely to highly plagioclase-olivine-phyric dolerite sill):									
12R-2, 38–41	15	5	—	36	33	10	1	—	25
Unit 9 (moderately to highly plagioclase-olivine-phyric basalt):									
12R-3, 66–67	3	12	—	26	32	20	1	6	29

Note: Ol = olivine, Pl = plagioclase, Cpx = clinopyroxene, Mes = mesostasis, Acc = accessory minerals, and Ves = vesicles.

[a] Secondary minerals include vesicle filling.

green and brown clays containing glass shards, lithic fragments, calcite, and limonite.

The rocks of Unit 1 are generally moderately plagioclase-olivine-phyric basalts, and parts of the unit are highly phyric and have more than 10% phenocrysts. The basalts contain 1%–5% (and uncommonly 10%) euhedral to subhedral olivine phenocrysts (0.2–0.5 mm) and 8%–15% plagioclase phenocrysts (1.0–3.0 mm). The olivine phenocrysts are totally altered to brown and green clays, and the plagioclase phenocrysts (An_{50-70}), which show normal compositional zoning, contain patches and zones of devitrified glass.

The groundmass varies from cryptocrystalline to fine and medium grained; it is generally hypocrystalline, with hyalopilitic, intersertal, and intergranular textures. The groundmass comprises 25%–33% plagioclase (An_{50-70}) as thin skeletal, hollow, swallow-tailed laths, generally 0.2–1.0 mm long, intergrown with 5%–55% clinopyroxene grains and skeletal prisms. Mesostasis (<27%) of crystallites of plagioclase and clinopyroxene and devitrified glass (5%–15%), containing numerous tiny grains of iron oxide (1%), makes up the rest of the groundmass.

The rocks contain a few unevenly distributed (maximum 2%) spherical vesicles up to 1.0 mm in diameter, filled with calcite and clay. Many of the rocks are nonvesicular. Alteration is generally slight and consists of the replacement of olivine by clays and the devitrification of the glassy groundmass.

Unit 2

Highly plagioclase-olivine-phyric basalt, pillow lava, and pillow breccia

Unit 2 is a light gray pillowed and brecciated unit that occurs between 442.7 and 452.2 mbsf, or between Sections 124-770C-4R-1 at 10 cm and the top of Section 124-770C-5R-1. The total thickness drilled in this unit is 9.5 m, and approximately 4 m was recovered. The actual upper contact with Unit 1 was not recovered; it occurs in Section 124-770C-4R-13 at 10 cm between Pieces 2 and 3. The presence of curved glassy and variolitic chilled margins and patches of hyaloclastic breccia indicates that Unit 2 is made up of pillows that are up to 1 m in diameter.

The upper 1.5 m of the unit is predominantly made up of pillows with very little breccia, and the remainder is much more brecciated. The pillows contain very few small vesicles, which are filled or lined with green clay and calcite. Veins and fractures from 0.5 to 2 cm wide are present throughout the unit and are filled with clay in which lithic and glassy clasts, limonite, and carbonate are present.

The rocks of Unit 2 are highly plagioclase-olivine-phyric basalts, containing 3%–5% euhedral to subhedral olivine phenocrysts (0.5–2.0 mm) and 10%–15% euhedral to subhedral plagioclase phenocrysts (0.3–3.0 mm). The olivine phenocrysts are totally altered to brown clay, and the plagioclase phenocrysts (An_{60}), which show some normal compositional zoning, contain angular patches and zones of devitrified glass.

The groundmass varies from cryptocrystalline to fine grained. The rocks are generally hypocrystalline, with hyalopilitic to intersertal textures. The groundmass comprises from 10% thin, hollow, and skeletal plagioclase laths and microliths, generally 0.1–1.0 mm long, set in a cryptocrystalline matrix (<70%) of turbid, iron-stained devitrified glass, full of tiny grains and plates of iron oxide. Incipient, arborescent aggregates of plagioclase and clinopyroxene are present in the matrix.

The rocks contain unevenly distributed (maximum 2%) spherical vesicles up to 1.0 mm, filled with brown clays. Many of the rocks are nonvesicular. Alteration is generally slight and consists of the replacement of olivine by clays and the devitrification of the glassy groundmass.

Unit 3

Moderately to highly plagioclase-olivine-phyric basalt and pillow breccia

Unit 3, which is gray to grayish brown amygdaloidal basalt, is present between 452.2 mbsf and 460.8 mbsf, or from the top of Section 124-770C-5R-1 to Section 124-770C-5R-7 at 70 cm. The total thickness of the unit penetrated by drilling is 8.6 m, and approximately 6.9 m was recovered. There is a gap of >5.5 m in the core above the top of this unit, and the nature of the contact with Unit 2 is unknown.

Unit 3 is a volcanic breccia made up of angular clasts of highly plagioclase-olivine phyric basalt 5–20 cm in diameter that are separated by a pervasive network of pink- and buff-colored calcite veins. These veins may be from 2 mm to 5 cm in diameter, and the larger ones contain angular clasts up to 2 or 3 cm that are surrounded by the carbonate. There are some small irregular patches in the volcanic rock that are made up of glassy and lithic clasts suspended in clay.

The rocks of Unit 3 comprise highly brecciated and veined, moderately to highly plagioclase-olivine-phyric basalt. They contain 2%–10% euhedral to subhedral olivine phenocrysts (0.5–1.0 mm) and 5%–15% euhedral to subhedral plagioclase phenocrysts (1.0–2.0 mm). The olivine phenocrysts are totally altered to brown clay and calcite, and the plagioclase phenocrysts show some normal compositional zoning; they also contain angular patches and zones of devitrified glass.

The groundmass varies and is generally hypocrystalline, with intersertal, intergranular, and intrafasciculate textures. It comprises about 40%–50% euhedral to subhedral plagioclase laths (approximately An_{50}), generally 0.3–0.6 mm long, and approximately 30% clinopyroxene prisms (0.3–0.6 mm) and grains that are intergrown with the plagioclase or are present between the plagioclase laths. About 1% large skeletal plates of ilmenite (<1.0 mm) is also present. Up to 15% devitrified glass is present in angular patches set between the plagioclase laths.

The rocks are extremely vesicular and contain up to 15% unevenly distributed spherical and irregular vesicles (0.2–3.0 mm), filled with layers of iron oxide, clays, and calcite. Alteration is generally slight and consists of the replacement of olivine by brown clays and the devitrification of the intersertal glass to a turbid mixture containing iron oxide.

Unit 4

Moderately to highly plagioclase-olivine-phyric basalt and brecciated, veined lava

This is a massive dark gray to brownish gray unit that occurs between 460.8 and 472.08 mbsf, or between Sections 124-770C-5R-7 at 70 cm and 124-770C-7R-1 at 78 cm. The thickness of the unit as defined by coring is 11.28 m, and about 7 m was recovered. The contact between Units 3 and 4 is not seen; it lies between Pieces 5 and 6 in Section 124-770C-5R-7, where nearly 2 m of Unit 3 may be missing. The unit is largely made up of angular fragments of moderately phyric basalt. The largest fragments range from 5 to 10 cm in diameter, separated by a pervasive network of veins of pink calcite. The veins may be up to 5 cm in diameter and contain numerous small (1–2 cm), angular fragments of basalt that are not in contact with each other but are suspended in the carbonate cement.

There are some very small irregular patches near the top of the unit that are made up of small angular fragments of lava in a green clay matrix. The absence of chilled pillow margins and the lack of glassy hyaloclastite suggests that the unit was formed by brecciation of an individual lava flow of amygdaloidal, moderately plagioclase-olivine-phyric basalt. The spherical to lobate

amygdules (0.5–7.0 mm) are irregularly distributed, make up 5%–15% of the rock, and are filled or lined with mixtures of calcite, limonite, and green clay.

The rocks of Unit 4 comprise highly brecciated and veined, moderately plagioclase-olivine-phyric basalt. They contain 0%–5% euhedral to subhedral olivine phenocrysts (0.5 mm) and 1%–5% euhedral to subhedral plagioclase phenocrysts (1.0–3.0 mm). The olivine phenocrysts are totally altered to brown clay, and the plagioclase phenocrysts show some normal compositional zoning and contain angular patches and zones of devitrified glass.

The groundmass is fine grained, with mainly intergranular and intrafasciculate textures with minor intersertal domains. The groundmass comprises <50% euhedral to subhedral plagioclase laths (approximately An_{60}), generally 0.5–1.5 mm long, intergrown with <35% clinopyroxene prisms and grains, in radial and parallel aggregates. About 1% tiny grains of ilmenite (<0.1 mm) are also present. These rocks contain <5% angular, intersertal areas of glass altered to clay.

The rocks are extremely vesicular and contain 5%–15% uniformly to unevenly distributed, spherical, lobate, and irregular vesicles (0.5–3.0 mm, and rarely up to 7 mm), with clay rims and cores filled with mixtures of clay and calcite. Alteration is slight to moderate and consists of the replacement of olivine by brown clays and calcite and the replacement of interstitial glass to clay.

Unit 5

Moderately to highly plagioclase-olivine-phyric basalt and brecciated lava

Unit 5 is a brecciated brownish yellow gray unit that occurs between 472.08 and 490.8 mbsf, or between Section 124-770C-7R-1 at 78 cm and the top of Section 124-770C-9R-1. It is 18.72 m thick, according to the drilling logs, and about 5.5 m was recovered. The contact of Unit 5 with Unit 4 above is difficult to place precisely; it lies somewhere between Pieces 6b and 8 in Section 124-770C-7R-1. It is marked by the appearance of abundant hyaloclastite breccia and some curved pillow margins, but its nature cannot be ascertained.

The unit is quite heterogeneous in structure but uniform in lithology. Identifiable pillows are uncommon and are between 10 and 20 cm in diameter. There are zones up to 1 m of brecciated lava, cut by irregular white carbonate veins 3–4 mm wide, which may be large pillows or thin flows. The lava comprises a sparsely to moderately plagioclase-olivine-phyric basalt, the detailed petrography of which is described below. The rocks contain 1%–5% generally spherical, unevenly distributed vesicles 1–2 mm in diameter. They are filled with layers of green and brown clay, carbonate, and silica.

One very small tabular intrusion, with a low dip, penetrates the base of this unit. The intrusion is in Section 124-770C-7R-6, Piece 5, and is approximately 5 cm thick with thin, planar, glassy and variolitic chilled margins. The interior of this very small intrusion is cryptocrystalline and sparsely plagioclase and olivine phyric; the groundmass is stained with limonite.

The rocks of Unit 5 comprise moderately to highly plagioclase-olivine-phyric basalt. They contain 1%–10% euhedral to subhedral olivine phenocrysts (0.5–1.0 mm) and 5%–15% euhedral to subhedral plagioclase phenocrysts (approximately An_{70}) from 1.0 to 3.0 mm. The olivine phenocrysts are totally altered to clay, and the plagioclase phenocrysts show some normal compositional zoning. They also contain angular patches and zones of devitrified glass.

The groundmass is fine grained to cryptocrystalline and is generally hypocrystalline, with hyalopilitic and intersertal textures. It comprises 5%–10% euhedral to subhedral, hollow, swallow-tailed plagioclase laths, generally about 1.0 mm long, set in a matrix of up to 75% devitrified glass. This matrix comprises cryptocrystalline radial aggregates of plagioclase(?) and clinopyroxene(?) microliths that are extremely difficult to identify, and turbid glass filled with minute granules of iron oxide. The rocks contain 1%–5% scattered, spherical vesicles (0.5 mm) filled with clay. Alteration is slight to moderate and consists of the replacement of olivine by brown clays and the oxidation of the glassy matrix.

Unit 6

Moderately to highly plagioclase-olivine-phyric basalt and lava(s)

Unit 6 is interpreted as a massive brownish gray lava or lavas that are penetrated by a number of flat-lying minor intrusions with glassy chilled margins and cryptocrystalline, limonite-stained interiors. The unit is present between 490.8 and 501.32 mbsf, or from the top of Section 124-770C-9R-1 to Section 124-770C-10R-1 at 82 cm. It is 10.52 m thick, according to the drilling records, and approximately 3 m was recovered. More than 12 m of Unit 5 was not recovered in the core, and the nature of the contact between it and Unit 6 cannot be determined.

Recovery was <30% in Unit 6, and the recovered rocks consist of numerous fragments, which made it very difficult to determine the lithology and cooling units of the host lavas. The recovered material suggests that the lava(s) are fine- to medium-grained, phaneritic rocks with vesicular tops and abundant larger olivine crystals near the base, above a chilled cryptocrystalline margin. If this interpretation is correct, then there are at least three separate cooling units (lavas) present, but their individual thicknesses cannot be determined. The vesicles are concentrated in zones, thought to represent flow tops, and are spherical (1–3 mm); they are filled or partly filled with green clays and calcite.

The rocks of Unit 6 are moderately plagioclase-olivine-phyric basalt. No thin sections of this unit were examined. They contain about 5%–10% euhedral to subhedral olivine phenocrysts (0.5–1.0 mm) and 2%–5% euhedral to subhedral plagioclase phenocrysts (1.0–3.0 mm). The olivine phenocrysts are altered to brown clay, and the plagioclase phenocrysts contain angular patches and zones of devitrified glass.

The groundmass is cryptocrystalline to fine grained and is generally hypocrystalline, with intersertal and intergranular textures. The rocks contain few vesicles (1%–3%) and show slight to moderate alteration.

Unit 7

Sparsely plagioclase phyric to aphyric dolerite sill

The massive, homogeneous, gray to brownish gray Unit 7 occurs between 501.32 and 512.48 mbsf, or between Section 124-770C-10R-1 at 82 cm and Section 124-770C-11R-2 at 78 cm. It is 11.16 m thick, according to the drilling records, and about 5.5 m was recovered. We are missing 7 m of section from Unit 6 above; and although the top of Unit 7 appears in the same section as the bottom of Unit 6 (Section 124-770C-10R-1), the contact is not visible. It is classified as a sill because of its massive and uniform lithology, its phaneritic texture, and the absence of the small intrusions that penetrate the lava units above and below (Units 6 and 9). The top is marked by a zone of about 25 cm in which vesicles are abundant.

The groundmass in this zone is phaneritic but slightly finer grained than the main body of the unit. The vesicles are spherical, from 1 to 2 mm in diameter, and make up about 10% of the rock volume in this zone. They are filled or partly filled with calcite, green clay, and iron oxide. Irregular, steeply dipping to horizontal fractures occur, but they are not abundant. They range from 1 to 3 mm in width and are filled with limonite, calcite, and green and brown clay.

The rocks of Unit 7 contain very few scattered plagioclase phenocrysts and comprise a massive unit of sparsely plagioclase-phyric to aphyric dolerite. The plagioclase phenocrysts

(<3%) are euhedral to subhedral in form and are 1.0–2.0 mm in diameter. They show minor compositional zoning and contain angular patches of devitrified glass. The groundmass, which makes up the vast majority of the rock, is fine grained and has intergranular, subophitic, and intersertal textures. It consists of 30%–40% stout plagioclase (approximately An_{60}) laths (0.3–0.8 mm), 38%–42% clinopyroxene prisms and grains (0.5–1.0) mm, and up to 20% devitrified glass.

Very minor olivine (1%) is present in some samples. Ilmenite occurs as subhedral plates and grains within the groundmass and as skeletal crystals intergrown with the clinopyroxene. Numerous vesicles occur in the top 20 cm of the unit, but there are very few within the main body of the intrusion. Alteration is slight and is limited to clay replacing the small amount of olivine present and to limonite staining of the groundmass adjacent to the fractures.

Unit 8

Sparsely to highly olivine-plagioclase-phyric dolerite sill

Unit 8 is a massive, brownish gray to dark gray unit that is present between 512.48 and 523.12 mbsf, or between Sections 124-770C-11R-2 at 78 cm and 124-770C-12R-3 at 22 cm. It is 10.64 m thick, according to the drilling records, and <3.5 m was recovered. The top contact was not seen, but it lies between Pieces 2 and 3 in Section 124-770C-11R-2. The body is classified as a sill because of its massive homogeneous lithology, phaneritic texture, lack of vesicles, and the absence of the small intrusions that cut the lava units above and below.

Unit 8 comprises a dolerite, with phenocrysts of plagioclase and olivine up to 3 mm, set in an intergranular, phaneritic groundmass made up of olivine, plagioclase, and clinopyroxene. The top 60 cm contains fewer olivine and plagioclase phenocrysts, is less coarse grained than the bulk of the body, and may represent part of the upper chilled margin. Veins and fractures are more abundant and thicker, particular in the center of this unit, than in the sill above. They range from 1 to 5 mm in thickness and may be vertical, steeply dipping or horizontal, and either irregular or planar; they are filled with mixtures of calcite and brown clay.

Unit 8 is a massive dolerite sill in which the rocks are finer grained and less porphyritic at the top and coarser grained and more porphyritic near the base. They contain 1%–10% subhedral to rounded olivine phenocrysts (0.5–3.0 mm, together with 0%–15% euhedral to subhedral plagioclase phenocrysts (1.0–3.0 mm). The olivine is completely altered to a mixture of clay, iddingsite, and limonite; and the plagioclase phenocrysts show limited, normal compositional zoning and patches of devitrified glass.

The groundmass is fine grained with intergranular and intersertal textures, made up of 35%–40% plagioclase laths (approximately An_{70}), about 35% clinopyroxene prisms, 1% small plates and grains of ilmenite (0.1–0.5 mm), and 10% interstitial glass. There are very few vesicles anywhere in this unit. Alteration is moderate: 15% clay and limonite replaces the olivine, and the interstitial glass is replaced by bright green clay.

Unit 9

Moderately to highly olivine-plagioclase-phyric basalt, and lavas with dikes

Unit 9 is interpreted as a moderately to highly olivine-plagioclase phyric, brownish gray lava with a fine-grained matrix that is penetrated by three flat-lying minor intrusions, from 5 to 20 cm wide with glassy chilled planar margins, and cryptocrystalline, limonite-stained interiors. The unit occurs between 523.12 and 529.5 mbsf, or between Section 124-770C-11R-2 at 78 cm and the bottom of the hole in Section 124-770C-12R-3. It is 6.38 m thick, according to the drilling records, and <2 m was recovered.

Only 3.5 m out of more than 10 m of Unit 8 was recovered in the core, and the relationship between it and Unit 9 below cannot be established. The lithology and cooling units of the host lavas cannot be determined with certainty because of the fragmentary recovery. However, the uniformity of the material between the intrusions suggests that it is all part of one lava flow.

Spherical vesicles (<10%) are irregularly distributed, range from 0.5 to 3 mm in size, and are filled with green clays, calcite, and limonite. Fractures and veins are less abundant and smaller in this unit than in Unit 8. They are generally steeply dipping to horizontal, from 1 to 3 mm thick, and filled with mixtures of carbonate and clay.

The rocks of Unit 9 comprise moderately to highly plagioclase-olivine-phyric basalt. They contain 1%–5% euhedral to subhedral olivine phenocrysts (0.2–1.0 mm) and 3%–12% euhedral to subhedral plagioclase phenocrysts (1.0–4.0 mm). The olivine phenocrysts are totally altered to clays, and the plagioclase phenocrysts show limited normal compositional zoning; they contain angular patches of devitrified glass.

The groundmass is fine grained, intergranular to intersertal, and comprises <30% euhedral to subhedral plagioclase laths (An_{60-70}), generally 0.2–0.8 mm long, intergrown with <35% clinopyroxene prisms and grains in radial and parallel aggregates. Devitrified, angular patches of glass (20%) are present among the plagioclase laths. Ilmenite (approximately 1%) occurs as plates and skeletal dendrites in the devitrified glass.

The rocks contain 5%–10% uniformly to unevenly distributed spherical vesicles (0.5–3.0 mm), with clay rims and cores filled with mixtures of clay and calcite. Alteration is slightly moderate and consists of the replacement of olivine by brown clays and the replacement of interstitial glass by greenish clay.

BASEMENT GEOCHEMISTRY

A total of 19 igneous rock samples from Site 770 basement were analyzed by X-ray fluorescence (XRF) during Leg 124 for their major element contents. For 12 of these samples, trace elements (Nb, Zr, Y, Sr, Rb, Zn, Cu, Ni, Cr, V, Ce, and Ba) were determined. The sample preparation technique and the analytical procedures are outlined in the "Explanatory Notes" chapter (this volume).

The petrography of the analyzed samples and their distribution in the basement lithologic units are reported in Table 12. The major and trace element analyses are listed in Tables 13 and 14 and the CIPW norms in Table 15. The normative values have been calculated on a dry basis with $Fe_2O_3/(Fe_2O_3 + FeO) = 0.15$. Major element chemistry shows marked differences in the compositions of the analyzed rocks as well as distinct distributions for each lithologic unit. Downhole variations of major element chemistry for the igneous rocks of Site 770 are shown in Figures 15 and 16.

The sparsely to moderately olivine-plagioclase phyric basalts from Unit 1 are olivine normative tholeiites with a low Mg# (MgO/[MgO + FeO]) normalized to $Fe_2O_3/(Fe_2O_3 + FeO) = 0.15$. The Mg# values range from 52 to 56. The TiO_2 values are homogeneous and distinctly higher than in the other lithologic types.

The highly plagioclase-olivine phyric basalts from Unit 2 are slightly to moderately olivine normative tholeiites with a distinctive high Al_2O_3 content (up to 19.23%) and Mg# in the range from 62 to 63. The TiO_2 values are distinctly lower than in Unit 1. The moderately to highly plagioclase-olivine phyric basalts from Unit 3 have variable silica and alkali contents, which are reflected in marked differences in their normative compositions.

Table 12. Summary of lithologic units, XRF analyzed samples, sample depth, and petrography of Site 770 basement rocks.

Lith. unit	Core, section, interval (cm)	Depth (mbsf)	Rock type unit (modal composition)
Hole 770B:			
1	124-770B-16R-4, 84–87	422.01	Ol-Pl phyric basalt (3% Ol, 18% Pl, 79% Ms)
1	124-770B-17R-3, 134–137	430.07	Ol-Pl phyric basalt (2% Ol, 63% Pl, 34% Ms, 1% Amg)
2	124-770B-18R-3, 141–143	439.95	Ol-Pl phyric basalt (10% Ol, 30% Pl, 2% Cpx, 58% Ms)
2	124-770B-19R-1, 99–102	446.09	Pl-Ol phyric basalt (6% Ol, 45% Pl, 48% Ms, 1% Amg)
2	124-770B-19R-2, 42–45	447.02	Pl-Ol phyric basalt (4% Ol, 30% Pl, 64% Ms, 2% Amg)
3	124-770B-20R-2, 102–105	457.18	Pl-Ol phyric basalt (10% Ol, 52% Pl, 30% Cpx, 5% Ms, 2% Amg)
3	124-770B 20R-3, 10–15	457.60	Pl-Ol phyric basalt (5% Ol, 49% Pl, 30% Cpx, 12% Ms, 1% Acc, 3% Amg)
5	124-770B-21R-1, 96–99	465.46	Ol-Pl phyric basalt (5% Ol, 40% Pl, 34% Cpx, 5% Ms, 1% Acc, 15% Amg)
5	124-770B-21R-4, 30–34	468.71	Pl-Ol phyric basalt (5% Ol, 48% Pl, 37% Cpx, 5% Amg)
6	124-770B-21R-6, 15–18	471.30	Pl-Ol phyric basalt (5% Ol, 39% Pl, 34% Cpx, 5% Ms, 2% Acc, 15% Amg)
Hole 770C:			
1	124-770C-2R-3, 59–62	426.76	Pl-Ol phyric basalt (1% Ol, 27% Pl, 5% Cpx, 42% Ms)
1	124-770C-3R-3, 125–128	437.15	Pl-Ol phyric basalt (2% Ol, 35% Pl, 56% Cpx, 5% Ms)
2	124-770C-4R-1, 27–30	442.87	Pl-Ol phyric basalt (3% Ol, 25% Pl, 70% Ms, 2% Acc)
5	124-770C-7R-25, 3-6	477.17	Pl-Ol phyric basalt (4% Ol, 20% Pl, 74% Ms, 1% Amg)
5	124-770C-7R-26, 44–47	478.84	Pl-Ol phyric basalt (3% Ol, 18% Pl, 75% Ms, 1% Acc, 3% Amg)
7	124-770C-10R-2, 43–47	502.43	Olivine dolerite (4% Ol, 32% Pl, 42% Cpx, 20% Ms, 2% Acc)

Note: Ol = olivine, Pl = plagioclase, Cpx = clinopyroxene, Opx = orthopyroxene, Ms = glassy or cryptocrystalline mesostasis, Amg = amygdules, Acc = accessory and secondary minerals.

Table 13. Major element composition of igneous rocks, Site 770.

Core, section, interval (cm)	SiO_2	TiO_2	Al_2O_3	Fe_2O_3	MnO	MgO	CaO	Na_2O	K_2O	P_2O_5	Total	LOI	Mg#
124-770B-													
[a]16R-4, 84-87	49.75	2.07	15.60	10.95	0.23	5.65	11.30	3.15	0.29	0.25	99.24	1.05	54
[a]17R-3, 134-137	49.40	2.16	16.05	10.80	0.19	5.20	11.65	3.25	0.19	0.27	99.16	0.84	52
18R-3, 141-143	49.58	1.32	18.61	8.21	0.18	5.74	12.93	2.60	0.18	0.10	99.45	1.43	62
19R-1, 99-102	49.16	1.28	19.23	8.60	0.16	6.09	11.90	2.22	0.43	0.15	99.22	2.80	62
[a]19R-2, 42-45	49.80	1.18	18.10	8.53	0.15	6.00	12.92	2.60	0.14	0.11	99.53	1.06	62
20R-2, 102-105	49.54	1.23	18.74	7.12	0.12	7.29	12.23	2.25	0.14	0.08	98.74	7.85	70
20R-3, 10-15	49.47	1.22	18.13	7.18	0.15	7.42	12.45	3.16	0.16	0.08	99.42	2.42	70
21R-1, 96-99	47.45	1.38	17.12	9.04	0.14	7.67	13.45	2.13	0.40	0.11	98.89	4.93	66
21R-4, 30-34	49.58	1.32	18.61	8.21	0.18	5.74	12.93	2.60	0.18	0.10	99.45	4.08	62
21R-6, 15-18	48.85	1.49	17.45	8.54	0.13	6.69	13.00	2.40	0.39	0.13	99.07	3.77	64
124-770C-													
2R-3, 59-62	49.90	2.15	16.10	9.80	0.31	5.37	11.70	3.15	0.19	0.27	98.94	0.87	56
[a]3R-3, 125-128	50.00	2.22	16.70	9.65	0.17	5.25	11.43	3.25	0.21	0.27	99.15	0.93	56
4R-1, 27-30	48.69	1.23	17.44	8.70	0.14	6.32	12.82	2.76	0.07	0.10	98.27	0.18	63
5R-2, 39-41	48.42	1.25	17.27	9.23	0.14	7.35	12.40	1.87	0.33	0.07	98.33	2.78	65
7R-5, 3-6	49.06	1.29	17.47	9.22	0.15	7.41	12.41	2.33	0.36	0.10	99.80	2.77	65
[a]7R-6, 44-47	49.70	1.62	16.90	9.92	0.14	5.70	12.27	2.85	0.36	0.18	99.64	1.44	57
[a]10R-2, 43-47	50.70	2.01	15.90	9.17	0.17	6.10	11./8	3.25	0.24	0.22	99.54	0.77	60
[a]12R-2, 38-41	48.90	1.33	15.52	10.63	0.20	8.67	11.70	2.45	0.24	0.14	99.78	2.73	65
12R-3, 64-66	49.06	1.29	17.47	9.22	0.15	7.41	12.41	2.33	0.36	0.10	99.80	2.70	65

Note: Major element compositions are given in wt% oxide. LOI = loss on ignition.
[a] On-board analysis revised at the University of Udine, Italy.

Table 14. Trace element contents of igneous rocks, Site 770.

Core, section, interval (cm)	Nb	Zr	Y	Sr	Rb	Zn	Cu	Ni	Cr	V	Ce	Ba	Zr/Y	Ti/Zr	Ti/V
124-770B-															
[a]16R-4, 84–87	7	163	40	195	7	98	63	117	206	331	19	6	4.08	76	37
[a]17R-3, 134–137	8	170	41	186	6	100	64	116	228	342	9	3	4.15	76	38
19R-1, 99–102	3	70	31	111	3	87	76	150	404	281	17	24	2.26	110	27
19R-2, 42–45	2	67	29	107	3	76	78	144	383	270	7	5	2.31	106	26
20R-2, 102–105	2	69	26	111	1	69	80	154	338	278	11	24	2.65	107	27
20R-3, 10–15	2	69	28	108	1	72	74	205	302	286	10	9	2.46	106	26
21R-1, 96–99	3	86	31	129	9	78	73	249	244	263	11	28	2.77	96	31
[a]21R-6, 15–18	3	95	31	141	6	78	76	152	238	244	13	13	3.06	94	37
124-770C-															
[b]7R-5, 3–6	5	182	25	110	7	na	na	117	na	na	na	3	7.28	42	
[b]7R-6, 44–47	5	113	36	143	11	na	na	94	305	265	na	na	3.14	86	37
[b]10R-2, 43–47	8	150	36	160	5	na	na	110	263	307	na	9	4.17	80	39
[b]12R-2, 38–41	4	52	52	68	7	na	na	132	418	250	na	<2	1.00	153	32

Note: Trace element compositions are given in parts per million (ppm).
[a] On board analysis revised at the University of Udine, Italy (except for Zn, Cu, and Ce).
[b] New analysis made at the University of Udine.

Table 15. CIPW norms of igneous rocks, Site 770.

Core, section, interval (cm)	Ne	Or	Ab	An	Di	Hy	Ol	Ap	Il	Mt	Total
124-770B-											
16R-4, 84–87	0	1.71	26.65	27.57	20.90	12.45	2.33	0.59	3.93	2.18	98.31
17R-3, 134–137	0	1.12	27.50	28.64	21.32	9.47	3.31	0.64	4.10	2.15	98.25
18R-3, 141–143	0	1.06	22.00	38.58	19.39	11.24	2.10	0.24	2.51	1.63	98.75
19R-1, 99–102	0	2.54	18.78	41.23	13.09	17.80	0.54	0.36	2.43	1.71	98.48
19R-2, 42–45	0	0.83	22.00	37.30	20.29	12.12	2.07	0.26	2.24	1.70	98.81
20R-2, 102–105	0	0.83	19.04	40.62	15.20	18.17	0.33	0.19	2.34	1.41	98.13
20R-3, 10–15	0.47	0.95	25.87	34.81	20.57	0	12.21	0.19	2.32	1.43	98.82
21R-1, 96–99	0	2.36	18.02	35.97	23.38	1.35	12.36	0.26	2.62	1.80	98.12
21R-4, 30–34	0	1.06	22.00	38.58	19.39	11.24	2.10	0.24	2.51	1.63	98.75
21R-6, 15–18	0	2.30	20.31	35.69	21.76	8.33	5.12	0.31	2.83	1.70	98.35
124-770C-											
2R-3, 59–62	0	1.12	26.65	29.23	21.05	13.09	0.29	0.64	4.08	1.95	98.10
3R-3, 125–128	0	1.24	27.50	30.36	19.13	12.87	0.46	0.64	4.22	1.92	98.34
4R-1, 27–30	0	0.41	23.35	34.99	21.76	5.68	7.02	0.24	2.34	1.73	97.52
5R-2, 39–41	0	1.95	15.82	37.75	18.14	17.83	1.66	0.17	2.37	1.83	97.52
7R-5, 3–6	0	2.13	19.71	36.15	19.28	11.27	5.95	0.24	2.45	1.83	99.01
7R-6, 44–47	0	2.13	24.11	32.26	21.36	9.94	3.53	0.43	3.08	1.97	98.81
10R-2, 43–47	0	1.42	27.50	28.09	22.51	11.45	1.65	0.52	3.82	1.82	98.78
12R-2, 38–41	0	1.42	20.73	30.64	20.62	11.83	8.66	0.33	2.53	2.11	98.87
12R-3, 64–66	0	2.13	19.71	36.15	19.28	11.27	5.95	0.24	2.45	1.83	99.01

Note: Values were calculated on the basis of an $Fe_2O_3/(Fe_2O_3 + FeO)$ ratio of 0.15 and normalized to 100%. Ne = nephaline, Or = orthoclase, Ab = albite, An = anorthite, Di = diopside, Hy = hypersthene, Ol = olivine, Ap = apatite, Il = ilmenite, and Mt = magnetite.

Samples 124-770B-20R-2, 102–105 cm, and 124-770C-5R-2, 39–41 cm, are slightly olivine normative tholeiites, and one sample (124-770B-20R-3, 10–15 cm) is nepheline- and highly olivine-normative and does not contain normative hypersthene. It is probable that the observed differences in chemistry of Sample 124-770B-20R-3, 10–12 cm, are mainly related to a secondary enrichment in Na. In fact, the basalts of Unit 2 are fairly uniform in terms of most major elements as well as of Mg# (65–70). Trace elements also give consistent indications of similar primary compositions. The TiO_2 values are uniform (1.22–1.25 wt%) and similar to those of the porphyritic basalts from Unit 2.

The moderately to highly phyric plagioclase olivine basalts from Unit 5 show a wide spectrum of chemical composition. The Mg# values range from 66 to 57, and CaO and Al_2O_3 values are variable, as is the CaO/Al_2O_3 ratio. The CIPW values indicate highly to moderately olivine normative tholeiitic compositions. Petrographic data suggest that some chemical differences may be related to changes caused by alteration, but it is also probable that primary compositions are reflected.

The moderately plagioclase-olivine phyric basalts from Units 6 and 9, which are similar petrographically, also show rather uniform olivine tholeiitic compositions, with Mg# values of 64–65, and low TiO_2 contents (1.29–1.49 wt%). They are similar to basaltic lithotypes from Unit 5.

The upper doleritic sill (Unit 7) is composed of olivine normative tholeiite characterized by fairly high TiO_2 (2.01%). In TiO_2 content, it is similar to the basalts from Unit 1, but it has a higher Mg# (60). For the lower dolerite sill (Unit 8), the analyzed sample shows a clearly distinct olivine tholeiitic composition with Mg# of 65 and low TiO_2 (1.33 wt%). Chemically, it is similar to the basalts from Unit 2.

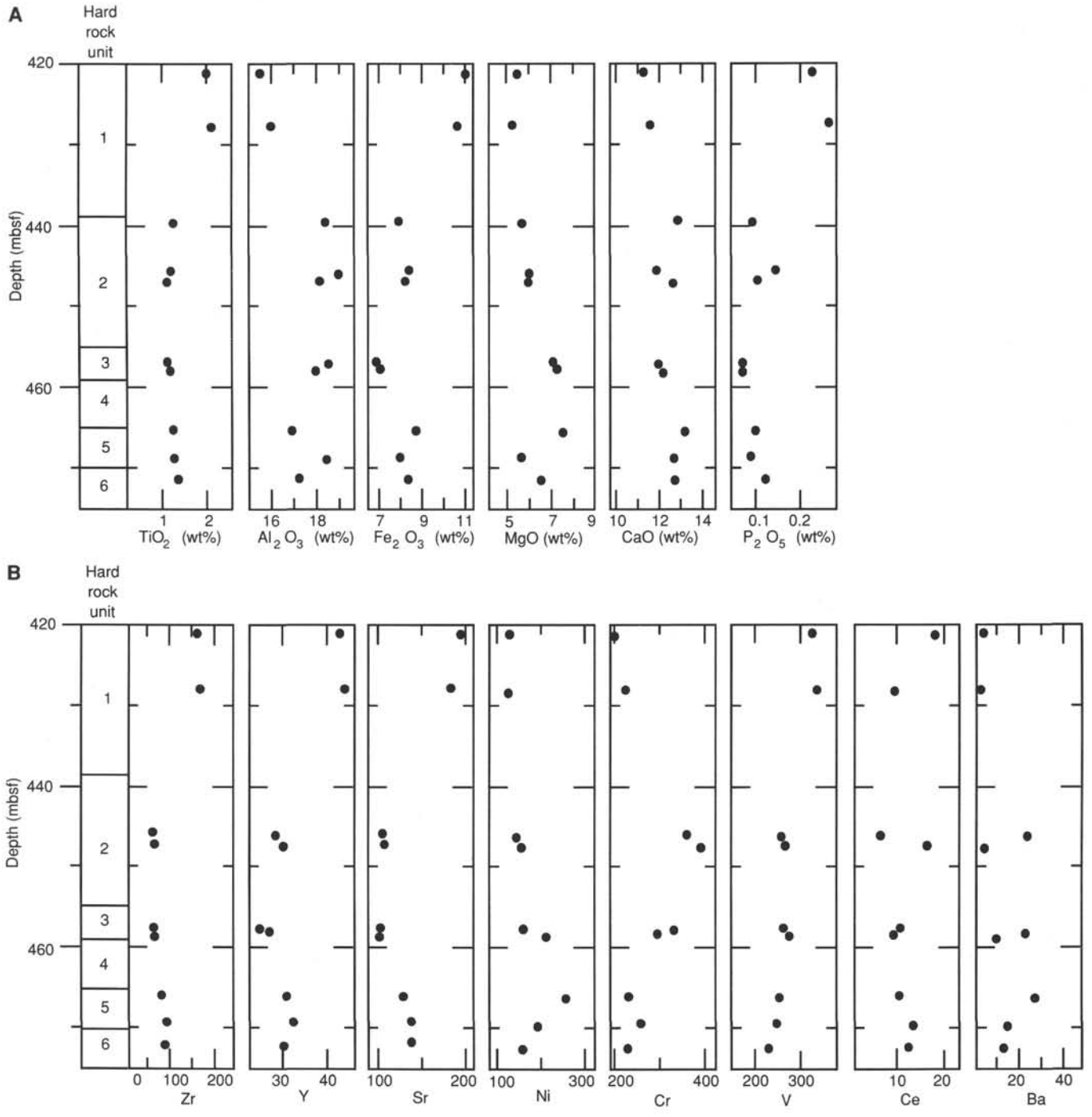

Figure 15. Downhole variations of selected major (**A**) and trace (**B**) elements in basement rocks, Hole 770B. The boundaries of the petrographically recognized hard rock units are indicated.

Preliminary interpretation of the major element chemistry indicates that the basement rocks of Site 770 are tholeiitic in composition and similar to primitive to moderately fractionated basalts of MORB type. This is confirmed by the petrographic data (i.e., by the mineralogy and crystallization sequence). Petrography suggests that plagioclase accumulation could have taken place in some porphyritic rock types, which might explain the chemical variations.

Available trace element contents (Table 14) were used to evaluate the major element variations and the magmatic affinities of the rocks studied. Marked variations were also displayed for most trace elements, with significant differences among the units distinguished by petrography, as shown in Figure 16. Two groups of rocks were recognized. The majority of the samples have low concentrations of incompatible elements and a wide range of ratios for Zr/Y, Ti/Zr, and Ti/V (Table 14). Their concentrations

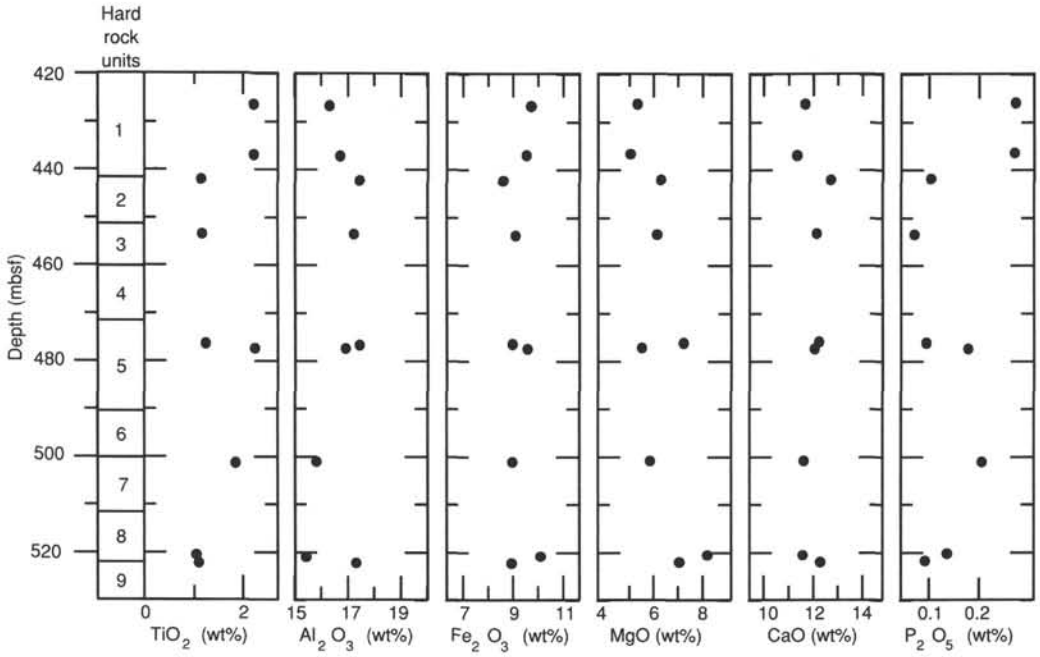

Figure 16. Downhole variations of selected major elements in basement rocks, Hole 770C. The boundaries of the petrographically recognized hard rock units are indicated.

and ratios lie in the general range of ocean-floor tholeiites (Sun, 1979; Holm, 1985). For two selected basalt samples (Samples 124-770B-20R-3, 10–15 cm, and 124-770B-21R-6, 15–18 cm), MORB-normalized minor and trace element patterns are shown in Figure 17.

A second group of samples, including basalt of Unit 1 and dolerite of Unit 6, is characterized by high concentrations of incompatible elements, which are consistent with high TiO_2 contents. Also, these rocks lie in the range of ocean-floor tholeiites, with an affinity to enriched types as indicated by the multielement pattern of a representative sample (124-770B-16R-4, 84–87 cm) shown in Figure 17. The covariations of Ti and Zr shown in Figure 18 demonstrate a clear distinction between the two groups of rocks.

The correlation of incompatible elements and their variation relative to Mg# indicate possible co-magmatic relations by fractionation processes between the two groups of rocks. We concluded preliminarily that the basement of Site 770 consists of ocean-ridge tholeiites erupted at various stages of fractionation from a common source.

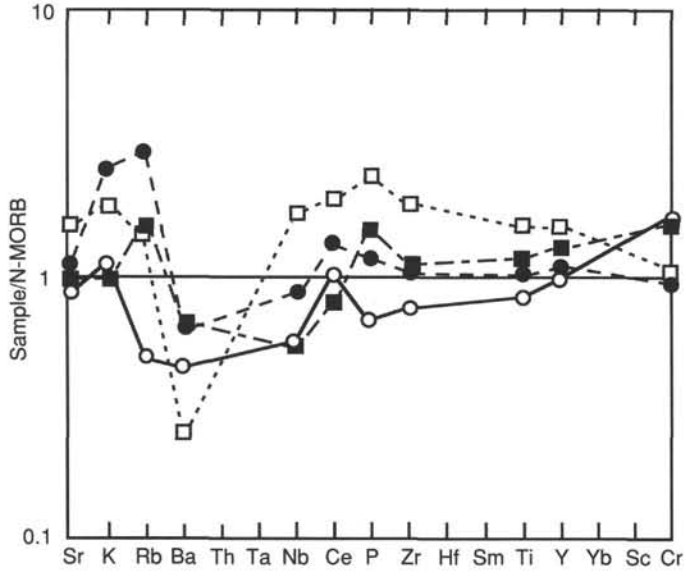

Figure 17. N-MORB normalized minor and trace element patterns of selected samples of basement rocks, Site 770. The pattern of a basalt from Site 767 is also shown for comparison. Normalizing values for normal MORB are from Pearce (1982). Closed square = Sample 124-767C-12R-CC, 36–39 cm; Open square = Sample 124-770B-16R-4, 84–87 cm; Open circle = Sample 124-770B-20R-3, 10–15 cm; Closed circle = Sample 124-770B-21R-6, 15–18 cm.

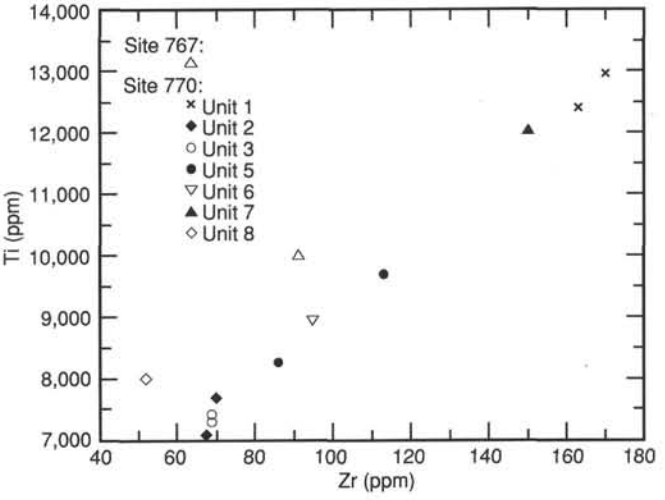

Figure 18. Ti-Zr variations of the igneous rocks from Site 770 and a basalt from Site 767.

DOWNHOLE MEASUREMENTS

Log Editing and Processing

The quality of most logs from Site 770 is very good. Logs from only three tools (velocity, lithodensity, and gamma spectrometry) required some shipboard reprocessing. Post-cruise reprocessing is warranted for these logs as well as the borehole televiewer log and the aluminum log.

The sonic velocity log exhibited severe cycle skipping in the basement and minor cycle skipping in sediments. The cycle skipping is caused by noise attributable to several sources: pulling pipe, tool drag on the borehole wall, and reverberation. Cycle skipping was aggravated by running the sonic tool without a caliper centralizer to decrease the risk of tool loss. Almost all of the cycle skipping was removed (Figs. 19 and 20) by reprocessing (see "Explanatory Notes" chapter, this volume). Eight short zones of 0.15–1.0 m length had no reliable velocity data; simple linear interpolation was applied across these intervals. Waveform processing is likely to improve the velocity log further, particularly in basement.

Raw logs from the gamma spectrometry tool were reprocessed as described in the "Explanatory Notes" chapter (this volume), with the representative interval from 214.3 to 305.7 mbsf used as a basis for removing the chlorine correlation. The normalized counts are used in Figures 21 and 22. Because all three Schlumberger strings were run at this site, post-cruise reprocessing should be able to convert from elemental count rates to dry-weight percentages of elements (see "Explanatory Notes" chapter, this volume). The raw aluminum log exhibited occasional spikes to high values, caused by inadequate speed correc-

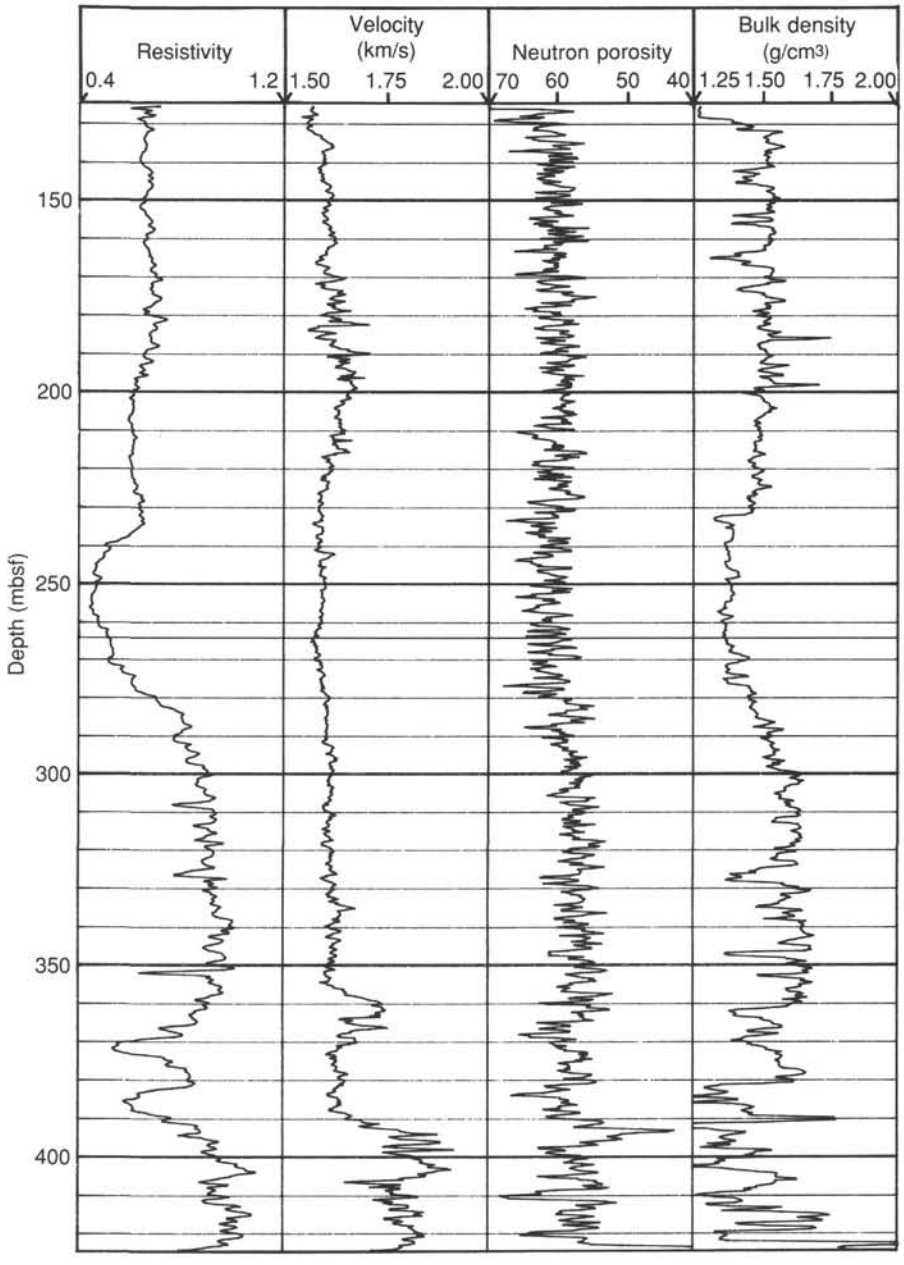

Figure 19. Logs of resistivity, velocity, neutron porosity, and bulk density in the portion of the Site 770 sedimentary sequence for which open-hole logs were obtained.

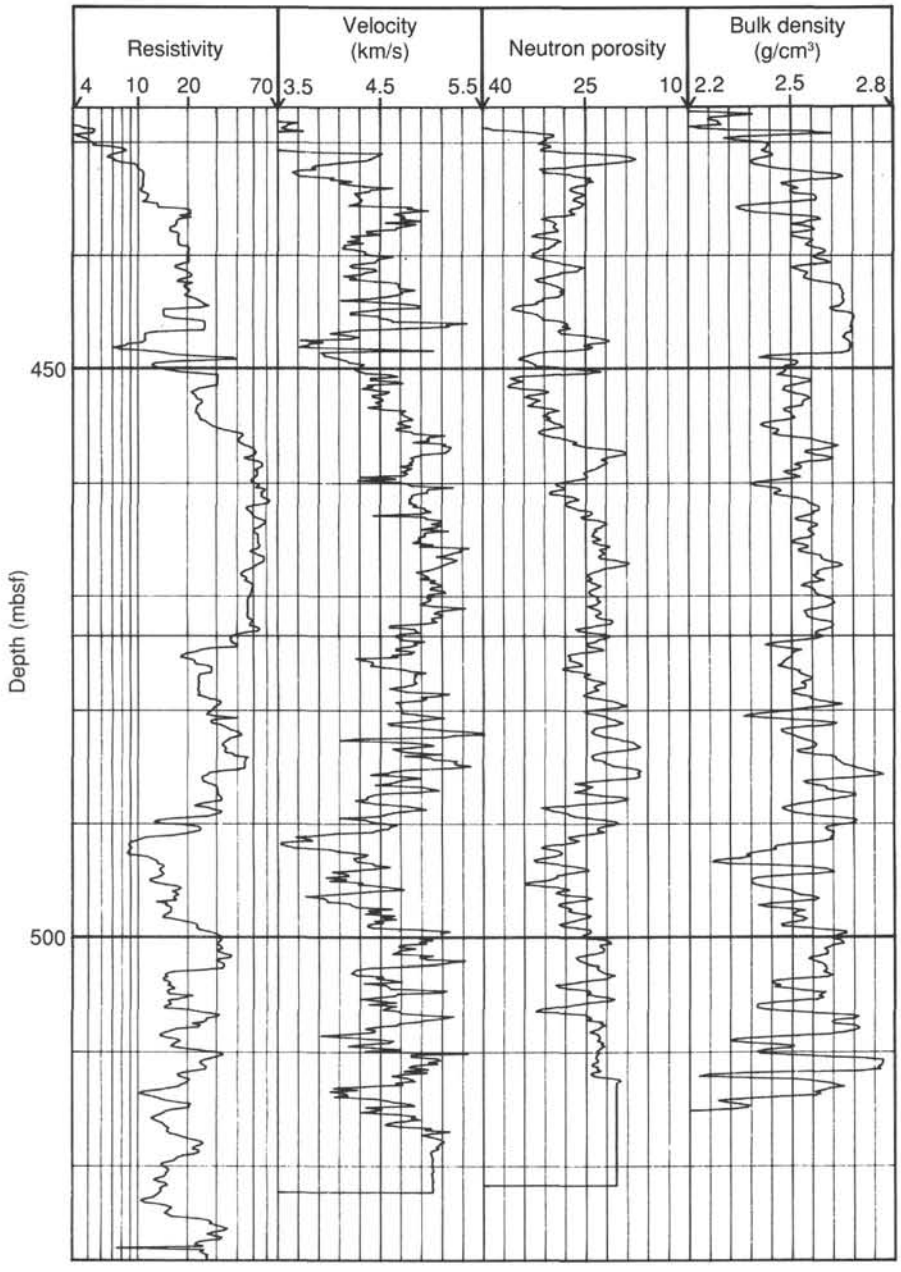

Figure 20. Logs of resistivity, velocity, neutron porosity, and bulk density for the basement section of Site 770.

tions in sticky portions of the hole. More accurate speed corrections are possible post-cruise.

The first two runs of the lithodensity tool (repeat basalt section and main log) yielded incorrect near-count rates caused by self-calibration on the wrong peak. Therefore, densities calculated with near- and far-count rates are much too low. Densities in Figures 19 and 20 use only the far-count rate and are generally reliable, except for somewhat greater sensitivity to borehole rugosity than is normal. However, densities for the interval from 361 to 427 mbsf are too low, on the basis of comparisons with other porosity-sensitive logs (Fig. 19) and to core densities (see "Physical Properties" section, this chapter). A short repeat section (126–232 mbsf) with reliable near-count rates well replicated the density values shown.

Two types of spurious spikes are obvious in some logs. Logging while pulling pipe requires careful coordination between the logging winch and drill floor. This coordination was imperfect on two occasions, and the top portion of the geochemical tool string entered the pipe temporarily. These excursions are evident as spikes at 150 and 320 mbsf on the two highest tools on this tool string: gamma ray (Fig. 23) and hole deviation (Fig. 24). The geochemical tool string was kept nearly stationary in the interval from 450 to 463 mbsf for 50 min while a telemetry problem was diagnosed and corrected. During this time, the adjacent pipe and formation were irradiated by the aluminum clay and gamma spectrometry tools. The memory of this formation irradiation creates a pair of very large spikes on the open-hole gamma-ray log obtained later by the same tool string in the interval from 450 to 463 mbsf (Fig. 23). The memory of pipe irradiation creates similar spikes at 48–60 mbsf on the same log, because the pipe was pulled to a shallow depth for through-pipe logging of the interval from 125.6 to 0 mbsf. Substantial irradia-

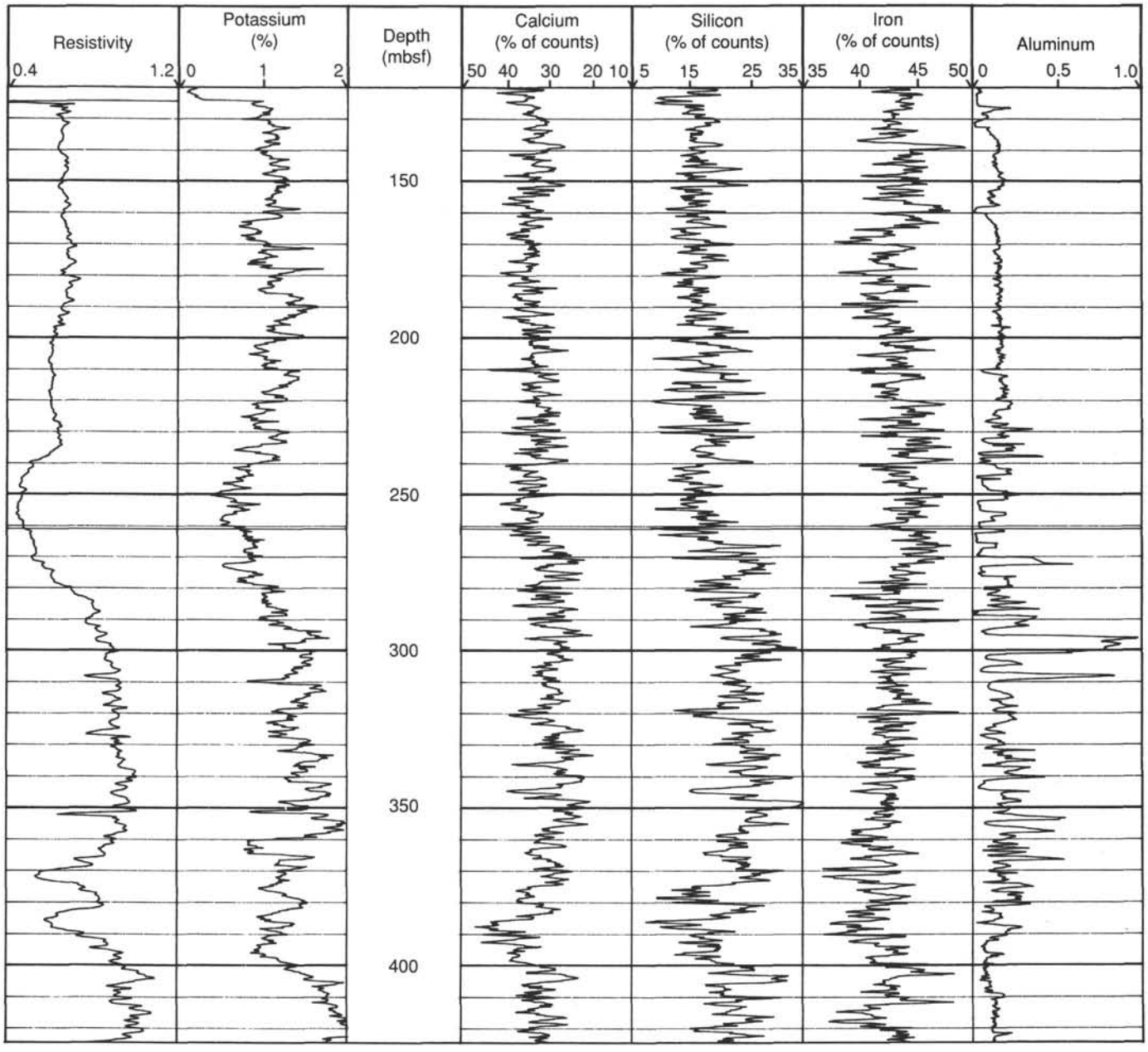

Figure 21. Geochemical logs for the portion of the Site 770 sedimentary sequence for which open-hole logs were obtained. Calcium, silicon, iron, and aluminum are expressed as uncalibrated relative abundances.

tion memory was retained even 18 hr later, as evidenced by similar but smaller gamma-ray spikes during logging with the lithoporosity tool string (Fig. 23).

All logs were depth shifted on the basis of pipe and seafloor depths. However, differential depth shifts of 1 m or perhaps more may be present within logs because of the cable stretching sometimes associated with sticky hole conditions (see "Explanatory Notes" chapter, this volume). For example, slight differences in the depth of the sediment/basement contact are evident on the three gamma-ray runs of Figure 23. Continuous depth shifting similar to that employed at Site 767 (see "Site 767" chapter, this volume) is warranted but has not been applied yet.

Only minimal pipe corrections of through-pipe logs have been undertaken. Spectral gamma-ray data (shown after the barrel sheets at the back of the book) for the interval from 0 to 122 mbsf have been reprocessed and then corrected within certain approximations for pipe attenuation by applying offsets. A more accurate subsequent pipe correction for the geochemical logs is possible, given the comparison of through-pipe and open-hole logs obtained over the same interval from 449.5 to 236.5 mbsf. In the preliminary interpretations that follow, only the open-hole interval below 122 mbsf is considered.

Sedimentary Units

Much of the sedimentary sequence at Site 770 was only spot cored. Thus, the continuous log records will be particularly important for determining lithologic variations in the uncored intervals.

Unit I (0–296.05 mbsf) consists of volcanogenic silty clay and clay, with rare thin beds of marl and ash. In general, the upper 200 m is dominantly silty clay, grading into clay in Cores 124-770B-6R (244.1–253.7 mbsf) and -7R (292.4–302.1 mbsf)

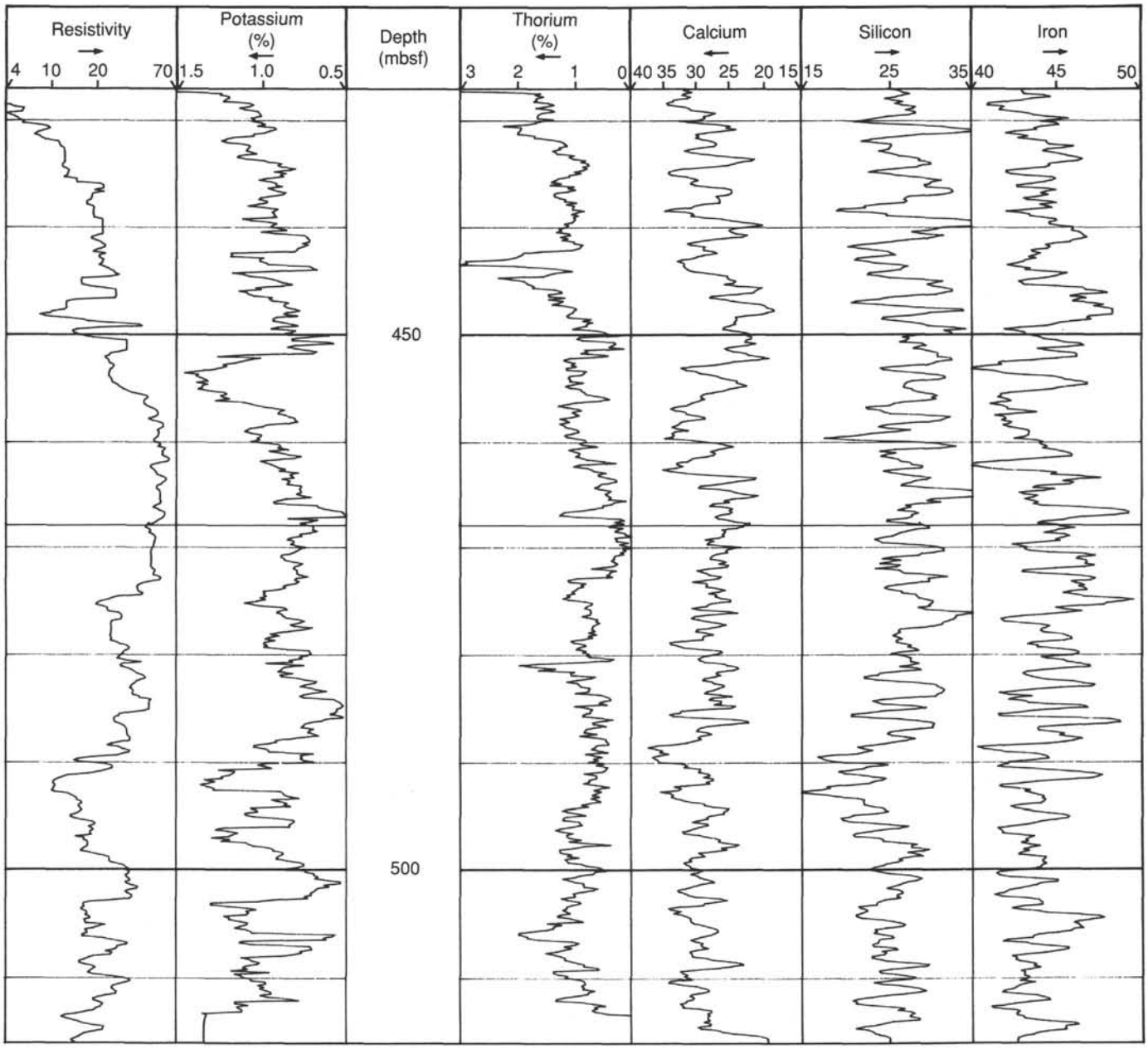

Figure 22. Geochemical logs for the Site 770 basement section. Calcium, silicon, and iron are expressed as uncalibrated relative abundances.

(see "Lithostratigraphy" section, this chapter). On the basis of the log responses, Unit I is composed of three subunits: 0–232, 232–277, and 277–293 mbsf.

The interval from 0 to 232 mbsf is quite uniform in physical properties (Fig. 19) and geochemistry (Figs. 21 and 23). Three exceptions are the gamma-ray peaks at about 36–40, 175, and 187 mbsf; slight depth shifts on different gamma-ray runs (Fig. 23) make these depths approximate. These three beds are probably thin clays, given the higher gamma-ray and porosity values they have than the adjacent silty clays. The small-scale variations that occur within the interval from 0 to 232 mbsf are probably caused primarily by variations in clay content.

The interval from 232 to 277 mbsf is higher in porosity and lower in density and resistivity than adjacent units (Fig. 19). This interval is most distinctive on the resistivity log, which exhibits the lowest resistivities in the interval from 246 to 258 mbsf, with flanking gradual rises toward the higher resistivities of adjacent subunits. This subunit is very low in potassium and apparently is also low in silicon and high in iron. A change from silty clay to clay is indicated by the porosity-sensitive logs (Fig. 19) and by spot cores. A change in composition is also evident from the geochemical log responses (Fig. 21). The change may be a clay mineralogy change toward greater smectite and lower illite in the interval from 232 to 277 mbsf compared with the bracketing intervals. Post-cruise geochemical log reprocessing followed by mineralogy inversion will provide a much more quantitative picture of the clay mineralogy changes.

The interval from 277 to 293 mbsf is a gradual transition from the high-porosity and low-potassium clays of the overlying subunit to the claystones of Unit II. The porosity decrease and density increase within this interval are too abrupt to be attributable to normal compaction. They are probably caused by a change in clay packing from the looser and more random packing of smectite above to the more parallel packing of illite be-

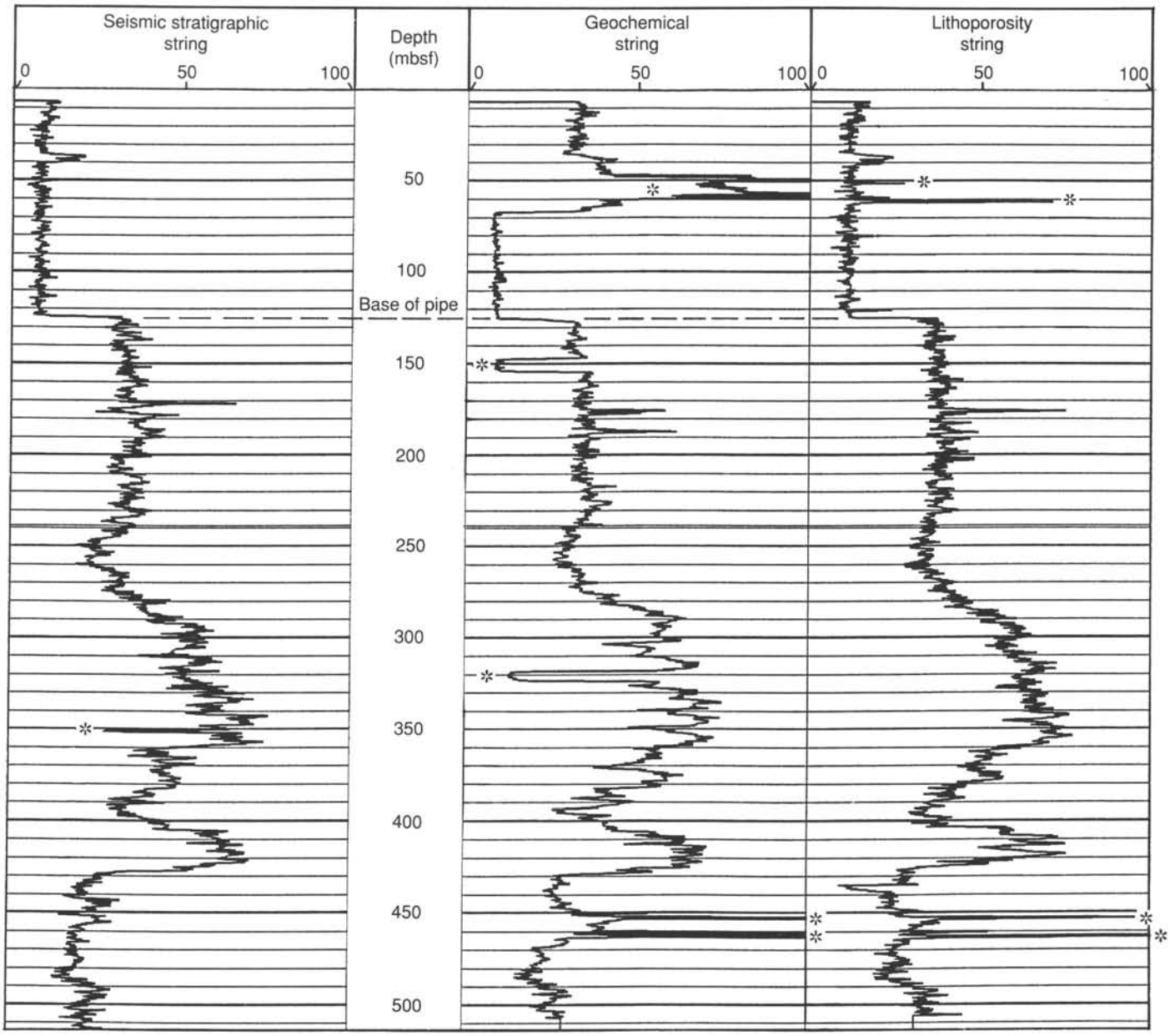

Figure 23. Comparison of the gamma-ray logs obtained on the three Schlumberger tool strings. See text for discussion of the spike artifacts (indicated by an asterisk).

low. A gradation from hemipelagic lower Unit I to pelagic Unit II is seen in spot cores (see "Lithostratigraphy" section, this chapter).

Unit II (296.05–420.9 mbsf) is composed of claystone and calcareous claystone. Three subunits are defined on the basis of variations in carbonate content. Subunits IIA (296.05–388.2 mbsf) and IIC (401.15–420.9 mbsf) are dominantly claystone with low carbonate content, whereas Subunit IIB (388.2–401.15 mbsf) is nannofossil claystone with up to 38% calcium carbonate (see "Lithostratigraphy" section, this chapter). On the basis of the log responses, Subunit IIA depths would be revised to 293–385 mbsf, Subunit IIB to 385–399 mbsf, and Subunit IIC to 399–427 mbsf.

Downhole logs indicate that Subunit IIA has two distinctive subintervals. The upper portion, from 293 to 360 mbsf, is marked by variable but gradually increasing potassium and resistivity (Fig. 21), corresponding to a continuation of the trend of downhole illite enrichment noted in the overlying unit. This trend is especially obvious on the gamma-ray logs of Figure 23. At 360 mbsf a sudden drop in potassium and gamma ray occurs. The lower portion of Subunit IIA, from 360 to 385 mbsf, has higher velocities and lower densities than the upper portion (Fig. 19). The cause of this unusual behavior is not known, although the high ash content could account for it.

The high calcite content of Subunit IIB is evident on the calcium log. The interval from 385 to 399 mbsf has the highest calcium counts of the entire sedimentary sequence at Site 770 (Fig. 21) and is shown in more detail in Figure 25. Calcium increases parallel decreases in potassium and thorium in this interval, indicating dilution of the clay-mineral component by calcite.

Subunit IIC includes a transition zone from 399 to 409 mbsf of increasing potassium and thorium (Fig. 25), overlying a uniform illite-rich clay from 409 to 427 mbsf. The contact with basement is tentatively placed at 427 mbsf, but it is subject to a

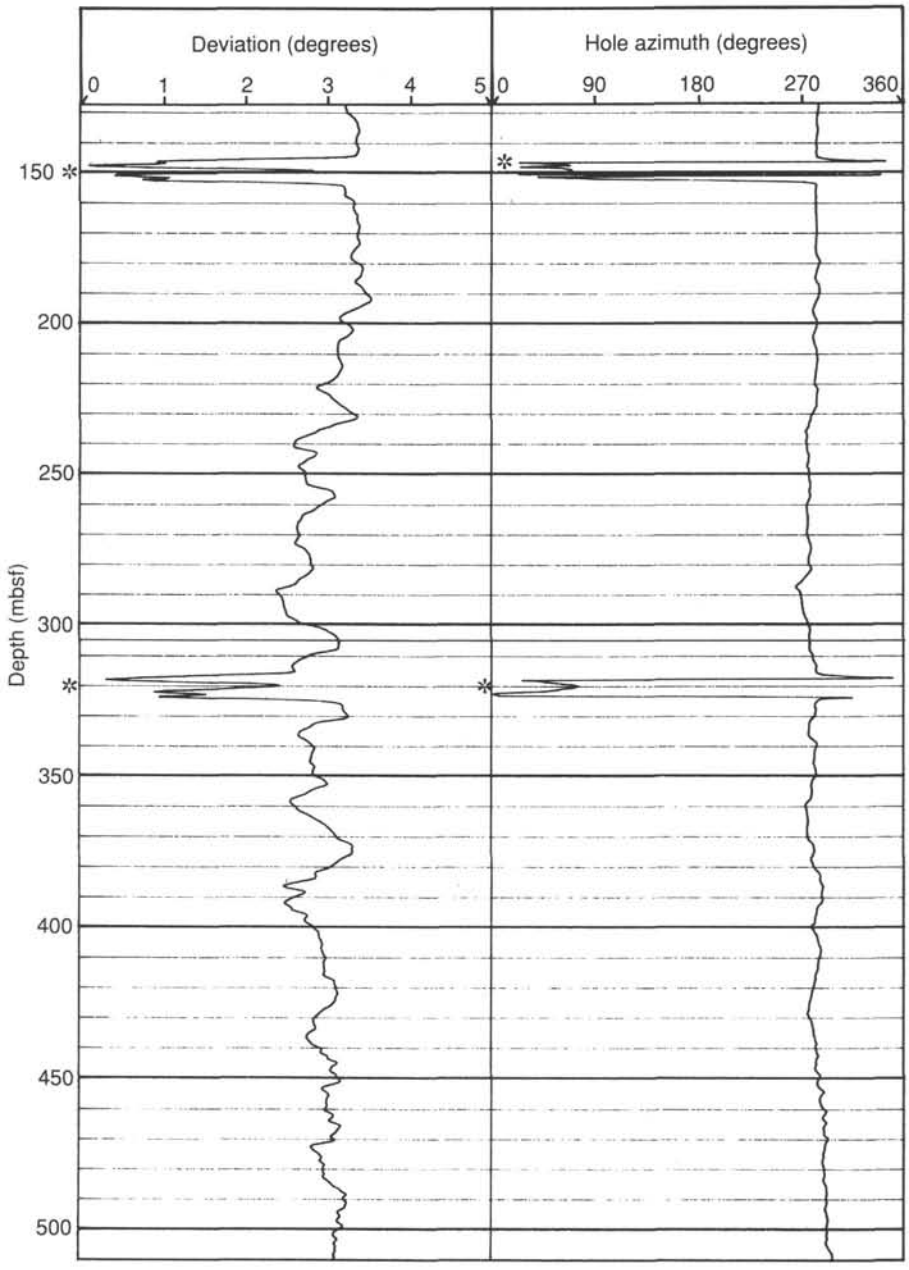

Figure 24. Hole deviation and the azimuth of that deviation, Hole 770C. Spikes (shown by an asterisk) are artifacts caused by the brief entry of part of the tool string into the pipe (see text).

2-m uncertainty because of residual depth shifts among the logs. The top of basement is certainly deeper than the estimate of 420.9 mbsf determined from the incomplete core recovery.

Basement

The basement at Site 770 was logged with geophysical (Fig. 20) and geochemical logs (Fig. 22). In addition, a three-component magnetometer (see "Explanatory Notes" chapter, this volume) was run (Fig. 26).

Geophysical properties of the igneous rocks of Site 770 are markedly different from Site 768 (see "Site 768" chapter, this volume) and typical upper oceanic crust. Compressional wave velocities are an unusually high 4–5 km/s, and this massive behavior is confirmed by very high resistivities (Fig. 20). Average density is 2.5–2.6 g/cm^3. In view of the high velocity and resistivity, the neutron porosity of 15%–35% must be almost entirely associated with bound water in clays rather than with free water in pores. All of the geophysical properties are consistent with basalts that have undergone advanced hydrothermal alteration with accompanying cementation. Substantial variations are evident within the penetrated section (Fig. 20). For example, the intervals from 455.5 to 474.5 mbsf, 484.0 to 485.3 mbsf, and 499.5 to 502.5 mbsf are particularly massive, and the uppermost interval from 427 to 436 mbsf is particularly porous.

A detailed interpretation of major-element geochemical variations must await the reprocessing of the geochemical logs. However, estimated potassium and thorium concentrations are unlikely to be changed significantly by reprocessing. Potassium and thorium are poorly correlated in the basement (Fig. 22), unlike in the overlying sediments. The thorium probably has been little affected by alteration, whereas nearly all of the potassium was removed from seawater during alteration. Consequently, a

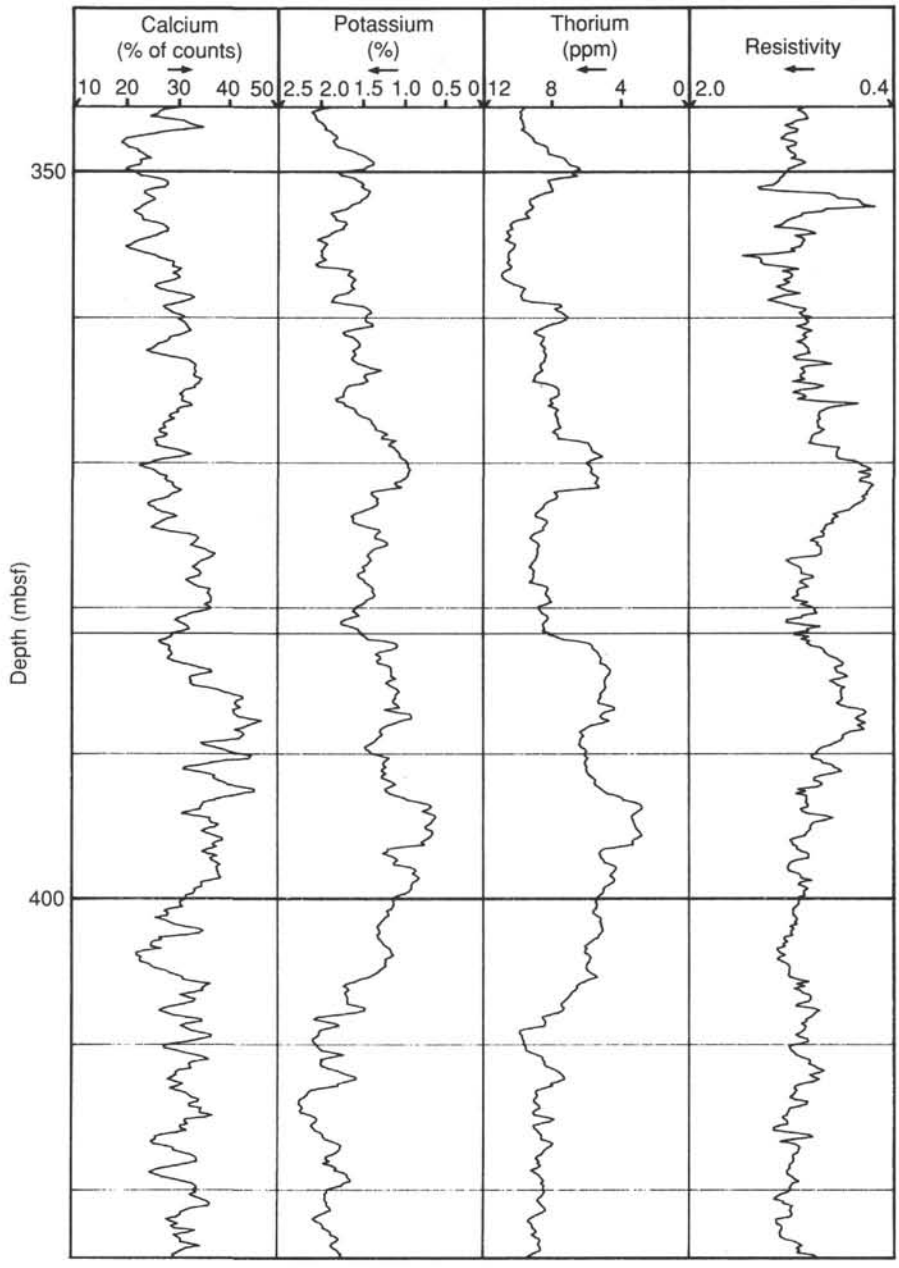

Figure 25. Expanded log plot for the lower portion of sedimentary Unit II, showing relative variations in the amount of calcium carbonate (calcium log) and clay minerals (potassium and thorium logs).

general inverse correlation is observed between resistivity and potassium, as expected if alteration is greatest in the least massive units. This pattern is the opposite of what would be expected from heterogeneous alteration-related cementation of an originally homogeneous-porosity sequence. Consequently, alteration has increased velocity and resistivity values but has not obscured the original heterogeneity in porosity.

Magnetometer records in the basement (Fig. 26) exhibit substantial character, with generally stronger magnetizations above 471 mbsf than below. These raw logs require some caution in interpretation, as slight variations in tool tilt can affect them. The hole deviation survey (Fig. 24), obtained by the same tool as the magnetometer record, shows oscillations of as much as 0.5°, which probably reflect tool wobble rather than true variations in hole deviation. Nevertheless, the overall hole deviation is clearly a fairly uniform 2.5°–3.0° to the west (Fig. 24) below 127 mbsf. Similarly, although tool wobble may cause some of the variation observed in the magnetometer record, it is not responsible for the overall magnetic pattern. The general inverse pattern of moment and inclination is most easily explained as a normal polarity with negative inclinations, implying crustal formation south of the equator.

The basement basalts and diabases of Site 770 have been subdivided into nine units (see "Basement Lithology" section, this chapter). We quote only approximate depths as described in cores for these units, but we do note that basement core recovery was only about 50%. Much more accurate depths can be determined from the logs after final depth justifications of the logs are undertaken.

The pillow lavas of Unit 1 (420–440 mbsf) exhibit gradual downhole increases in magnetization, density, and resistivity and a corresponding potassium decrease indicative of gradually

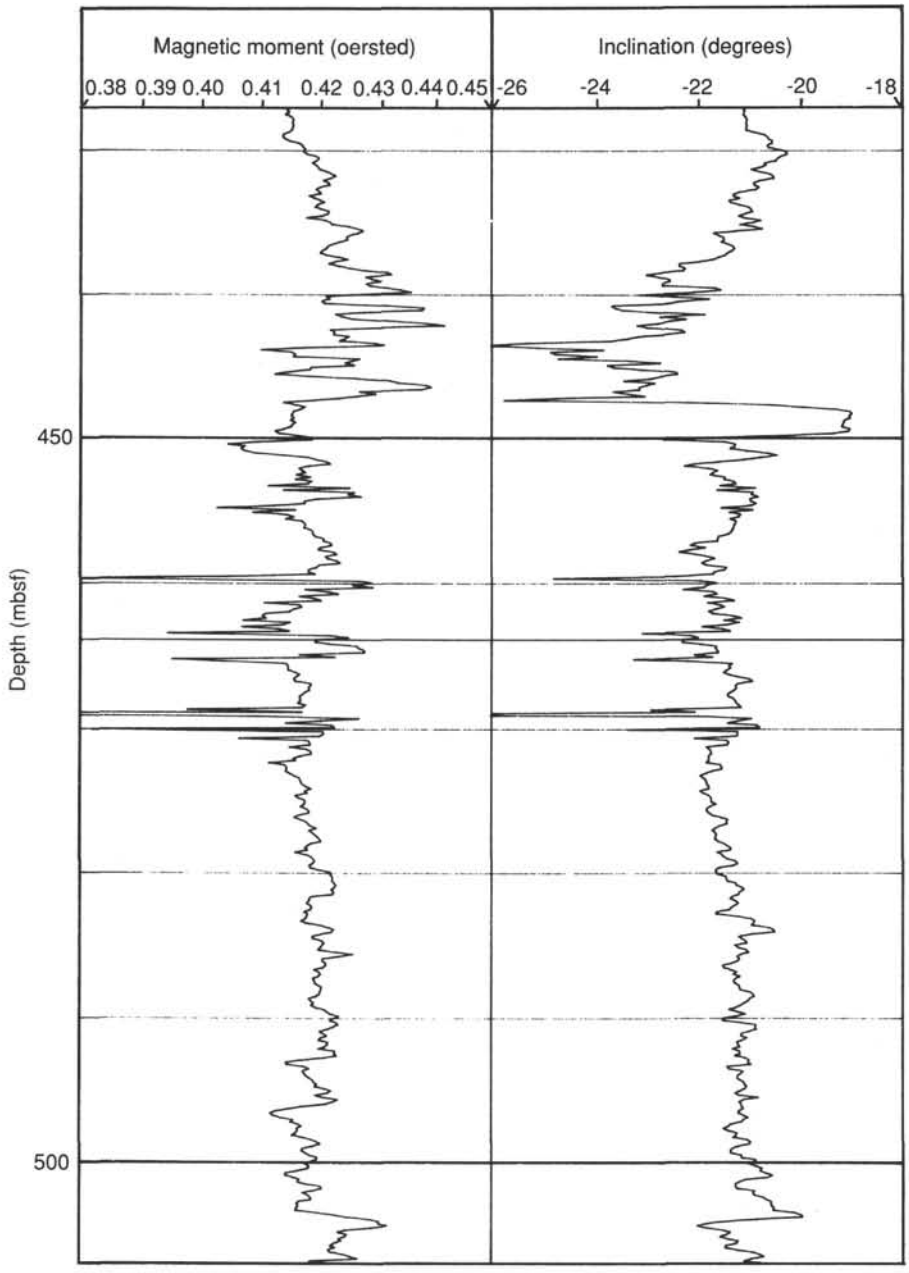

Figure 26. Magnetic logs for the Site 770 basement section.

decreasing alteration. A sharp drop in thorium and change in magnetization mark the contact with Unit 2 at 443 mbsf. The pillow lavas and breccia of Unit 2 (440–450 mbsf) are quite heterogeneous, with a general downhole increase in thorium and with high calcium and iron. The interval from 447.6 to 450.0 mbsf may be of opposite (reversed?) polarity. A further thin subinterval from 443 to 444 mbsf is strongly magnetic and very low in thorium. The brecciated and veined lavas of Units 3 (450–460 mbsf) and 4 (460–470 mbsf) are very massive, with high resistivity and velocity and low neutron porosity. Little addition of potassium to this unit has occurred. Magnetization is heterogeneous, and several very thin, very strongly magnetic zones are evident.

The pillow lavas and pillow breccia of Unit 5 (470–490 mbsf) are lower in resistivity and magnetization than are Units 3 and 4, yet they are similar in neutron porosity, density, and potassium. The basalt lavas and dikes of Unit 6 (490–500 mbsf) are more porous, weathered, and uncemented than Units 3–5, on the basis of the very low resistivity, density, and velocity and high neutron porosity. The base of Unit 6 is probably 499 mbsf rather than 501 mbsf, given the log responses. The "sills" of Units 7 (500–513 mbsf) and 8 (513–524 mbsf) may actually be an alternation of 1–5-m-thick massive sills and much more porous pillows, given the blocky, bimodal character of the log responses. Unit 9 (524–530 mbsf) was not reached by most logging tools.

STRESS MEASUREMENTS

Stress orientation was measured at Site 770 with the BHTV (see "Downhole Logging" section, this chapter, and "Explanatory Notes" chapter, this volume) to observe the ellipticity of the hole and occasional breakouts. The acoustic intensity pattern recorded by the televiewer allows determination of the shape of the borehole. If the tool were centered in a circular hole of con-

stant reflectivity at all azimuths, the record would be uniformly bright. The televiewer records in the basement showed a consistent pattern of a weakly reflective sector, 90° in width, within a stronger reflectivity record. Down the center of the weakly reflective zone is a narrow line of high reflectivity. This pattern can be interpreted as the result of poor reflectivity along the semi-major axis of the ellipse, on the far side of the asymmetrically hanging tool. The narrow line of high reflectivity would be caused by reflection along the exact axis of the ellipse, giving us a very precise indication of the shape of the hole. This interpretation is supported by the observation that in some instances the two broad, dark areas of low reflectivity coalesce into one, more narrow band, indicating the start of a breakout.

An alternate explanation for the reflectivity pattern is also possible. The pattern may indicate an off-center placement of the tool caused by the departure of the hole from vertical. A deviation of 3° was measured in the basement. The azimuth of this deviation was 290°. As the long axis of the ellipse (see below) lies at an azimuth of 136 (316)°, it seems unlikely that hole deviation is responsible for the asymmetric reflectivity pattern seen in the BHTV record at Site 770.

The orientation of the long axis of the ellipse and the direction of the breakouts, where present, were measured in 38 locations along the record. Most of the measurements were made at regular 1.5-m intervals. The range of measurements varied from 120° to 155°, with a mean of 136° and a standard deviation of 7.6°. This orientation marks the direction of the minimum horizontal stress axis, and the maximum horizontal stress direction lies at right angles to it, with a mean of 046°. The range of values lying within one standard deviation is 039°–054°.

A northeast trend for the maximum horizontal stress axis is consistent with the trend of the Cagayan and Sulu ridges, which are colliding with the Philippine Mobile Belt. It is likely that this collision is responsible for imparting deviational stress not only to the ridges but also to the intervening basins. This trend is nearly normal to that of the Cotabato Trench. It lies about 20° to the east of the maximum horizontal stress direction measured in the Sulu Sea at Site 768 (see "Stress Measurements" section, "Site 768" chapter, this volume). Should these differences be borne out after careful post-cruise analysis, they may indicate a change in the stress field toward the south, possibly caused by the influence of the Molucca Sea collision zone.

It should be emphasized that these data are only preliminary and will be extensively reprocessed after the cruise. At that time it is possible that some of the conclusions here will be altered.

SEISMIC STRATIGRAPHY

Site 770 is located on multichannel seismic Line SO49-02 acquired on board the *Sonne* in April 1987 and processed by the BGR in February 1988 (see Hinz and Block, this volume). In addition, pre-site single-channel seismic reflection data were shot on board the *JOIDES Resolution* prior to drilling on 20 December 1988 (see Lewis et al., this volume). *Sonne* navigation was obtained with transit satellites, Loran C, and doppler sonar. The *JOIDES Resolution* used the GPS for the entire survey.

Site 770 is located on a slightly uplifted fault block within the Celebes Basin, 45 km northeast of the Site 767 location. The water depth over Site 770 is 4505 m, or 400 m above the level of Site 767. The trend of the fault block is not well constrained, but given the tentative correlation between Line SO49-2 and the seismic line of the *JOIDES Resolution*, we mapped a trend of 063° (Fig. 27), or parallel to that of the magnetic anomaly pattern found to the southwest (Weissel, 1980). The bounding fault lies to the southwest of Site 770, and the tip of the scarp appears to crop out at the seafloor (Fig. 28).

The sedimentary section is divided into two seismic sequences (Fig. 29). Seismic Sequence 1 is 380 m thick and comprises most

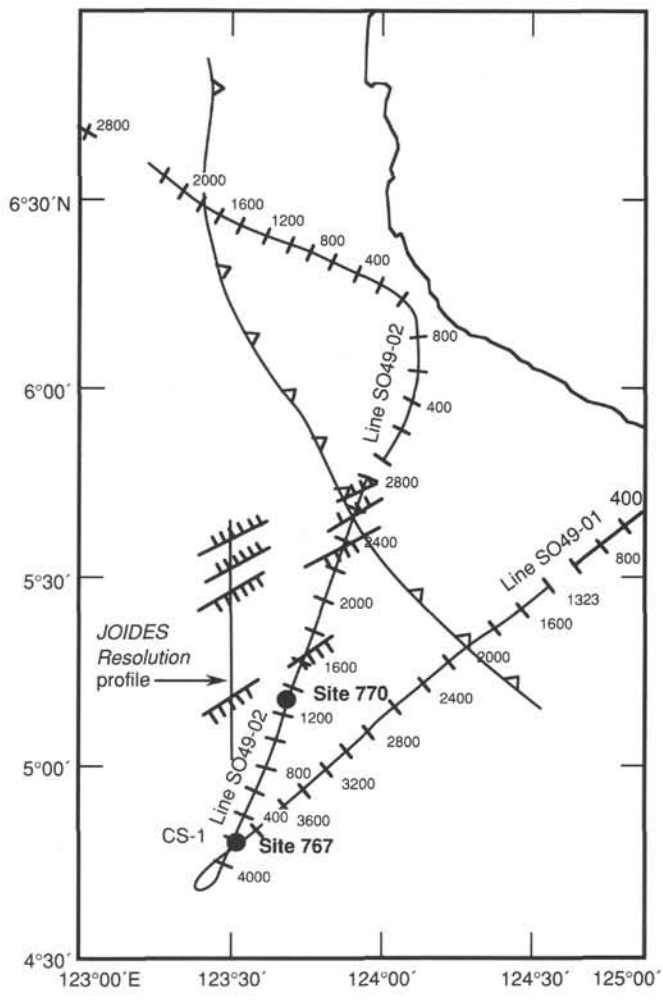

Figure 27. Tracks of the *Sonne* and *JOIDES Resolution* in the Celebes Sea, showing the location of Site 770. Also shown are the possible orientations of faults mapped on these profiles.

of the section here. It is weakly reflective and appears to be pelagic in origin. It has a clay or silty clay composition, with occasional marly interbeds. Seismic Sequence 2 shows up as a weak reflector on the *JOIDES Resolution* seismic line (Fig. 30). The sequence is 35 m thick and is composed of carbonate-rich ooze and clays. The difference in measured velocities between the ooze and the clay is very slight, indicating that the strong reflector at the base of the section on the *Sonne* line is not the interface between these two sequences. The basalt velocity is about 5 km/s and produces a strong contrast with the sediments.

The difference in traveltimes to basement on the *JOIDES Resolution* line (0.5 s) and the *Sonne* line (0.45 s) may indicate a rapid change in sediment thickness over a small area in the vicinity of the site. The small difference in location caused by inaccuracies in reading the *Sonne* track map may be enough to produce the observed differences in thickness.

SUMMARY AND CONCLUSIONS

The objectives of Site 770 were to obtain basement rocks and log records within basement at a location close to Site 767, which had to be abandoned just after hitting basement. Except for the lack of a packer run, the objectives were satisfied very well here.

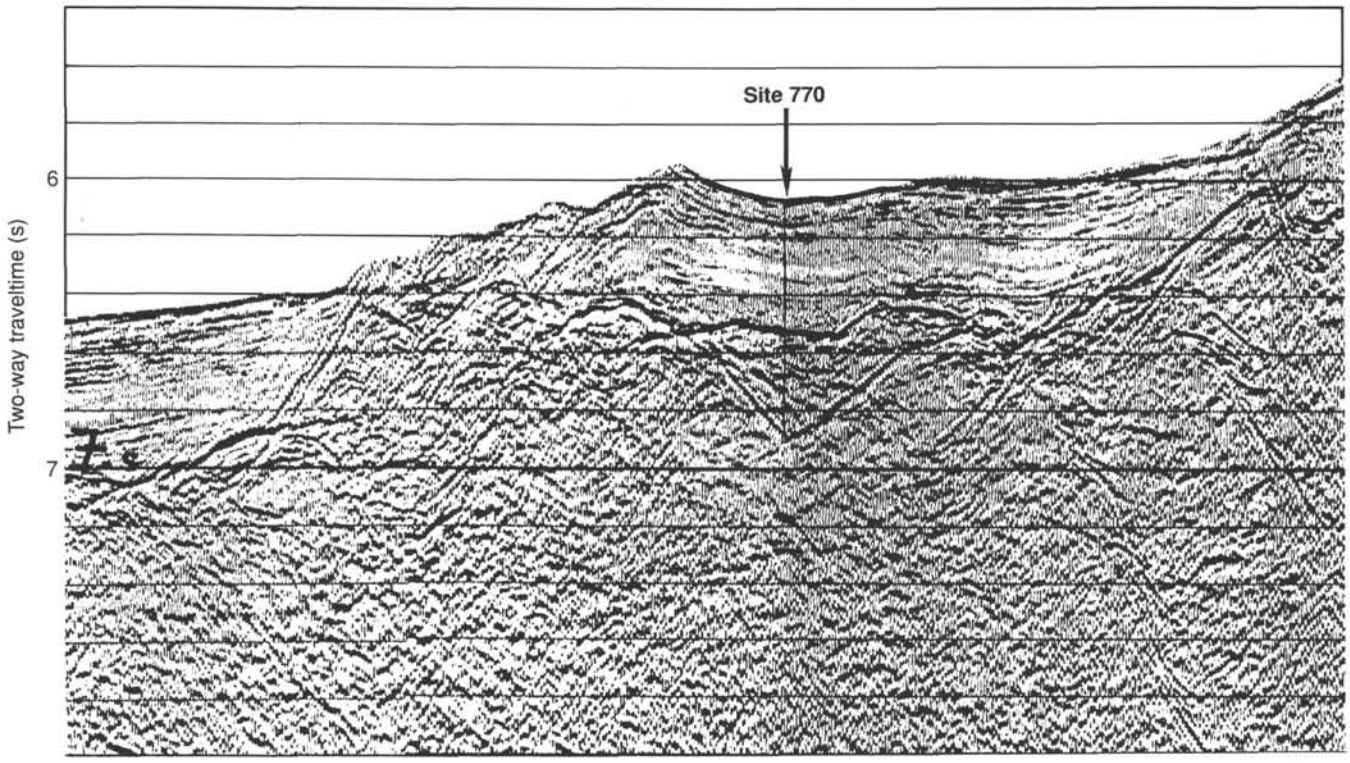

Figure 28. Multichannel seismic reflection profile of Line SO49-2, showing the location of Site 770.

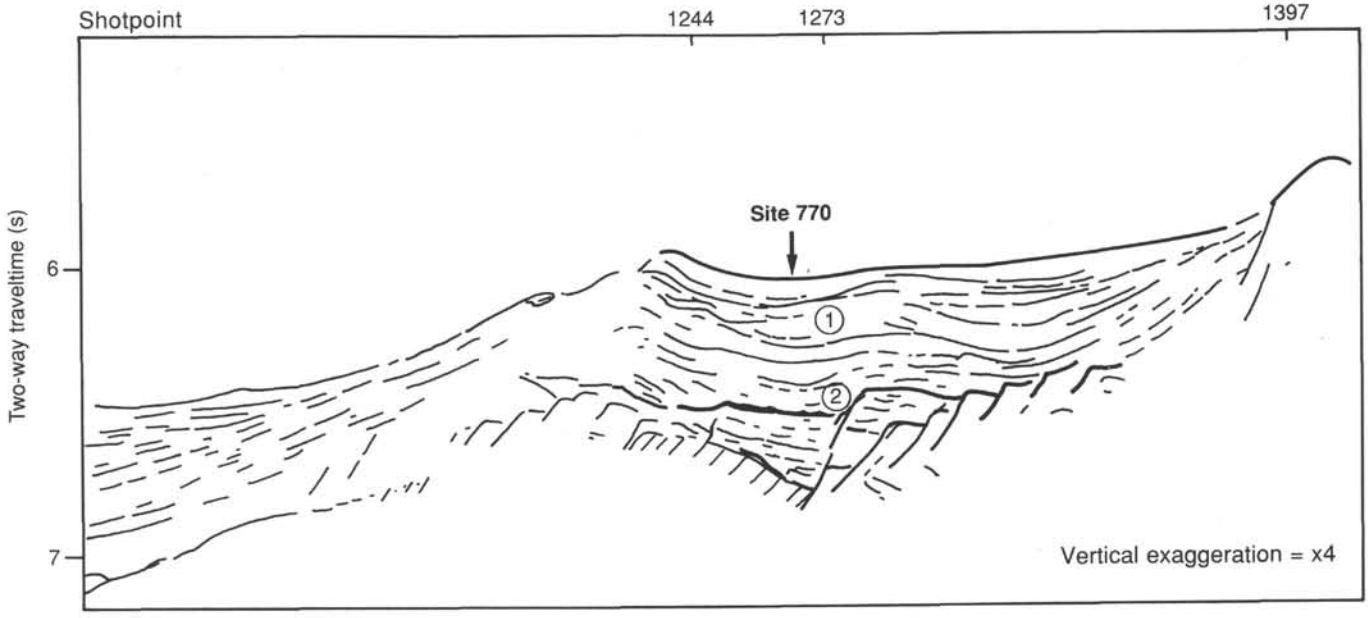

Figure 29. Line-drawing interpretation of seismic reflection profile of Line SO49-2.

Site 770 consists of two main lithologic units:

Unit I (0–296 mbsf) is middle(?) Miocene to Holocene in age, with dominant rock types composed of volcanogenic silty clay and clay with sparse thin beds of marl and volcanic ash.

Unit II (296–421 mbsf) is late middle Eocene to middle(?) Miocene in age and consists of claystone and calcareous claystone, with sparse interbeds of silty to sandy claystone and porcellanite clay mixed sediment. The unit is divided into three subunits, mainly on the basis of carbonate content.

Subunit IIA (296–388 mbsf) is late Oligocene to middle(?) Miocene in age. Claystone is the dominant lithology, but the subunit also contains minor interbeds of volcanogenic claystone with silt, sand, and porcellanite-mixed sediment. The claystone is grayish brown in the upper part, becoming brown to yellowish brown in the lower part.

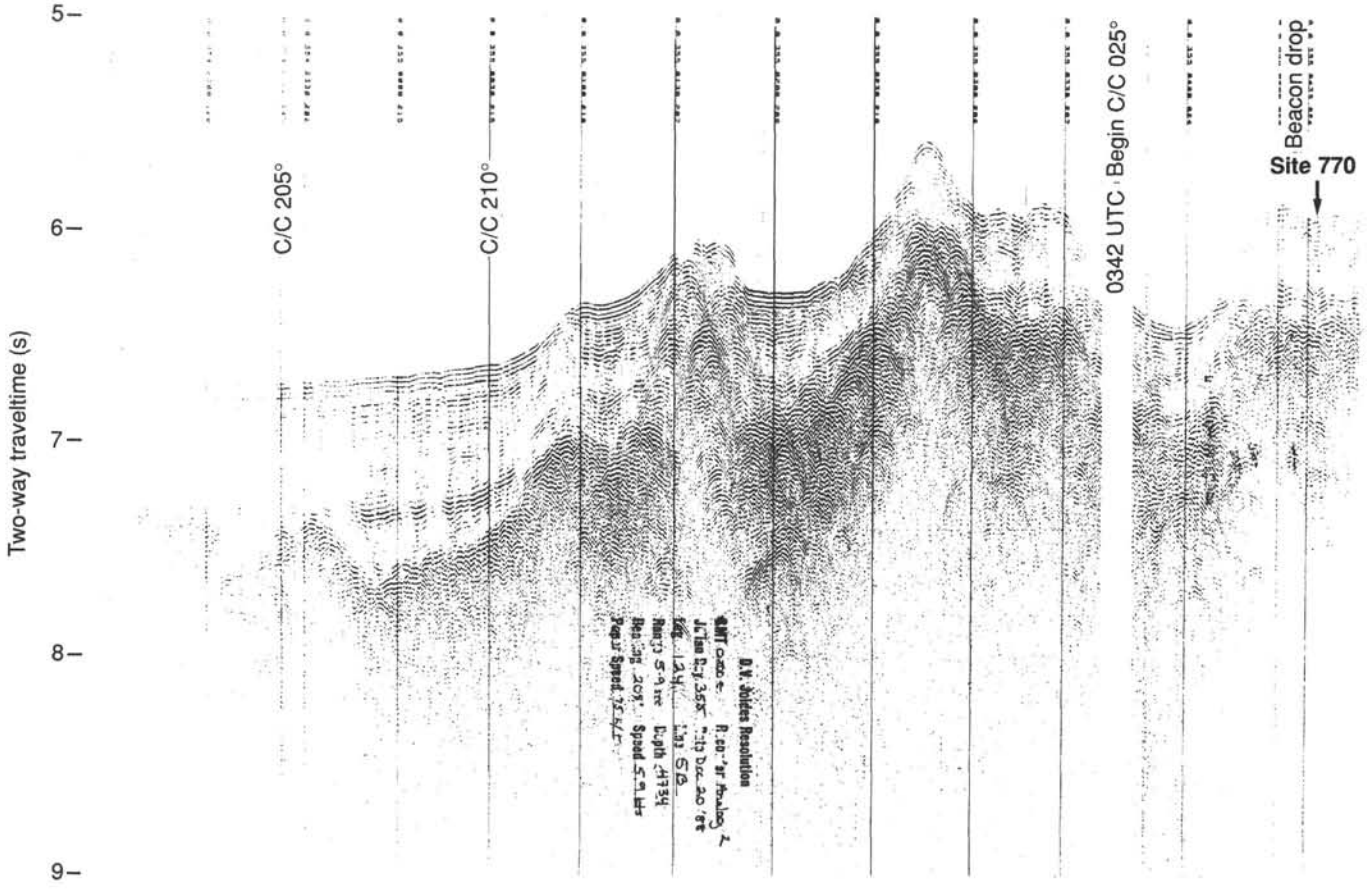

Figure 30. Single-channel seismic reflection profile from *JOIDES Resolution*, showing the location of Site 770.

Subunit IIB (388–401 mbsf) is early to late Oligocene in age and consists of pale brown nannofossil claystone with carbonate contents up to 38%. It is interpreted to be pelagic in origin.

Subunit IIC (401–421 mbsf) is late middle Eocene to early Oligocene in age. The upper part of the subunit consists of brown claystone and nannofossil claystone with a lower carbonate content than Subunit IIB (maximum of 25%). The lower part, which overlies basement, is made up of sandy clay and silty claystone.

The sedimentary section at Site 770 is about half the thickness of Site 767, yet the basal ages are identical. The difference reflects the higher elevation of Site 770, which protects the site from turbidite influence and allows it to lie just above the CCD in the lowest part.

Basement was recovered from 421 to 529 mbsf. We were able to identify nine lava units by means of their mineralogy, texture, and structure. Units 1 and 2 are pillow basalt sequences, Unit 3 is a pillow breccia, and Units 4, 5, and 6 are brecciated, massive, amygdaloidal lavas. In Hole 770C, Unit 6 is a massive lava or lavas that show penetration by a number of flat-lying minor intrusions. Units 7 and 8 are identified as sills, and Unit 9 is made up of lavas penetrated by small dikes. The boundaries, rock types, and thicknesses of these units are described below, with the caution that the uncertainly about depths is a result of core recovery of only about 50%:

Unit 1 (421–440 mbsf) is moderately plagioclase-olivine-phyric basalt and pillow lava. The upper part of the unit is made up mainly of small fractured and veined pillows. In the lower part of the section, the pillows are larger, varying from 40 cm to 1 m in diameter.

Unit 2 (440–450 mbsf) is highly plagioclase-olivine-phyric basalt, pillow lava, and pillow breccia. This is a light gray, pillowed, brecciated unit.

Unit 3 (450–460 mbsf) is moderately to highly plagioclase-olivine-phyric basalt and pillow breccia, made up largely of angular fragments of highly porphyritic lava that are 5–10 cm in diameter.

Unit 4 (460–470 mbsf) is moderately to highly plagioclase-olivine-phyric basalt and brecciated, veined lava, interpreted as resulting from the brecciation of an individual lava flow.

Unit 5 (470–490 mbsf) is a moderately to highly plagioclase-olivine-phyric basalt and brecciated lava. All of the recovered section is uniform in lithology, and the unit is thought to comprise one lava flow.

Unit 6 (490–500 mbsf) is moderately to highly plagioclase-olivine-phyric basalt and lava. A number of flat intrusions, with glassy chilled margins, penetrate the massive brownish gray lava(s) in Hole 770C. It is thought to be composed of at least three separate cooling units.

Unit 7 (500–513 mbsf) is a sparsely plagioclase phyric to aphyric dolerite sill. It has a massive and uniform lithology and a phaneritic texture, and it lacks the small intrusions that penetrate the lava units above and below.

Unit 8 (513–524 mbsf) is a sparsely to highly olivine-plagioclase-phyric dolerite sill. The body has a massive homogeneous lithology and a phaneritic texture. Veins and fractures are more abundant and thicker than in the sill above.

Unit 9 (524–530 mbsf) is a moderately to highly olivine-plagioclase-phyric basalt lava. It is penetrated by three flat-lying minor intrusions.

Stress orientation data were obtained with the BHTV logs. Preliminary interpretation of hole ellipticity and break-out data indicate a maximum horizontal stress direction of 050°, or slightly more easterly than the results from Site 768 in the Sulu Sea.

REFERENCES

Berggren, W. A., Kent, D. V., Flynn, J. J., and Van Couvering, J. A., 1985a. Cenozoic geochronology. *Geol. Soc. Am. Bull.,* 96:1407–1418.

Berggren, W. A., Kent, D. V., and Van Couvering, J. A., 1985b. The Neogene: Part 2, Neogene geochronology and chronostratigraphy. *In* Snelling, N. J. (Ed.), *The Chronology of the Geological Record.* Geol. Soc. Mem. (London), 10:211–260.

Haq, B. U., Hardenbol, J., and Vail, P. R., 1987. Chronology of fluctuating sea levels since the Triassic (250 million years ago to present). *Science,* 235:1156–1167.

Holm, P. E., 1985. The geochemical fingerprints of different tectonomagmatic environments using hygromagmatophile element abundances of tholeiitic basalts and basaltic andesites. *Chem. Geol.,* 51: 303–323.

Ling, H. Y., 1973. Radiolaria: Leg 31 of the Deep Sea Drilling Project. *In* White, S. M. (Ed.), *Init. Repts. DSDP,* 31: Washington (U.S. Govt. Printing Office), 703–762.

Martini, E., 1971. Standard Tertiary and Quaternary calcareous nannoplankton zonation. *In* Farinacci, A. (Ed.), *Proceedings of the Second International Conference on Planktonic Microfossils, Roma, 1970:* Rome (Tecnoscienza), 2:739–785.

Pearce, J. A., 1982. Trace element characteristics of lavas from destructive plate boundaries. *In* Thorpe, R. S. (Ed), *Andesites: Orogenic Andesites and Related Rocks:* New York (Wiley): 525–548.

Riedel, W. R., and Sanfilippo, A., 1978. Stratigraphy and evolution of tropical Cenozoic radiolarians. *Micropaleontology,* 23:81–96.

Sanfilippo, A., Westberg-Smith, M. J., and Riedel, W. R., 1985. Cenozoic radiolaria. *In* Bolli, H. M., Saunders, J. B., and Perch-Nielsen, K. (Eds.), *Plankton Stratigraphy:* Cambridge (Cambridge Univ. Press), 631–712.

Sclater, J. G., Meinke, L., Bennett, A., and Murphy, C., 1985. The depth of the ocean through the Neogene. *In* Kennett, J. P. (Ed.), *The Miocene Ocean: Paleoceanography and Biogeography.* Mem. Geol. Soc. Am., 163:1–20.

Sun, S. S., Nesbitt, R. W., and Sharanskin, A. Y., 1979. Geochemical characteristics of mid-ocean ridge basalts. *Earth Planet. Sci. Lett.,* 44:119–38.

Weissel, J. K., 1980. Evidence for Eocene oceanic crust in the Celebes Basin. *In* Hayes, D. E. (Ed.), *The Tectonic and Geologic Evolution of Southeast Asian Seas and Islands.* Am. Geophys. Union Monogr., 23:37–47.

124A-113

NOTE: All core description forms ("barrel sheets") and core photographs have been printed on coated paper and bound as Section 3, near the back of the book, beginning on page 423.

Summary Log for Site 770

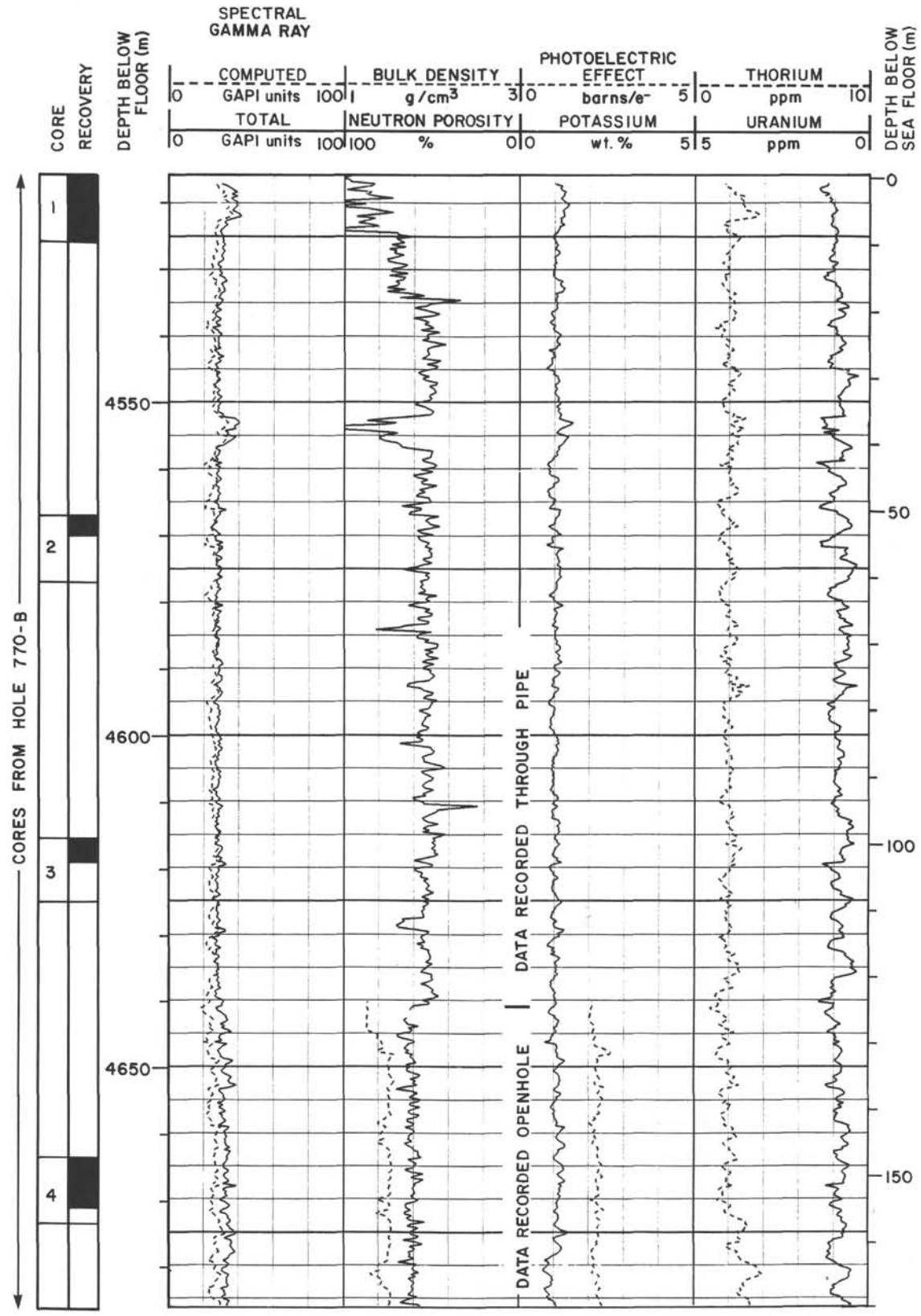

Summary Log for Site 770 (continued)

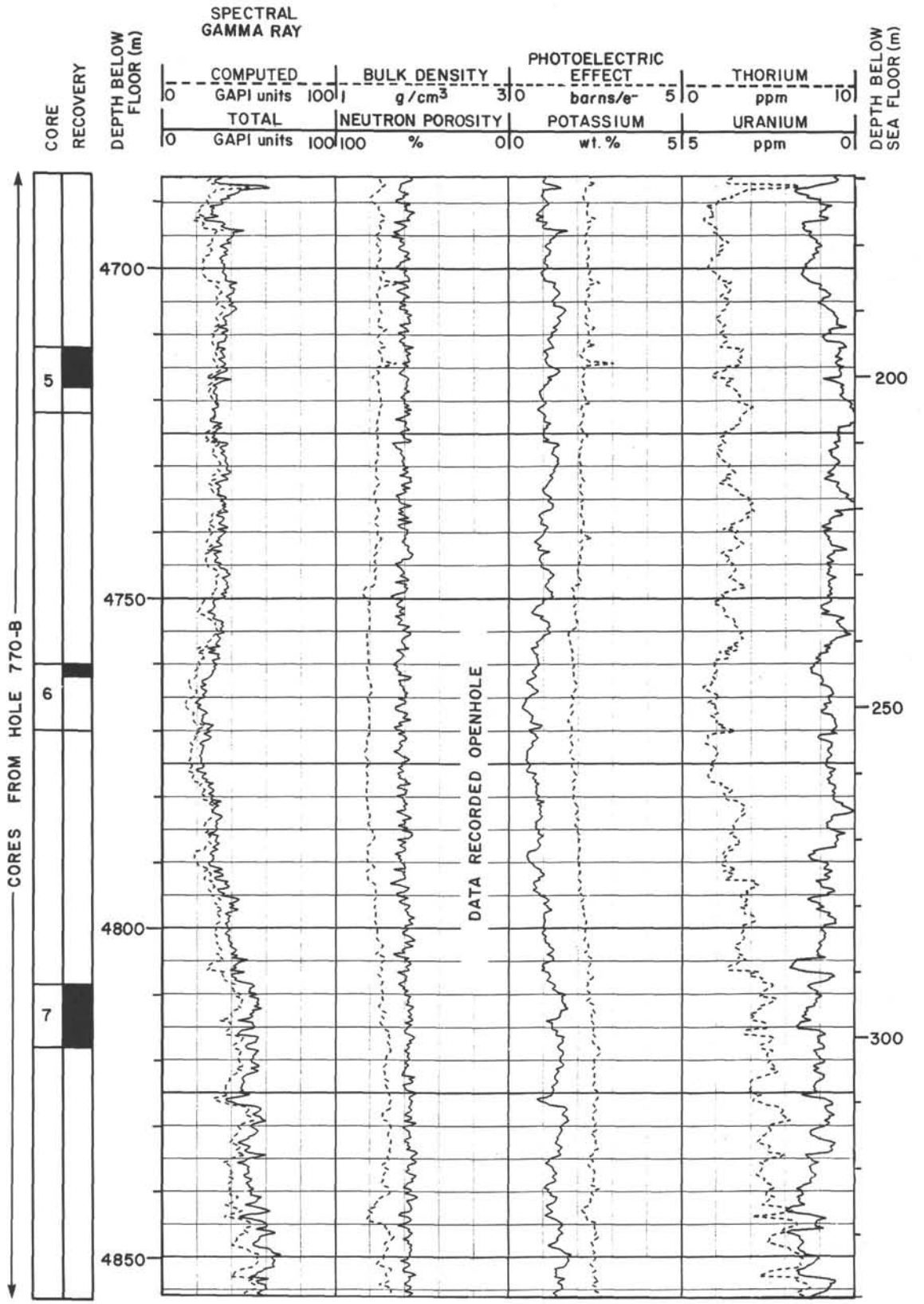

Summary Log for Site 770 (continued)

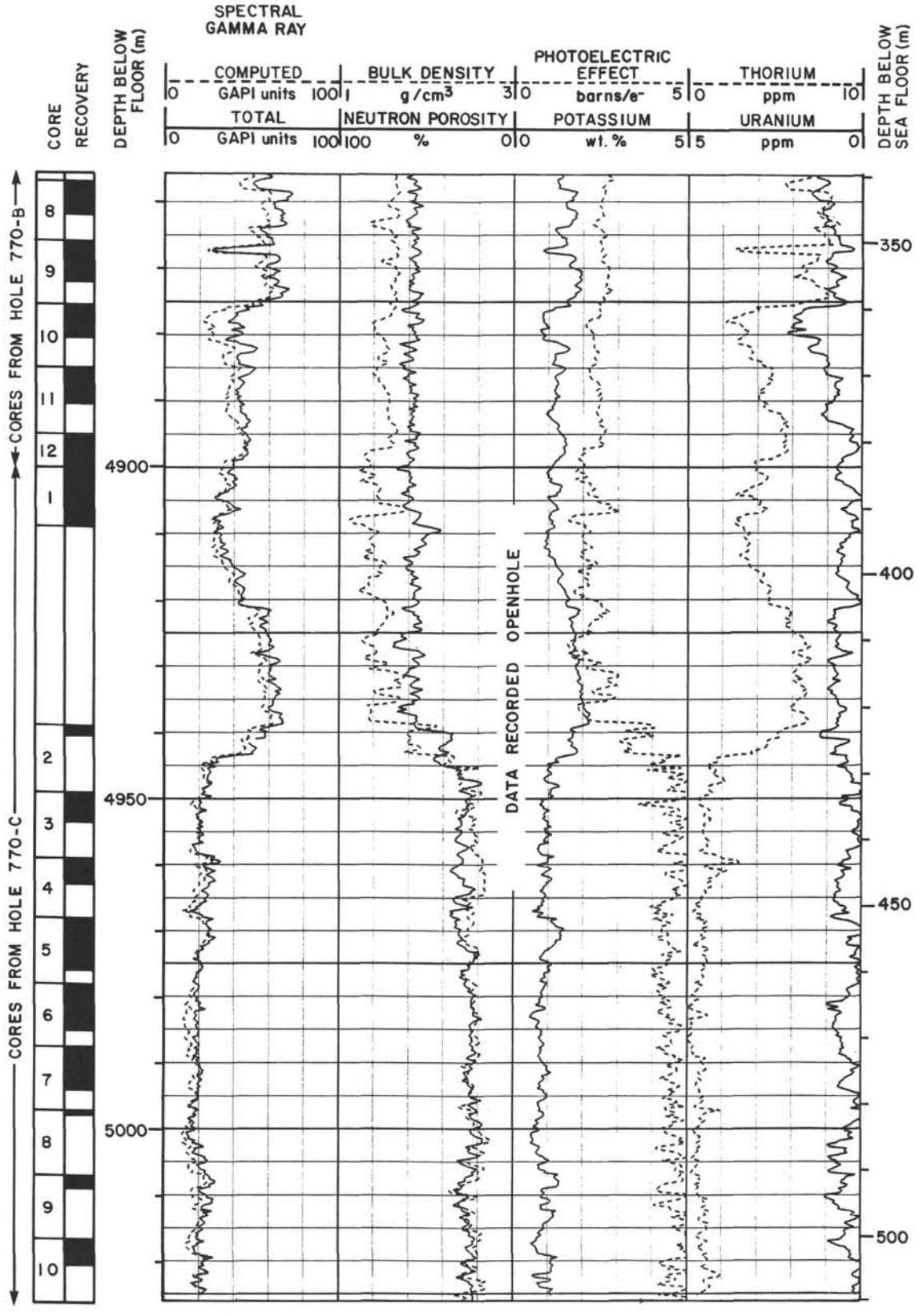

Summary Log for Site 770 (continued)

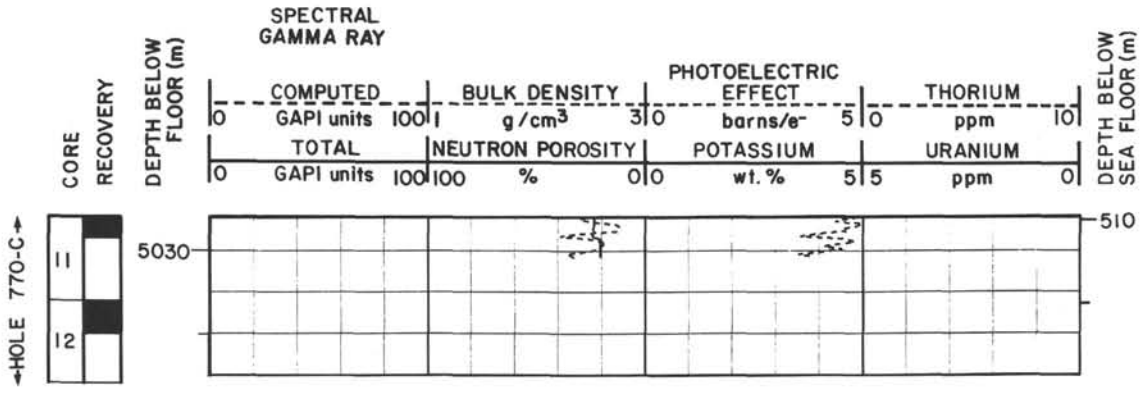

Summary Log for Site 770 (continued)

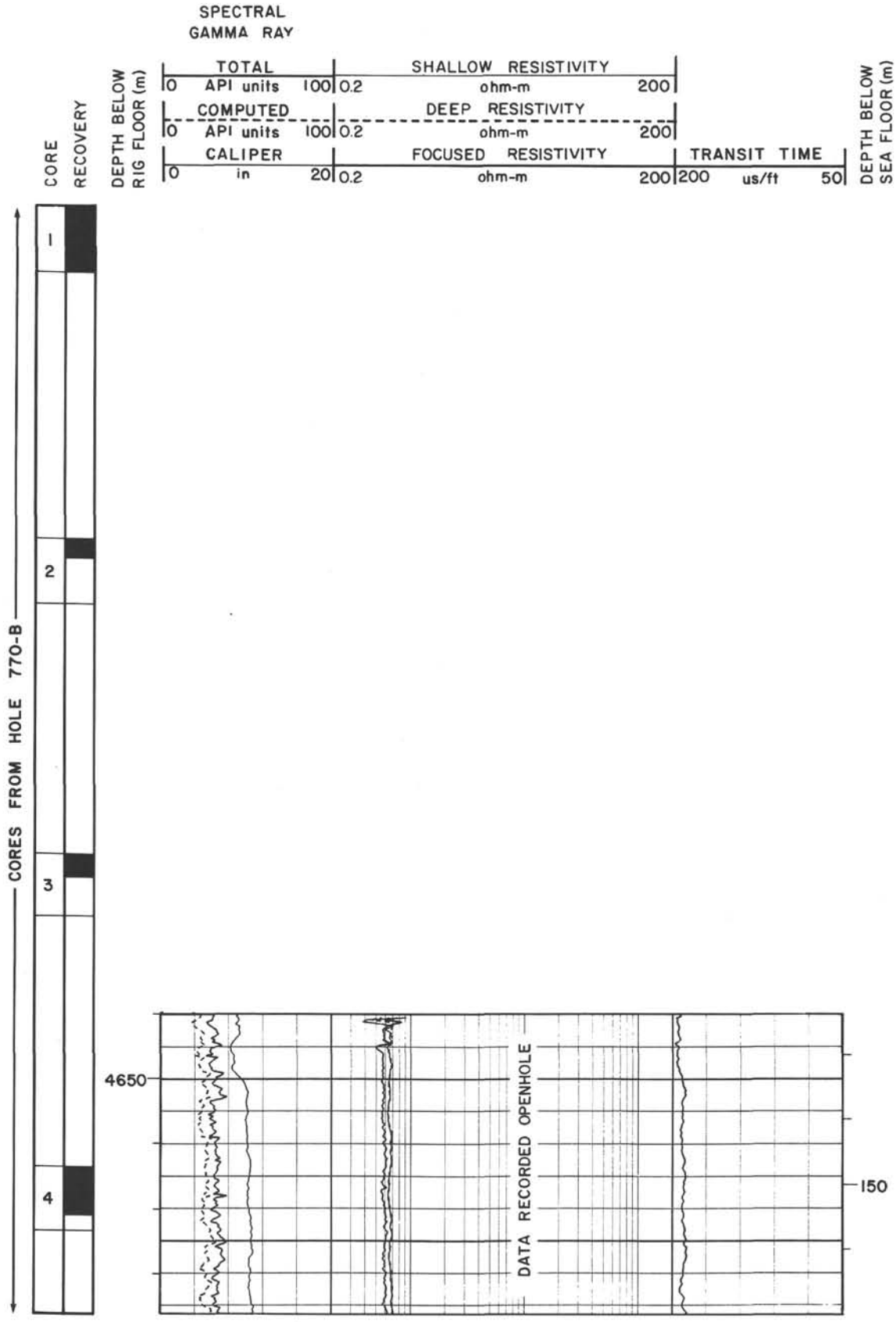

Summary Log for Site 770 (continued)

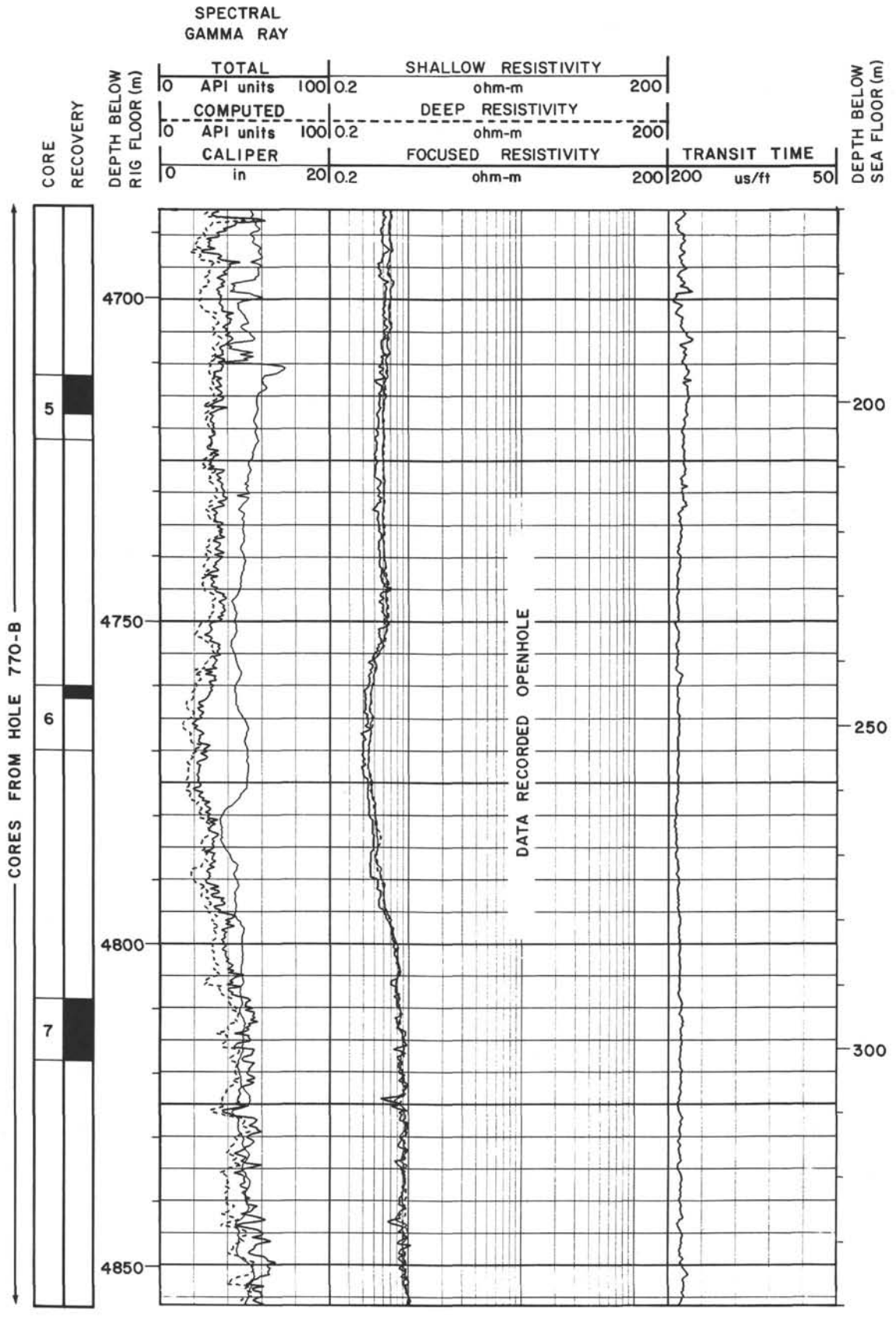

Summary Log for Site 770 (continued)

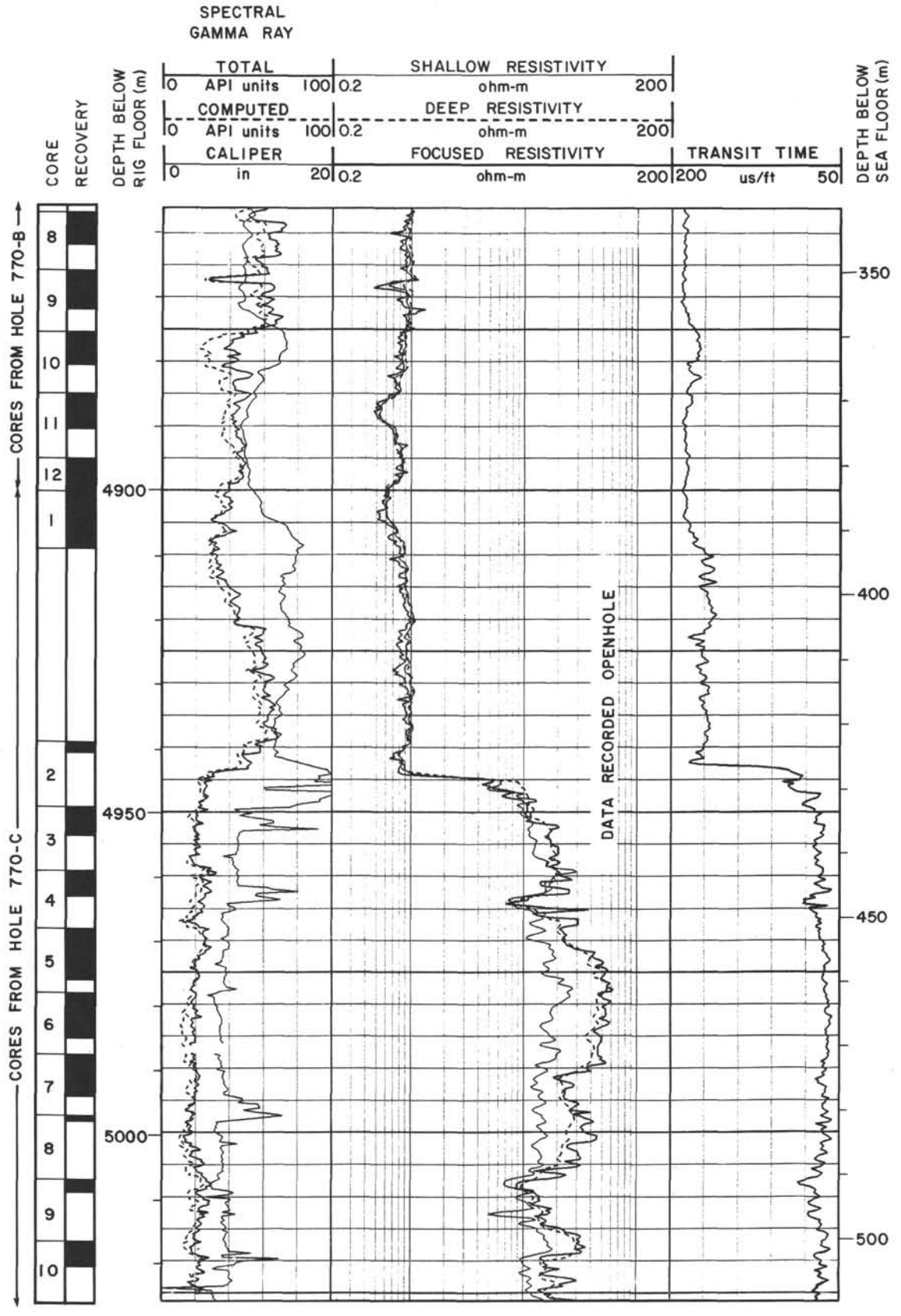

Summary Log for Site 770 (continued)

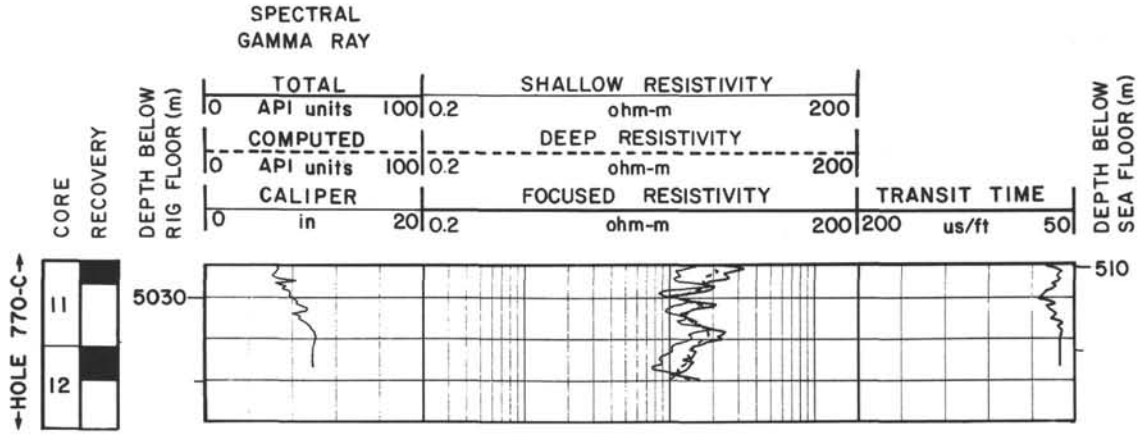

Summary Log for Site 770 (continued)

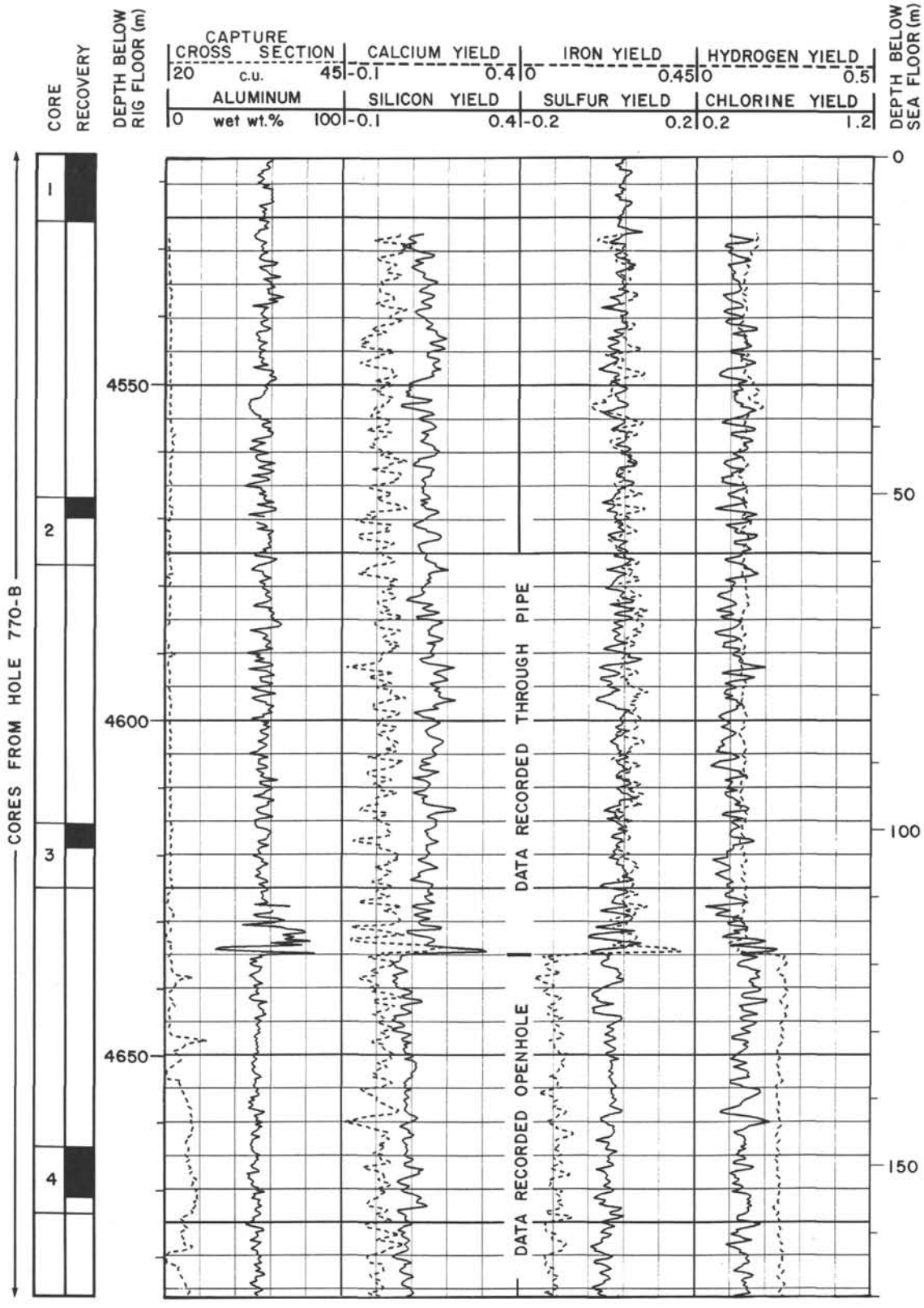

Summary Log for Site 770 (continued)

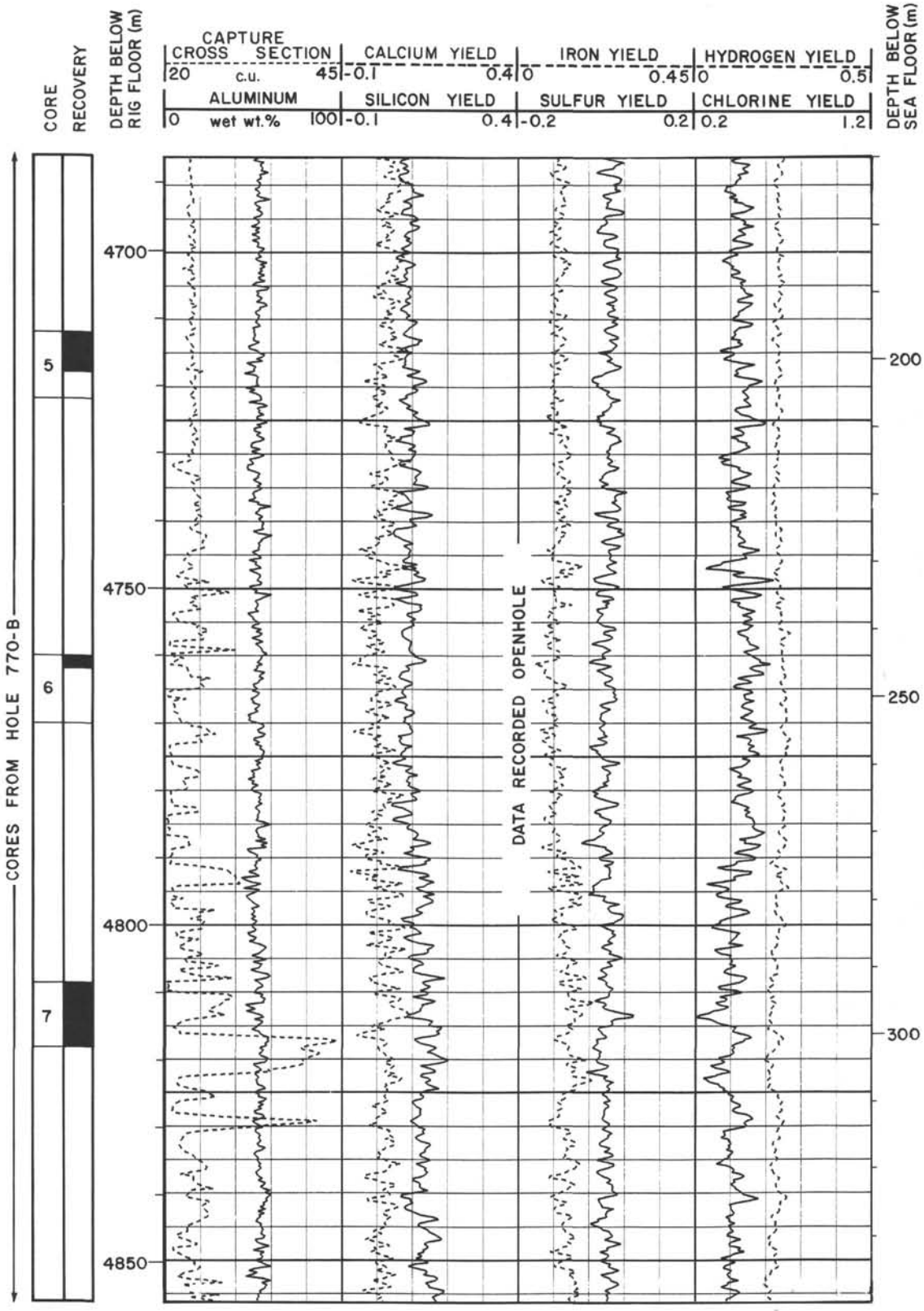

Summary Log for Site 770 (continued)

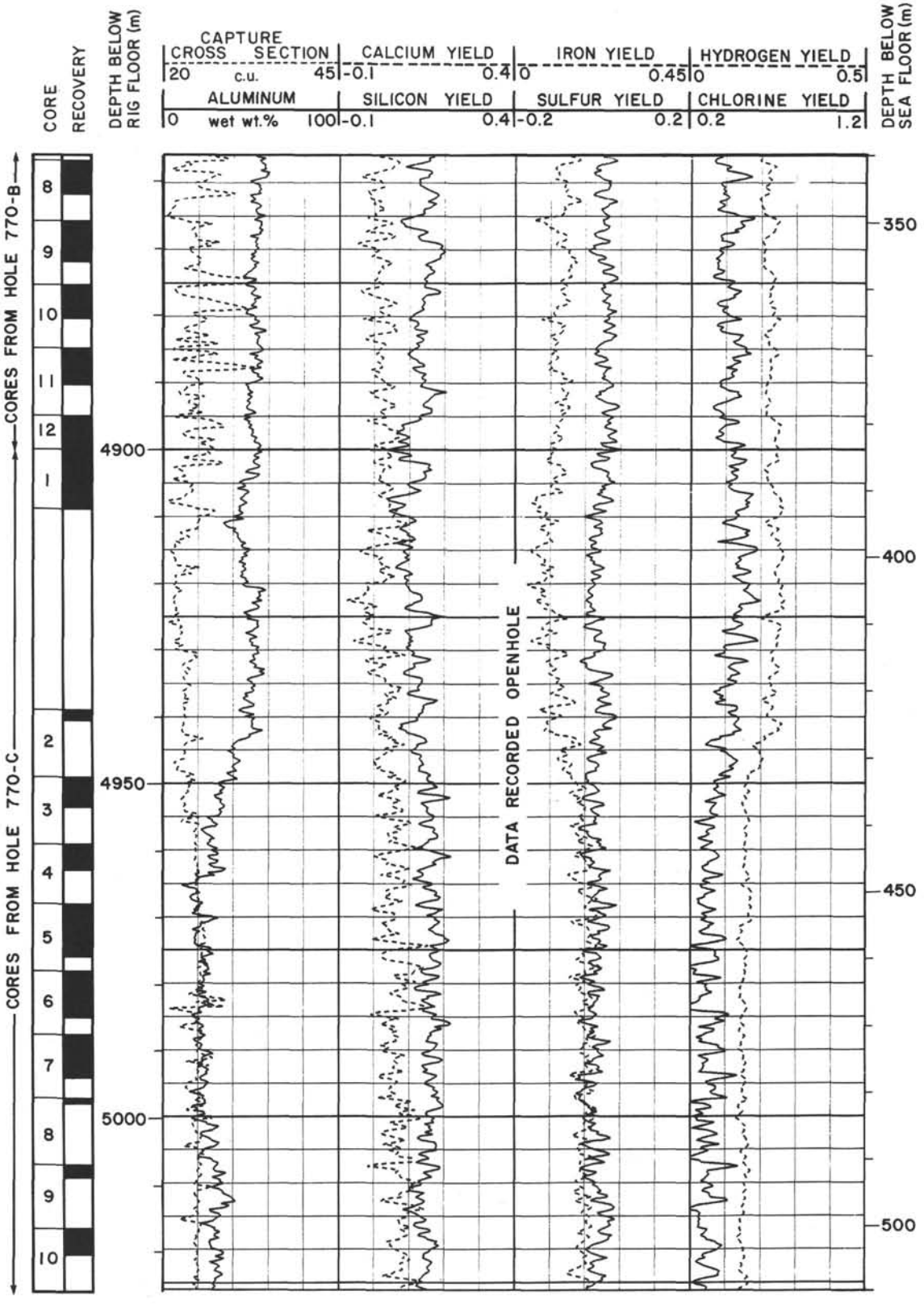

Summary Log for Site 770 (continued)